Doctoral Dissertation

A study of direction of arrivals estimation systems with virtual planar array antenna for multipath propagation

(仮想平面アレーアンテナを用いた電波到来方向推定システムに関する研究)

December 16, 2005

Under the Supervision of

Professor Hiroyuki Arai

Presented by

Akimichi Hirota

Department of Electrical and Computer Engineering,
Yokohama National University, Yokohama, Japan

Abstract

Due to the recent increases in the requirement for higher speed mobile communication, there has been a great deal of research and development into technologies for high-speed mobile communications. Among these methods, a microcellular system has been put into practical use. In the microcellular system, coverage is divided into microcells to respond to the increase in number of subscribers and the demand for high-speed mobile communication. Although propagation in urban areas has become complex due to implementation of the microcellular system, it is important to maintain the quality of mobile communication, particularly in urban areas.

Thus, antennas are installed, and the antenna angles are adjusted to ensure that the quality of mobile communication is suitable for practical use when a base station is set up. However, in urban areas, further complex multipath fading occurs due to reflection, diffraction, and scattering because of microcellular systems. Therefore, many arrival waves significantly in excess of the number of rake fingers reach the receivers. In addition, there are repeaters that amplify and transmit the same signal as nearby base stations. Although repeaters improve the quality of mobile communication, they may produce interference waves for other base stations when the transmitted waves from the repeaters reach other cells. Thus, it is difficult to maintain the quality of mobile communication at certain locations.

To address these problems, the transmitters of the interference waves are estimated. Moreover, the area design should be improved. However, it is insufficient to measure the arrival waves at each point and identify base stations by analysis of pilot signals in code division multiple access (CDMA) systems, such as IS-95 and CDMA2000. This is because repeaters in an area use the same pilot signals as the base station for that area; therefore, it is impossible to distinguish between the repeaters and the base station. Thus, it is important to estimate the direction of arrival (DOA) to distinguish between the arrival waves from the base stations and those from the repeaters. Such information is effective in improving the area design. Therefore, it is necessary to estimate DOA and field intensity of electromagnetic waves as well as the base stations that transmit these waves.

Radio waves from base stations arrive from several directions in the horizontal plane. Further, the arrival directions of these waves may be proximate. Therefore, systems based on super-resolution DOA estimation algorithms using a planar array antenna are useful for measurement of multipath propagation. However, when a planar array is used, forward/backward spatial smoothing, which facilitates DOA estimation of correlated waves,

requires many elements, resulting in a high expenditure on receivers with corresponding increases in weight and size of the estimation system. Such a heavy and large-sized system cannot be transported in an outdoor environment to measure the arrival waves.

This dissertation presents a method for estimating DOA with a virtual planar array synthesized by shifting a T-shaped array antenna. The advantages of this method are low cost because of the reduction in number of receivers, reduction of mutual coupling between elements, and weight saving. In the proposed system, it is important to synthesize the data of the virtual planar array by shifting the T-shaped array. Thus, three methods are proposed for synthesizing the data of the virtual planar array: the first method, which assumes that arrival waves are sinusoidal waves, uses the periodicity of received signals; the second method uses pilot signals in the CDMA system; and the third method uses eigenvectors of correlation matrices.

Chapter 2 introduces the method for synthesizing virtual planar arrays and base characteristics of the virtual planar array by shifting the T-shaped array antenna in DOA estimations, when it is assumed that arrival waves are sinusoidal. In simulations, the average of estimation errors was within 3° at an SN ratio within 5 dB when there are influences, such as position errors, frequency fluctuation, *etc*. The average of DOA estimation error is 2.06° when the number of arrival waves is one in an echoic chamber. In addition, the proposed method can estimate DOA of two arrival waves in an anechoic chamber. These basic evaluations confirmed the effectiveness of the system using data received by the virtual planar array.

Chapter 3 describes a method for estimating the DOA using pilot signals in the CDMA system. We evaluated the proposed method by performing simulations and experiments in an anechoic chamber and outdoor environment. In the simulations, the DOA was estimated accurately, and the effectiveness of the proposed method was confirmed. Moreover, the average estimation errors were approximately 1° in the anechoic chamber, and arrival waves from base stations could be estimated in the outdoor environment. These results confirmed that the proposed method provides effective DOA estimation.

Chapter 4 proposes a method for DOA estimation using eigenvectors and described an evaluation of the proposed method by performing simulations and experiments in an anechoic chamber. Simulation results indicated that DOA was estimated correctly within 3° although the system suffered from the influence of position errors and SN ratio was poor. The performance of the method was evaluated by performing experiments in the anechoic chamber, and the average estimation error was about 0.5°. Further, the proposed method could estimate DOA of two arrival waves. These results confirmed that the proposed method is effective for DOA estimation.

Acknowledgments

I wish to express my gratitude to my supervisor, Professor Hiroyuki Arai, for his continuous guidance throughout this study. I am grateful to Professor Yasuo Kokubun, Professor Toshihiro Baba, Associate Professor Koichi Ichige, and Associate Professor Nobuhiro Kuga of the Yokohama National University for their helpful discussions and critical reading of the manuscript. In particular, I would like to thank Associate Professor Koichi Ichige for advice and constructive criticism regarding my research work, and Associate Prof. Nobuhiko Kuga for his kind advice regarding my special research work.

I am indebted to Mr. Masayuki Nakano of KDDI Corporation, Professor Tatsuo Itoh of University of California, Los Angeles, Professor Kyeong-sik Min of Korea Maritime University, Associate Professor Atsushi Sanada of Yamaguchi University, and Mr. Takehiro Miyamoto of Nihon Dengyo Kosaku Co. Ltd. for helpful discussion and encouragement.

I would like to express my appreciation to Mr. Hirofumi Hirono of KDDI Corporation, Dr. Masahiro Karikomi, Mr. Yukio Sato, Ms. Yurie Shiwa, and Mr. Bryan Robinson of Nihon Dengyo Kousaku Co. Ltd., Mr. Dong-chul Kim, and Mr. Jung-hun Kim of BGTECH Co. Ltd. for their helpful research co-operation.

I would like to thank Dr. Kohei Mori of Sony Corporation, Dr. Naobumi Michishita of National Defense Academy, Dr. Minseok Kim of Brains Corporation, and Dr. Yuki Inoue of NTT DoCoMo, Inc. for helpful discussion.

My appreciation is also due to Mr. Jun Yaezawa for his research cooperation. I would also like to extend my gratitude to everyone in the laboratories of Prof. Arai, Prof. Ichige, and Prof. Kuga. I acknowledge JSPS (Japan Society for the Promotion of Science) for their scholarship. Finally, I acknowledge my parents and my family for their support.

Contents

Chapter 1 Introduction

This chapter introduces the requirement for direction of arrival (DOA) estimation systems for a mobile communication and presents the problems associated with such systems. First, a history of developments for mobile communication systems is presented. Problems regarding mobile communication are introduced, and technologies developed to solve these problems are described. In addition, technologies to achieve further high-speed communication are also presented. DOA estimation systems are necessary for solution of the problems in current and next-generation mobile communication systems. Conventional DOA estimation systems are introduced, and the problems associated with such systems are discussed. Finally, the advantages of the proposed system are described, along with an outline of this dissertation.

1.1 Background

The major advantage of wireless communication is the ability to communicate while moving. It was first proposed immediately after the experiment of Marconi about 100 years ago, and the development of mobile communication systems had been proposed since the development of technologies for wireless communication. However, such systems were limited to military and police use before the end of the second world war, with systems for use by private organizations and individuals proposed after the war.

The first mobile telephone system for business use by private organizations was MTS (Mobile Telephone System) introduced in the United States in 1946, which was followed by IMTS (Improved Mobile Telephone System). However, these systems had insufficient capacity because they did not use cellular methods. AMPS (Advanced Mobile Phone Service), which is currently the most widely used system in the United States, was introduced in 1983. The most important feature of AMPS was the reduction of the radius of cells covered by any one base station, and adoption of the cellular system that recycles the same frequencies in distant areas. However, other countries developed original and analog cellular systems, with service beginning in Europe in the 1980s. Typical systems include NMT (Nordic Mobile Telephone) in Northern Europe and TACS (Total Access Communication system) in the UK. In Japan, an analog cellular telephone service was introduced by NTT in 1979, and a high-capacity system using narrowband was developed in 1989.

However, the capacities of these previous analog systems were too low to cope with the

increase in demand for cellular phones. Therefore, digital cellular systems were developed in Europe, the United States, and Japan. Europe standardized on a GSM (Global System for Mobile communication) system, IS-54 based on TDMA (Time Division Multiple Access), while the United States standardized on IS-95 based on CDMA (Code Division Multiple Access). On the other hand, the PDC (Personal Digital Cellular) system was introduced in Japan in 1992. In addition to these systems, PHS (Personal Handy-phone System) [1] and DECT (Digital European Cordless Telephone) [2] were also developed from cordless phone systems. PHS systems have in excess of 80 million subscribers all over the world, and have become the third most common type of mobile communication system after to GSM and CDMA [3].

The analog and digital cellular systems described above are known as the first- and second-generation systems, respectively. The recent spread of globalization and use of the Internet in business has necessitated the provision of a worldwide high-speed mobile communication service. However, although the first- and second-generation systems do not provide service in all regions, because they are different in each country. Thus, common communication systems for high-speed communication were discussed in ITU-R (International Telecommunication Union Radio communication Section), and IMT-2000 (International Mobile Telecommunications-2000) was standardized as the communication method of the third-generation system (3G). In Japan, the third-generation systems now have in excess of 34 million subscribers [4]. In addition, the number of subscribers of the second- and third-generation systems exceeds 90 million [5], and cellular phones have become indispensable.

High-speed communications systems with speeds ranging from dozens to several hundred Mbps have been developed using optical fibers. To provide seamless service with these fixed communication networks, an increase in speed to the same level is thought to be indispensable for mobile communication. Therefore, further increases in speed are required in wireless communication. There is a great deal of active research and development into Beyond 3G (Beyond 3rd Generation), such as HSDPA (High Speed Downlink Packet Access) and the 4G system [6], and these systems will be developed further in the future. Fig. 1-1 shows the development of data transmission speed in Japan.

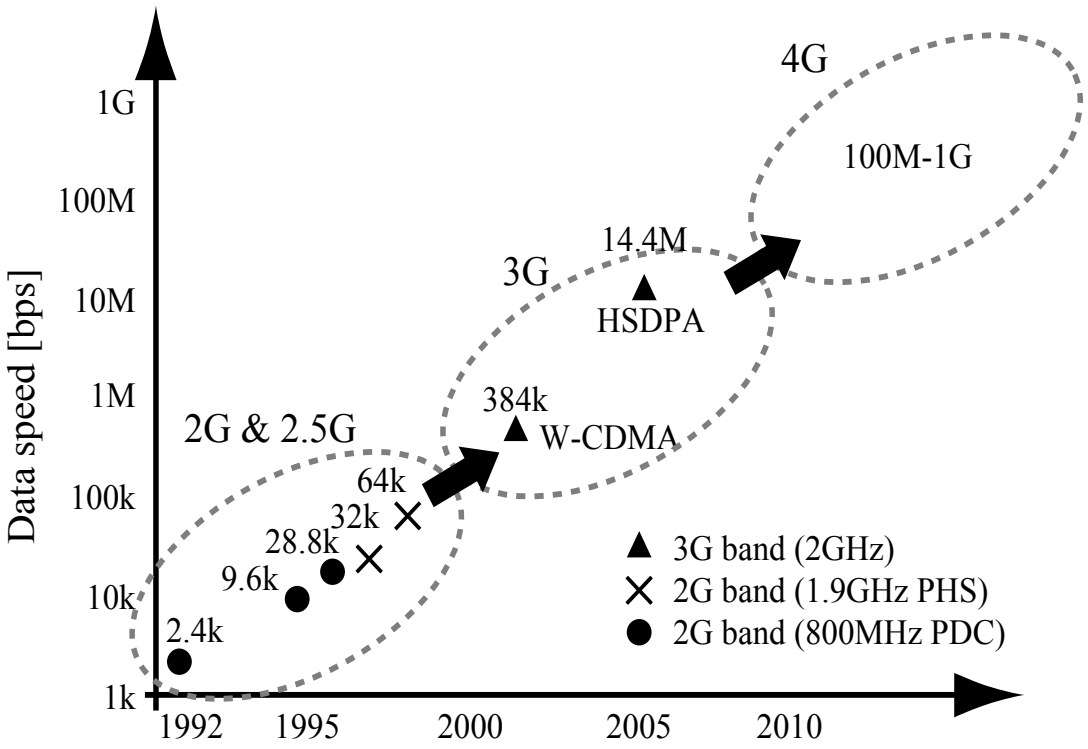

Fig. 1-1 Development of mobile communication data speed in Japan

1.2 Wireless communication

1.2.1 Characteristics of electromagnetic wave propagation

In mobile communication, there are many arrival waves from base stations due to reflection, diffraction, and scattering, as shown in Fig. 1-2. Moreover, many electromagnetic waves travel through various paths in indoor environments, such as wireless LANs, while reflecting from the walls and other scattered objects. There are various strong and weak points in electric fields because of the different routes taken by the signals. In urban areas, cars, people, receiving terminals, *etc*., move, and thus reception level changes over time.

This is called multipath fading, in which the reception level changes due to the large number of arrival waves [7]. There are two types of multipath fading, *i.e.*, uniform and frequency-selective fading. In general, multipath fading is considered to be uniform fading when the delay times of arrival waves can be disregarded. On the other hand, the delay times cannot be disregarded when the bandwidth of the transmitted signal is wide, because the delay time of each arrival wave becomes the same as one symbol length; this is called

frequency-selective fading. In mobile communication, compensation technologies for signal degradation due to multipath fading are important. As compensation methods differ according to the differences between uniform and frequency-selective fading, many compensation methods have been studied [7]–[68].

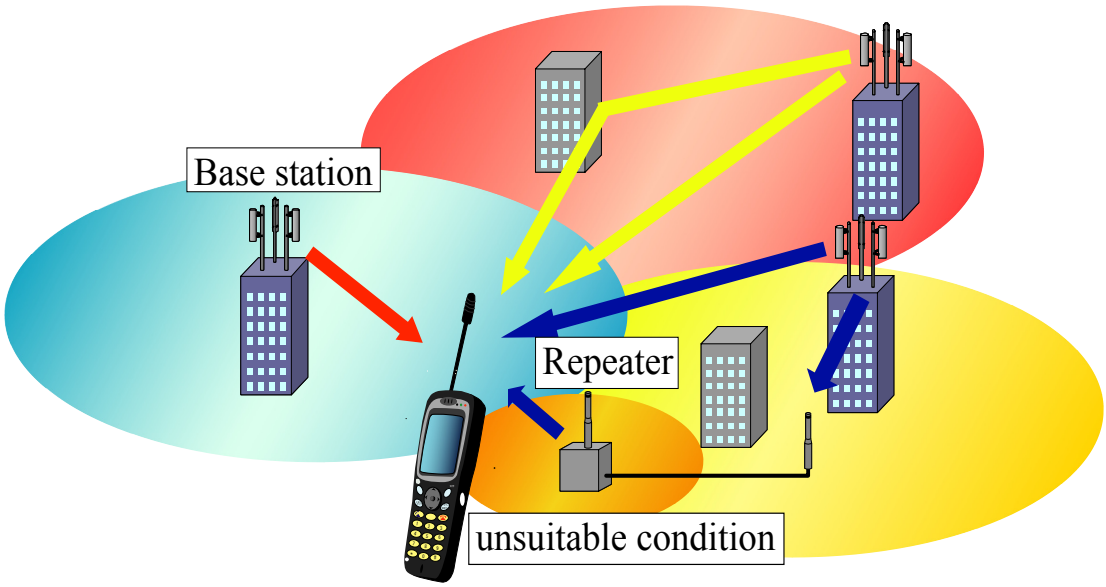

Fig. 1-2 Propagation characteristics in urban areas

In designing wireless communication systems, a propagation model is important for evaluation of the signal degradation due to multipath fading. The propagation model is based on the probability distribution to allow calculation of statistics, and the Rayleigh distribution and Nakagami-Rice distribution are generally used. The Rayleigh distribution appears as that of signal strength when large numbers of waves of random phase signals arrive. The Rayleigh distribution is used when considering multipath fading in mobile communication systems, such as non-line-of-sight systems, in which there many scattered waves and no directional waves [7]. The Nakagami-Rice distribution is used for fading in line-of-sight, *e.g.*, in satellite communications for ships with sea clutter or for land mobile radio [7]. Fading is actually simulated not only with modeling by statistical approaches but also by computer for the evaluation of wireless systems, and fading simulators have been reported [8]–[12]. In addition, experiments to clarify the propagation characteristics have been conducted by measurement of electrical fields and delay profiles in indoor and outdoor environments [13]–[31].

1.2.2 Techniques for multipath fading

It is necessary for high-efficiency mobile communication systems to consider efficiency with regard to frequency, electrical power, and performance taking fading into account. Methods for modulation and demodulation have been proposed taking these characteristics into consideration. From the last half of the 1970s to the early 1980s, there was a great deal of research and development into envelope modulation technologies to increase the efficiency of electrical power and resistance to amplitude fluctuations due to fading. Thus, GSMK (Gaussian-filtered Minimum Shift Keying)[32][33], PLL-QPSK (Phase-Locked Loop Quaternary Phase Shift Keying)[34], 4-value FM (Frequency Modulation)[35], and Tamed FM[36] were proposed; GSMK was adopted for the GSM system developed in Europe. The capacity shortages of the analog cellular phone system became a problem in the mid-1980s, and linear modulation methods were studied to increase efficiency [37]. Based on the results of these studies, FQPSK (Feher QPSK) and FQAM [38] were proposed. π/4QPSK was developed, and it has been adopted for the PDC system.

When electromagnetic waves modulated by these modulation methods are demodulated, delay or synchronous detection are generally adopted as the detection method. Compensation methods for fading were not examined in the mid-1980s, because it was considered that the delay detection method was better than the synchronous detection method. The reasons for this were that circuit composition is easy, and the BER characteristics of delay detection were better than synchronous detection in fading channels. However, with appropriate compensation methods for fading, synchronous detection has better characteristics than delay detection. In addition, there was an increase in demand for high-speed mobile communication, and therefore researchers began to apply synchronous detection to mobile communication. In the second half of the 1980s, multiple value modulation methods, such as 16 QAM, were studied for application to wireless communications. In this case, greater accuracy of the compensation technologies for fading were needed, because the information is included in not only the phase but also the amplitude [39] [41].

A problem in synchronous detection is that errors can occur that cannot be compensated, because it is not possible to follow the phase of CW (Continuous Wave) output of PLL to the fading channel. There are two types of method to address these problems—which are distinguished by the use or lack of use of pilot signals. As examples of the latter, methods using ACT (Adaptive Carrier Tracking) or based on LMS (Linear Mean Square) algorithm have been proposed [42]–[44]. However, these methods are not efficient due to the necessity of using a differential code. In contrast, technologies using pilot signals are very effective. In these methods, fading is compensated by estimation of fading using well-known pilot signals. It is

possible to divide into three methods, *i.e.*, pilot tone, pilot symbol, and pilot code methods, according to the method used to insert the pilot signal, as shown in Fig. 1-3. The pilot tone method multiplexes one or more sinusoidal waves and modulated signals on the frequency axis, such as TCT (Tone Calibration Technique) [45][46], DTCT (Dual Tone Calibration Technique)[47]–[50], and TTIB (Transparent Tone-In Band)[51]–[53]. This method is used mainly in FDMA (Frequency Division Multiple Access) systems. In the pilot symbol method, well-known pilot symbols are multiplexed with the information symbols on the time axis. In this method, the spectrum of the fading channel is limited to a given band and the fluctuation is very smooth [54]–[57]. In general, TDMA (Time Division Multiple Access) systems use the pilot symbol method. The pilot code method involves multiplexing a well-known pilot channel, which is spread by an orthogonal code to traffic channel and has the same frequency as the traffic channel. Especially, the pilot code method is used for CDMA (Code Division Multiple Access) systems [58], such as cdmaOne, cdma2000, and W-CDMA, for fading compensation when synchronization between terminals is taken with the base station. Diversity techniques have been studied and put into practical use as other methods for fading compensation [60]–[62]. These methods secure a steady received power by selecting or synthesizing the received power, because different fading occurs if the position, polarization, frequency, and radiation pattern of antennas are different.

These techniques achieves a sufficient effect in case of uniform fading; however, further fading compensation is needed when arrival waves are late by more than one symbol length, as in frequency-selective fading. Thus, adaptive equalizers [63] are adopted for frequency-selective fading. In particular, MLSE (Maximum Likelihood Sequence Estimation), which uses the Vitarbi algorithm and DFG (Decision Feedback Equalizer) have been developed and put into practical use [64]–[68]. These algorithms were used for the adaptive array antenna described later.

Conventional methods for fading are not sufficient to provide communication quality adequate for next generation systems for mobile communication [6]. Thus, further research and development are currently in progress. In modulation/demodulation technologies, multi-carrier wireless systems, such as OFDM (Orthogonal Frequency Division Multiplexing), MC/DS-CDMA, and MC-CDMA, have attracted a great deal of attention [69][70]. Moreover, with regard to encoding technology, the LDPC (Low-Density Parity-Check) code has been studied [71][72]. On the other hand, the adaptive array antenna and MIMO (Multiple Input Multiple Output) technology with two or more antennas have attracted attention as antenna techniques [6][7][73]. Especially, the adaptive array antenna system has been used as the base stations for PHS systems [74], and MIMO systems have been put into practical use, and these technologies are expected to be developed further in the future.

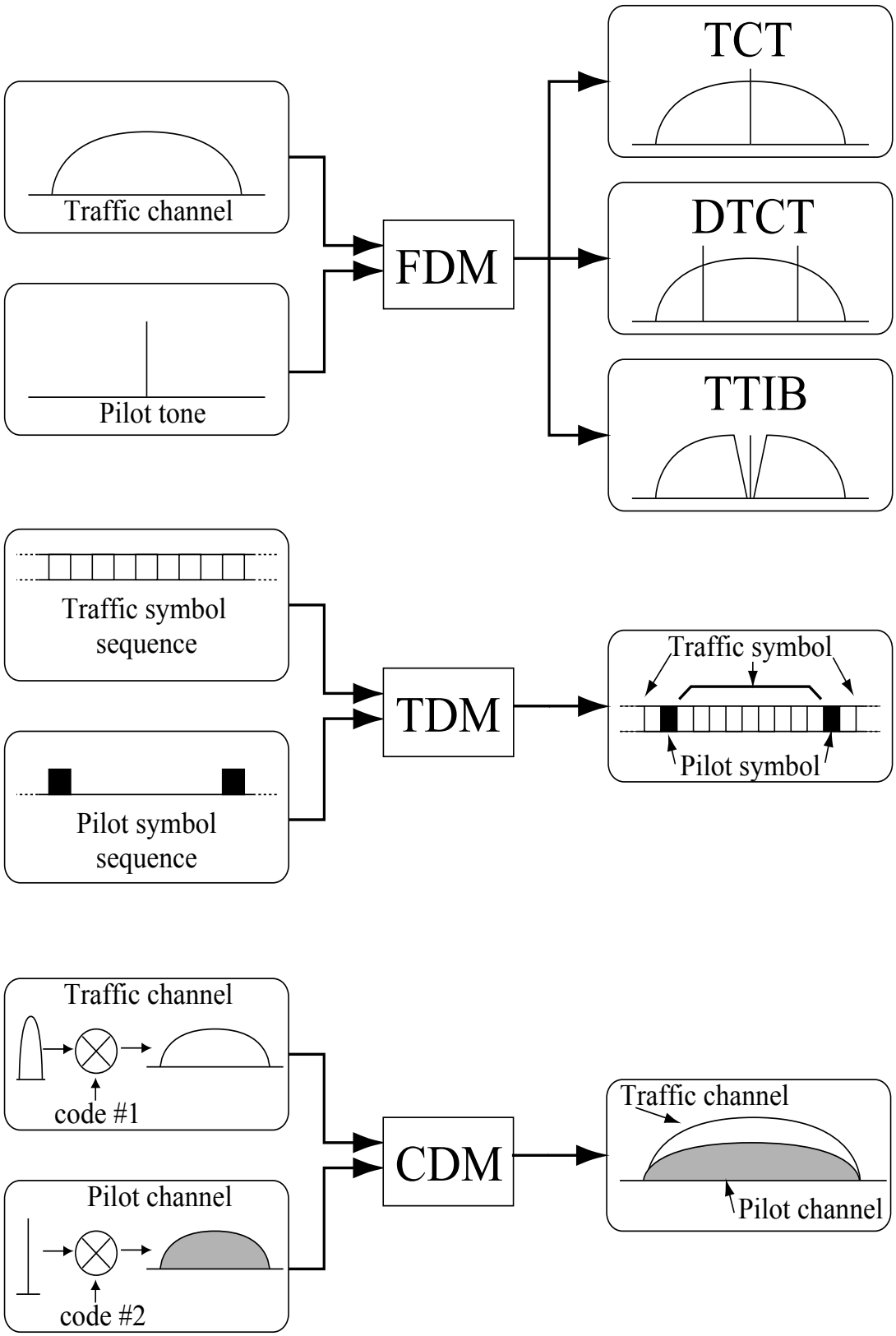

Fig. 1-3 Fading compensation schemes using pilot signals

1.2.3 Problems in mobile communications

The cellular system has been used in mobile communication to improve the efficiency of frequency as shown in Fig. 1-2. Due to the increases in both number of subscribers and demands for high-speed mobile communication, microcellular systems in which the radii of the cells are small have been applied in areas where the density of users is high, such as urban areas. There is a possibility of interference waves of the same frequency from base stations of nearby cells in microcellular systems, because electromagnetic wave can propagate along distances of the order of several hundred meters [75]. The propagations of actual microcellular systems are more complex than the macrocellular systems in which the radii of cells range from one to a few kilometers, because the cell structures are not ideal circles and are geographically irregular. In addition, the influence of such the problems grows in the system of B3G and 4G because it is expected that the size of the cells in B3G and 4G systems will become smaller than those in conventional systems. Moreover, repeaters are used to amplify and transmit the same signal as nearby base stations. Repeaters improve the quality of mobile communication. When the transmitted waves from the repeaters reach other cells, they may become interference waves for other base stations. On the other hand, there are illegal repeaters that transmit interference waves, such as noise, in urban districts [76]. In fact, these illegal repeaters have become a problem because the quality of mobile communication is degraded by these interference waves.

Conventional methods for fading are not sufficient to maintain the quality of mobile communication under these conditions because of a reduction in the electric field intensity. To deal with these problems, the transmitters of the interference waves are estimated to allow the area design to be improved. However, it is insufficient to measure electrical intensity at each point and base stations and repeaters are identified by analysis of the measurement data including pilot signals. This is because repeaters in an area use the same pilot signals as those used by the base station for that area; therefore, it is impossible to distinguish between the repeaters and the base station. Moreover, it is necessary to discover and remove the illegal repeaters that cause degradation of communication. Thus, it is important to estimate the direction of arrival (DOA) to distinguish between the arrival waves from the base stations and those from repeaters. Such information is effective in improving the area design. On the other hand, the adaptive array antenna and MIMO systems have been examined as methods to compensate for fading and interference waves. However, these techniques have not been studied sufficiently to allow their application to cellular systems in urban areas. For such research, it is also necessary to analyze propagation. For these reasons, DOA estimation systems are very important.

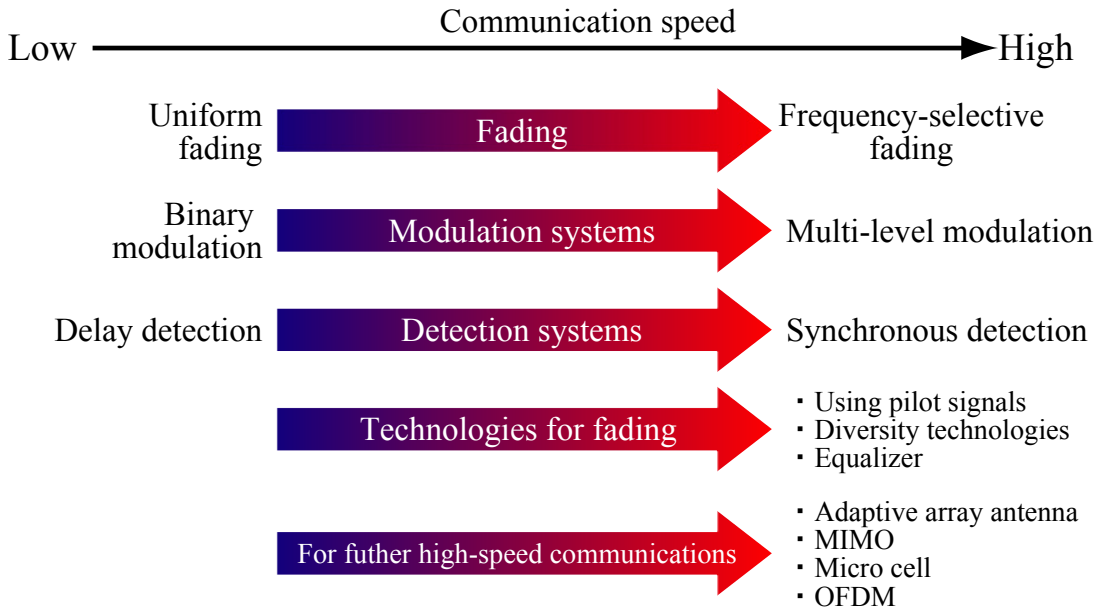

Fig. 1-4 Technologies for wireless communications

1.3 DOA estimation system

1.3.1 Basic methods for measurement of multipath fading

The technologies for DOA estimation have been developed chiefly as military radar technology. The radar system used for the first stage is CW radar [77]. This method estimates distances from targets by transmitting 2 waves with different frequencies alternately and calculating the differences in phase of the received signals. However, it is difficult to classify targets with the same relative velocity. The FMCW method was proposed to solve this problem [78][79]. This method estimates distances and velocities of targets by sweeping frequency and Fourier transform of the received data. Moreover, pulse radars and Doppler radars have also been developed. Pulse radars are those in which pulse signals are transmitted and the times of reflected waves are measured [80]. These radars have been adopted not only for military use but also in air traffic control and as weather radars [81]–[83]. First, these methods measure electrical intensities in all directions by rotating a reflector antenna for DOA estimation. However, these methods have problems due to clutter, consisting of unnecessary reflected waves due to scattering around targets, as well as poor resolution. Therefore, algorithms with array antennas described later [81] [84][85] have also been proposed.

On the other hand, in mobile communication, the conventional method for determining propagation characteristics involves measurement of electrical intensity at each position with a

monopole antenna [13]–[31]. However, radio sources that transmit interference waves cannot be distinguished because detailed propagation characteristics cannot be explained by this method. Thus, it is impossible to apply this method to the problems of fading in microcellular systems.

To measure propagation in more detail, radars technologies have been applied for measurement of the propagation environment of mobile communication. As a typical example, a multipath estimation method, which measures the magnitude and angle of the direction waves received by rotating the antenna with sharp directivity, has been reported [86]–[88]. This method requires an antenna with an effective aperture area that is sufficiently large to improve angular resolution. As the rotation of a large antenna requires a large drive unit, the total size of the system increases.

In addition, there is a method that measures the delay profile while moving a non-directional antenna at a constant velocity in a straight line [89]–[91]. This method estimates the DOA by using the Doppler shift data obtained from the Fourier transform of the measured delay profile data. Although this method can estimate the DOA continuously at each position, its disadvantages include the inability to discriminate between symmetrical directions and the forward direction and poor angular resolution.

1.3.2 DOA estimation algorithm with array antennas

The conventional methods have a number of problems in that the angle resolution is insufficient to measure propagation and the sizes of the systems are large. Thus, DOA estimation systems with array antennas have been studied to improve performance [92]–[148]. The most basic method in DOA estimation algorithms with an array antenna is the beam-former method, which is based on the same principle as the Fourier transform [92][93]. This method is used to measure the electrical power of an array output in all direction by scanning with the main lobe of a uniform excitation array antenna. However, this method may estimate incorrect directions when the array output becomes large due to receiving arrival waves with side lobes of the array antenna, and therefore this method is not useful for measurement in urban areas.

The Capon method, which involves measurement of electrical power by scanning in all directions while keeping a null radiation pattern to other arrival waves with an array antenna, was proposed [94]. The resolution characteristics of the Capon method depend on the beamwidth of the main beam due to scanning the main beam at all angles. That is, a narrow beamwidth is necessary to achieve high resolution, and large numbers of elements are necessary. On the other hand, it is possible to estimate DOA with high resolution by scanning all angles with null, because the beamwidth of null is narrower than the main beam. Based on these considerations, the linear prediction (LP) method were proposed [95]. Moreover, the Min-Norm

method [96] and Pisarenko method [97] have also been proposed. Weight assumptions of these methods are extended from the LP method. Although DOA estimation algorithms have been developed in addition to the adaptive array antenna, DOA estimation algorithms use the characteristics of the adaptive array antenna, because the principle is closely related to the adaptive array antenna [92][98][99]. For example, the principle of the Capon method is equal to the DCMP adaptive array antenna [100], the LP method is equivalent to the side lobe canceller and a power inversion adaptive array antenna [101][102]. It is possible in LP and Min-Norm methods to make the nulls at directions where there are no arrival waves. Thus, it is necessary to confirm the existence of arrival waves to estimate electrical power.

To resolve these problems, the multiple signal classification (MUSIC) method was proposed [103]. The MUSIC method makes use of the characteristic that eigenvectors correlated to the noise subspace of a correlation matrix are orthogonal to the mode vectors that express phase differences to a base point. Although the computational method of the MUSIC method is more complex than that of the beamformer method, the MUSIC method has higher resolution than conventional methods. [104] – [106]. The MUSIC method cannot estimate DOA correctly when the accuracy of the correlation matrix is insufficient, and has higher computational costs due to scanning the MUSIC spectrums. Due to these problems, the Root-MUSIC method has been proposed [107]. Moreover, the Unitary MUSIC method, which uses the Unitary transformation that can replace the calculation by complex numbers with real numbers, was proposed to reduce the computational complexity and to achieve better speed of the algorithm [108][109]. On the other hand, the estimation of signal parameters *via* rotational invariance techniques (ESPRIT), which is used to compute phase differences between subarray antennas, has been proposed [110]. A spectrum search is unnecessary in ESPRIT, although it has essentially the same accuracy as the MUSIC method. ESPRIT can be classified into LS-ESPRIT (Least-Squares) [110] and TLS-ESPRIT(Total-Least-Squares)[111] according to the methods used for calculating the phase differences of two subarrays. The method using the Unitary transformation has been proposed as well as the case of the MUSIC method [112][113]. Moreover, these algorithms have been extended to 2D or 3D, and can simultaneously estimate not only DOA in the horizontal plane but also the directions of elevations and delay time [114] – [117].

Recently, DOA-based adaptive array antennas have been studied. When using DOA-based adaptive array antennas in the fading channel, it is necessary to estimate DOA very early because of rapid changes in propagation characteristics [118].

To deal with these problems, the BiSVD (Bi-Iteration Singular-Value Decomposition) method [119] [121], PAST (Projection Approximation Subspace Tracking) method [122], and PASTd (Projection Approximation Subspace Tracking) method [122] have been proposed and investigated. These methods are characterized by successively updating eigenvectors in the

signal subspace of a correlation matrix, and have been applied to MUSIC and ESPRIT methods.

1.3.3 Specifications of DOA estimation systems

The performance of the conventional method during DOA estimation was evaluated by performing simulations. For example, the accuracy of the method, which measures the magnitude and the angle by rotating the antenna, was evaluated. The antenna pattern in this simulation is shown in Fig. 1-5 (a). The half-bandwidth of the antenna is 30°. The result in the case of one arrival wave at an angle of 0° is shown in Fig. 1-5 (b). This result indicated that DOA can be estimated correctly. Then, the case of two arrival waves was simulated. Fig. 1-6 (a) shows the results for arrival waves at 0° and 35°, and again the results confirmed that DOA can be estimated in this case. On the other hand, Fig. 1-6 (b) shows the magnitude of received signals at each angle with arrival waves of 0° and 25°. The estimation result was 11°, and therefore this system could not distinguish between the two arrival waves. These results suggest that it is possible for the DOA estimation error to be about 11° with this system.

Then, the specification of MUSIC was carried out. A simulation was conducted, in which two arrival waves had angles of 0° and 25°. The array antenna was a 2 × 2 planar array with an interval between elements of 0.4 wavelengths. The size of this array antenna became about 15 × 15 cm at 900 MHz. Fig. 1-7 shows the MUSIC spectrum of this simulation, and the results indicated that this system can distinguish between the two waves and estimate DOA correctly.

It is necessary to search the range of about 100 meters in the radius if the distance between transmitters and the system is 500 meters and DOA is estimated at two points, as shown in Fig. 1-8. Thus the efficiency of using this system for area design is not good. To resolve this problem, the half-bandwidth of the antenna used is sharper than the resolution needed for DOA estimation systems. However the size of the system becomes large due to the requirement of the large antenna for high resolution, and this results in the high cost of the system. On the other hand, it was confirmed that systems using MUSIC are better for efficiency area design than conventional methods, because the range of transmitters in the case of MUSIC is narrowed to a greater extent than in the case of an antenna with a shape pattern, as shown in Fig. 1-5 (a).

$$D(\theta) = \begin{cases} \cos^{\Theta_H}(\theta) & \left(-90^\circ \le \theta \le 90^\circ\right) \\ 0 & \left(-90^\circ \le \theta \le 90^\circ\right) \end{cases}$$

$$\Theta_H = -\frac{\log_{10} 2}{\log_{10}\left\{\cos\left(\Theta_H / 2\right)\right\}}$$

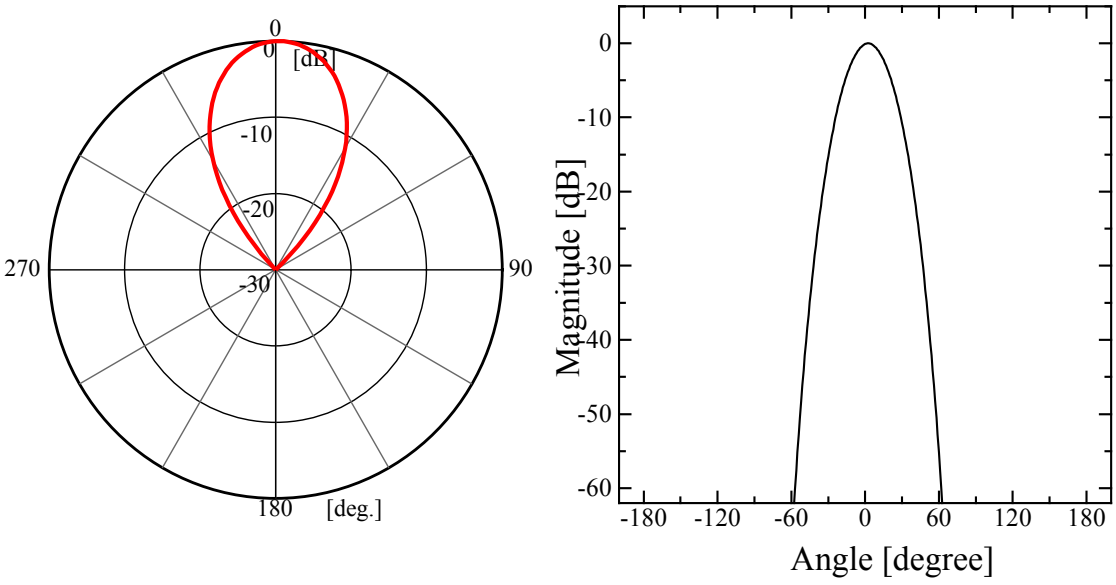

(a) Antenna pattern (b) Eletrical intensity (one arrival wave)

Fig. 1-5 Antenna pattern and simulation results (one arrival wave)

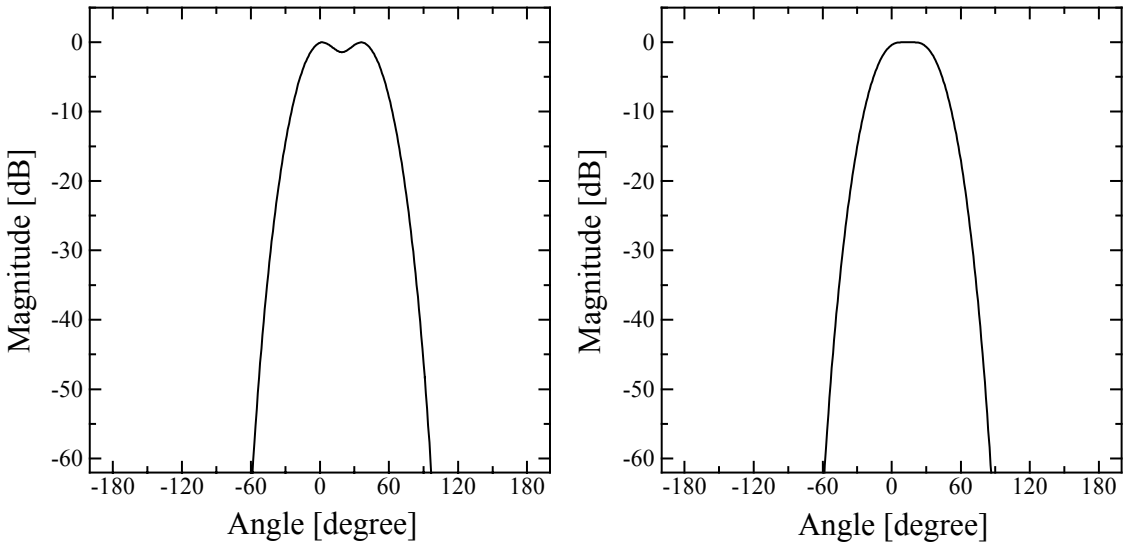

(a) Eletrical intensity (0, 35 [degree]) (b) Electrical intensity (0, 25 [degree])

Fig. 1-6 Estimation results with rotation of the antenna

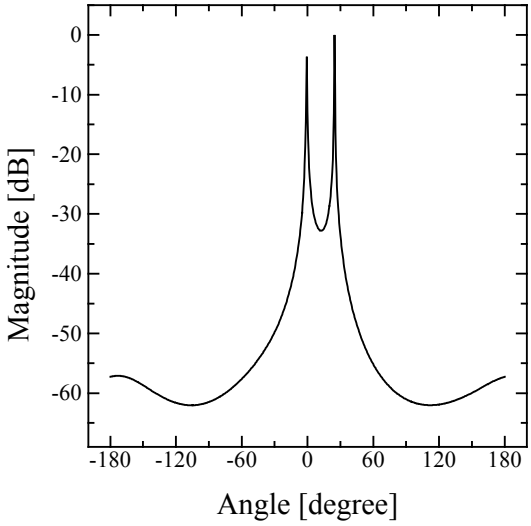

Fig. 1-7 MUSIC spectrum (0, 25 [degree])

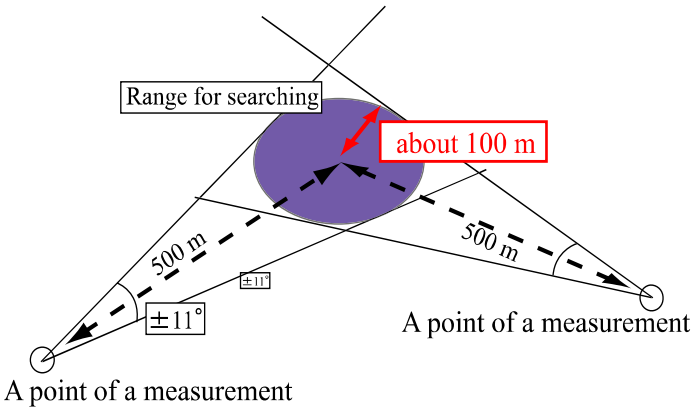

(a) The case of the conventional method

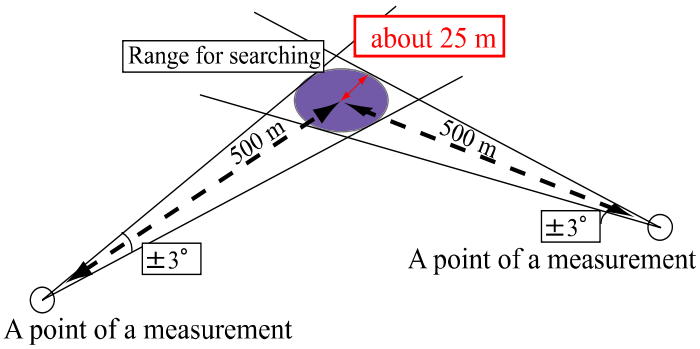

(b) The case of the MUSIC method

Fig. 1-8 Search ranges

1.3.4 DOA estimation system for reducing system costs

The advantages of DOA estimation systems using the array antenna are that DOA can be estimated with higher accuracy and resolution using super-resolution methods, such as the MUSIC method, and it is possible to estimate arrival waves in all directions. Thus, DOA estimation systems with array antennas using MUSIC or ESPRIT are desired for designing areas in cellular systems [76].

However, when the array antenna is used, forward/backward (F/B) spatial smoothing [123], which facilitates DOA estimation of correlated waves, requires many elements; this results in a high expenditure on receivers with an increase in the weight and size of the estimation system. Such a heavy and large-sized system cannot be transported in an outdoor environment to measure the arrival waves. Although the method that uses the Fourier transform is useful for reducing the effects of correlated waves [124], it is difficult to apply this method for estimation of DOA in urban areas because it is assumed that correlated waves originate from fixed or regularly moving transmitters. Thus, F/B spatial smoothing is required for DOA estimation in urban areas.

As a solution to these problems, a method has been developed in which a linear array or a planar array is translated to sweep or rotate an area and DOA are estimated using data obtained by synthesizing these data [128][129]. This method can achieve performance equivalent to that of a planar array occupying an area of a similar size, and can be applied to super-resolution methods such as MUSIC. The performance of the moving linear array is expected to be similar to that of a real antenna array that occupies the same area as that swept by the linear array of antenna elements. Therefore, the moving linear array system has been termed a “virtual planar array.” This method cannot be used to estimate the DOA when carrier synchronization has not been established because when the linear array moves, there may be a phase difference between the carrier frequencies of the wave transmitter and receiver. Therefore, the phase difference cannot be calibrated accurately as measurements at each position are obtained at different times. Therefore, this method can estimate DOA, when synchronization is achieved by connecting transmitters to receivers using cables, because the synchronization can compensate for the time differences between linear arrays at each position. However, in indoor environments this measurement can be conducted and DOA can be estimated, while in the case of outdoor environments this measurement cannot estimate DOA because base stations cannot be connected to the DOA estimation system using cables.

A method was developed in which measurement of receiving power can be achieved by scanning the main beam or null with an analog phase shifter as shown in Fig. 1-9 to reduce the cost of DOA estimation systems [130][131]. However, the accuracy during DOA estimation is

not better than the MUSIC method using a planar array. Thus, a DOA estimation system has been proposed in which data measured by several radiation patterns of the array antenna using analog phase shifters are applied to beamspace algorithms, such as beamspace MUSIC. Moreover, a DOA estimation system was developed that uses an electronically steerable parasitic array radiator (ESPER) antenna, which can change the radiation pattern by parasitic elements [135]–[138]. However, as the measurement times using each beam are different in these methods, synchronization between transmitters and DOA estimation systems is needed, and thus these systems cannot be used to estimate DOA in outdoor environments.

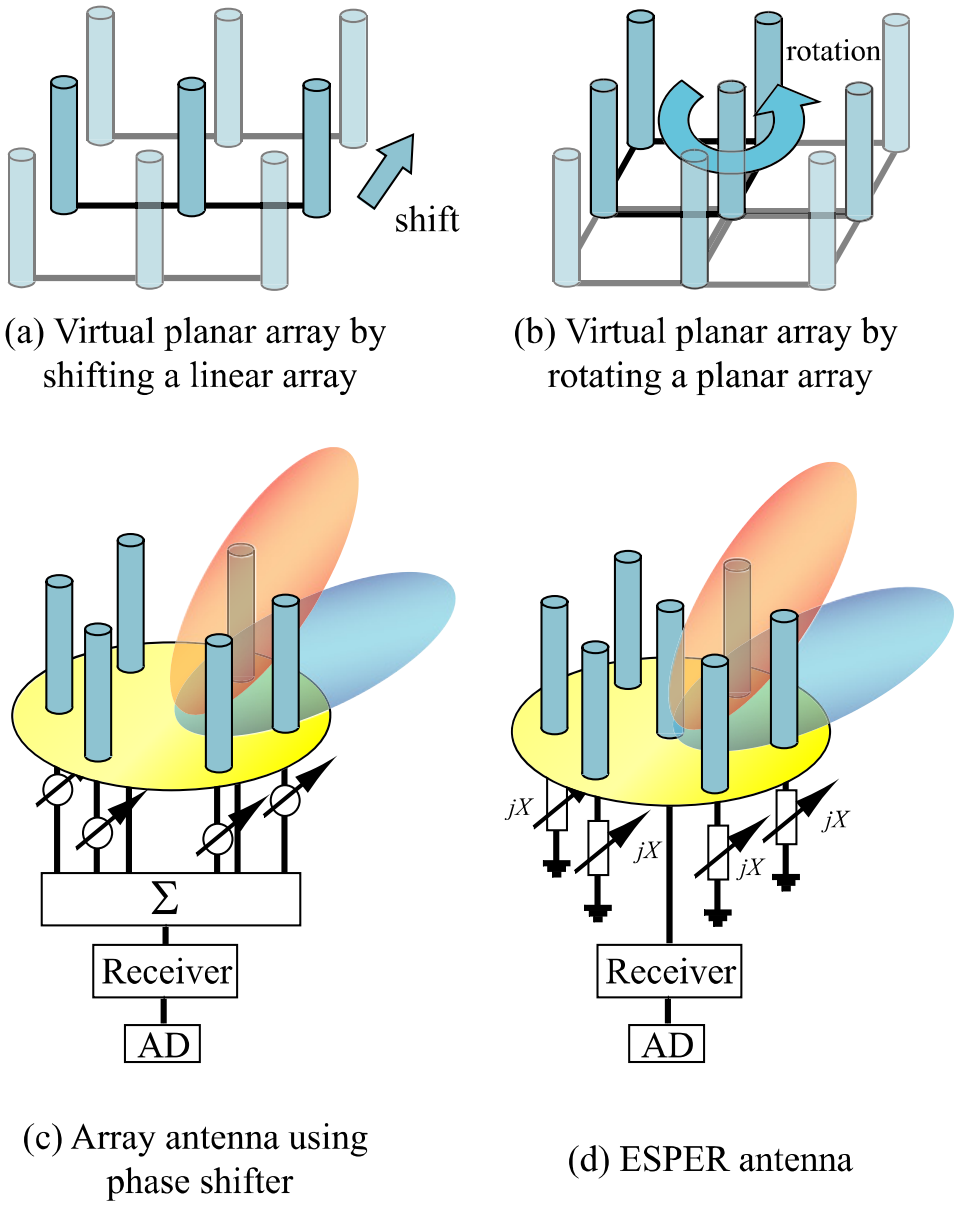

(a) Virtual planar array by shifting a linear array

(b) Virtual planar array by rotating a planar array

(c) Array antenna using phase shifter

(d) ESPER antenna

Fig. 1-9 DOA estimation method for reducing the system cost

1.4 Proposed system for DOA estimation

1.4.1 Virtual planar array antenna with a T-shaped array antenna

As described above, a method using an array antenna with a super-resolution method, such as MUSIC, is desired for DOA estimation system. However, the large number of elements required for F/B spatial smoothing procedures results in a high system cost. Although there are systems that use shifting of the array antenna or several antenna patterns to reduce system cost, methods for compensation of phase differences between data have not been examined in sufficient detail to allow these systems to be applied in outdoor environments.

This dissertation presents a DOA estimation system that correctly estimates DOA, while reducing the system cost. In this system, DOA can be estimated using data obtained from the virtual planar array antenna synthesized by shifting in parallel and measuring with a T-shaped array antenna, in which a linear array is added to an element used to correct phase differences.

Fig. 1-10 shows an outline of the propsed method with the T-shaped array antenna for synthesizing data received by the virtual plane array. First, arrival waves are measured with T-shaped array antenna at certain position, then, it is shifted in parallel. In this case, the T-shaped array is shifted so that the central element of the original position and the outstanding element after movement may overlap as shown in Fig. 1-10. The overlapping data of two elements is compared and the data of the next line is synthesized. Repeating this operation, the data received by virtual planar arrays is obtained, DOA can be estimated with its data.

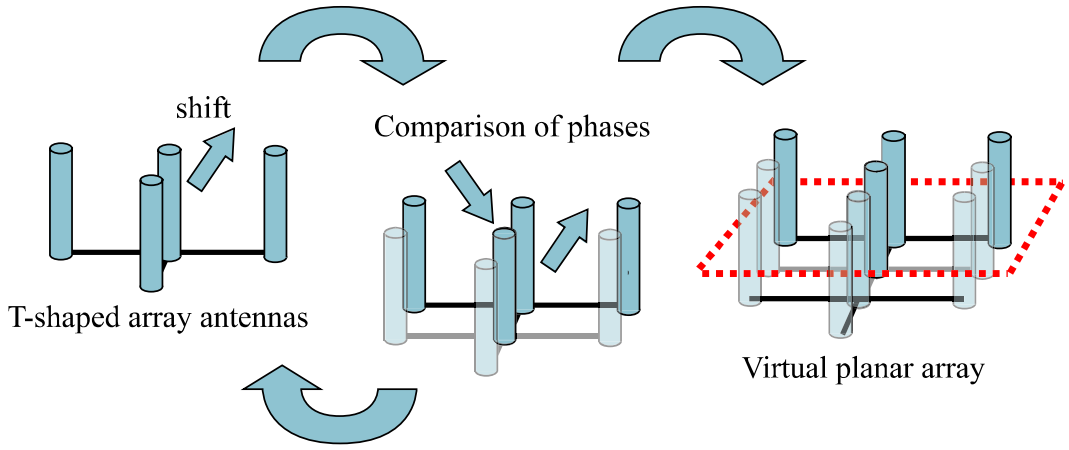

Fig. 1-10 The proposed method

This method can reduce the number of antenna elements required, and thus has the following advantages:

- Reduced system cost
- Can be applied to super-resolution methods, such as MUSIC, with an array antenna

Another advantage may be reduction of the influence of mutual coupling between antenna elements.

The number of shifting operations is determined by the number of elements in the virtual planar array required for the DOA estimations and the T-shaped array antenna. For example, when an $N \times N$ planar array is used for DOA estimation, the number of shifting operations is $N - 1$ times those of an $N + 1$ T-shaped array antenna. In fact, the proposed method can replace the $N \times N$ planar array with an $N + 1$ T-shaped array. Although the proposed system requires a unit for array shifting, if the cost of the unit is the same as that of a receiver and an analog-digital converter, the cost of the proposed system is reduced when the number of shifts required becomes greater than or equal to three. The cost of the unit for the shifting of the array antenna for the experiments described here was practically less than 1/100 as compared with that of the receiver and the ADC. Therefore, the proposed method is effective in reducing the system cost. In urban areas, it is easier for individuals to measure the DOA while walking as the estimation system is small and lightweight. Moreover, it is possible to apply the proposed method to DOA estimation systems with phase shifters or ESPER antennas that install elements for corrections of difference phases due to differences in measurement times. Thus, the systems with phase shifters or ESPER antennas may be able to estimate DOA when it is impossible to synchronize between transmitters and receivers.

1.4.2 Methods of synthesizing data received by virtual planar array antenna

In this proposed system, it is important to compare data of overlapping elements. Three methods synthesizing virtual planar array are proposed in this dissertation. The first method is to synthesize data of the virtual planar array by comparing data of overlapping elements of the T-shaped array antenna and correcting the different phases between linear arrays, assuming that arrival waves are sinusoidal waves of the same frequency only. This method is based on the proposed system.

The second method uses the pilot signal in CDMA systems to correct the different phases between linear arrays. When the arrival waves are modulated by random signals, the method using the virtual planar array cannot estimate the DOA. The shift in phase cannot be determined

as the phases of the received waves change randomly. Thus, it is impossible to calibrate the phase differences between linear arrays because the measurements at each position are performed at different times. That is, the method in which it is assumed that arrival waves are sinusoidal waves cannot estimate DOA in urban areas. However, on the assumption that the arrival waves are only emitted by the transmitters of CDMA systems, such as IS-95 and CDMA2000, pilot signals for the compensation of fading and the synchronization of spreading codes are always included in the arrival waves and in identical repeated signals, as described in Sec. 1.2.2. Therefore, the pilot signals can only be obtained by despreading the received signals. Moreover, it is possible to calculate the phase differences at each position by despreading these signals. Using these characteristics, the data of the virtual planar array are synthesized, and DOA can be estimated in urban areas.

The last method involves synthesizing data received by the virtual planar array using eigenvectors of correlation matrices. The method with pilot signals of CDMA systems cannot estimate DOA when arrival waves do not include pilot signals. Although it is important for area designs in urban areas to discover illegal repeaters that transmit interference waves, the method using pilot signals cannot distinguish the illegal repeaters, because the waves from these illegal repeaters are sinusoidal due to oscillation or wide band noise without pilot signals. To resolve this problem, a method using eigenvectors of correlation matrices calculated from data received by the T-shaped array antenna was proposed to estimate arrival waves that are random signals. This method makes use of the characteristic that eigenvectors of correlation matrices have phase information of mode vectors corresponding to the angles of arrival waves.

In this study, the MUSIC method was used as the DOA estimation algorithm, although the three methods can be applied to most DOA estimation algorithms using array antennas. As MUSIC has a high degree of accuracy, super-resolution, and is generally more efficient than ESPRIT when using a planar array. Although DOA can be estimated correctly with super-resolution algorithms when there are no mutual couplings between antenna elements, the effects of mutual coupling and errors reduce the accuracy of estimations in real systems. If DOA estimation error is within 3°, the DOA estimation system can distinguish the transmitters located 500 meters from the system in the range of radius of 25 meters; thus, the DOA system can find the transmitters effectively [76]. Therefore, the target of accuracy of DOA estimation is within 3°.

1.5 Outline of Dissertation

This dissertation is organized as shown in Fig. 1-11. In Chapter 2, the basic characteristics of

the proposed method are described. In Chapters 3 and 4, the development of the proposed method is described, along with its application to DOA estimation when arrival waves are waves in a CDMA system or random signals, such as noise.

Chapter 2 presents the base characteristics of the virtual planar array by shifting the T-shaped array antenna in DOA estimations, when it is assumed that arrival waves are sinusoidal. In the proposed method, the estimation accuracy is thought to be influenced by the synthetic accuracy of the data received by the virtual planar array antenna to use data with different measurement times. In addition, there is a possibility of position errors due to parallel shifting of the T-shaped array antenna. Therefore, these influences on estimation errors were evaluated by carrying out simulations and experiments in an anechoic chamber, and the effective and limited characteristics of the proposed method were confirmed.

Chapter 3 describes the synthesizing method using pilot signals in the CDMA system. This method can be used to estimate the arrival waves transmitted by CDMA systems, such as IS-95 and CDMA2000. The simulation results confirmed that the accuracy of the estimation based on the virtual planar array was the same as that based on the real planar array. Then, the effectiveness of the proposed system was demonstrated by experiments in the anechoic chamber and an outdoor environment.

Chapter 4 described the method of DOA estimation with a synthesized virtual planar array using eigenvectors of correlation matrices calculated from data received by a T-shaped array. This method can be used to estimate DOA when arrival waves are coherent waves, which are random signals. The performance of the proposed method was demonstrated through simulations and experiments in an anechoic chamber, and the results confirmed the effectiveness of this method. Chapter 6 presents the conclusions.

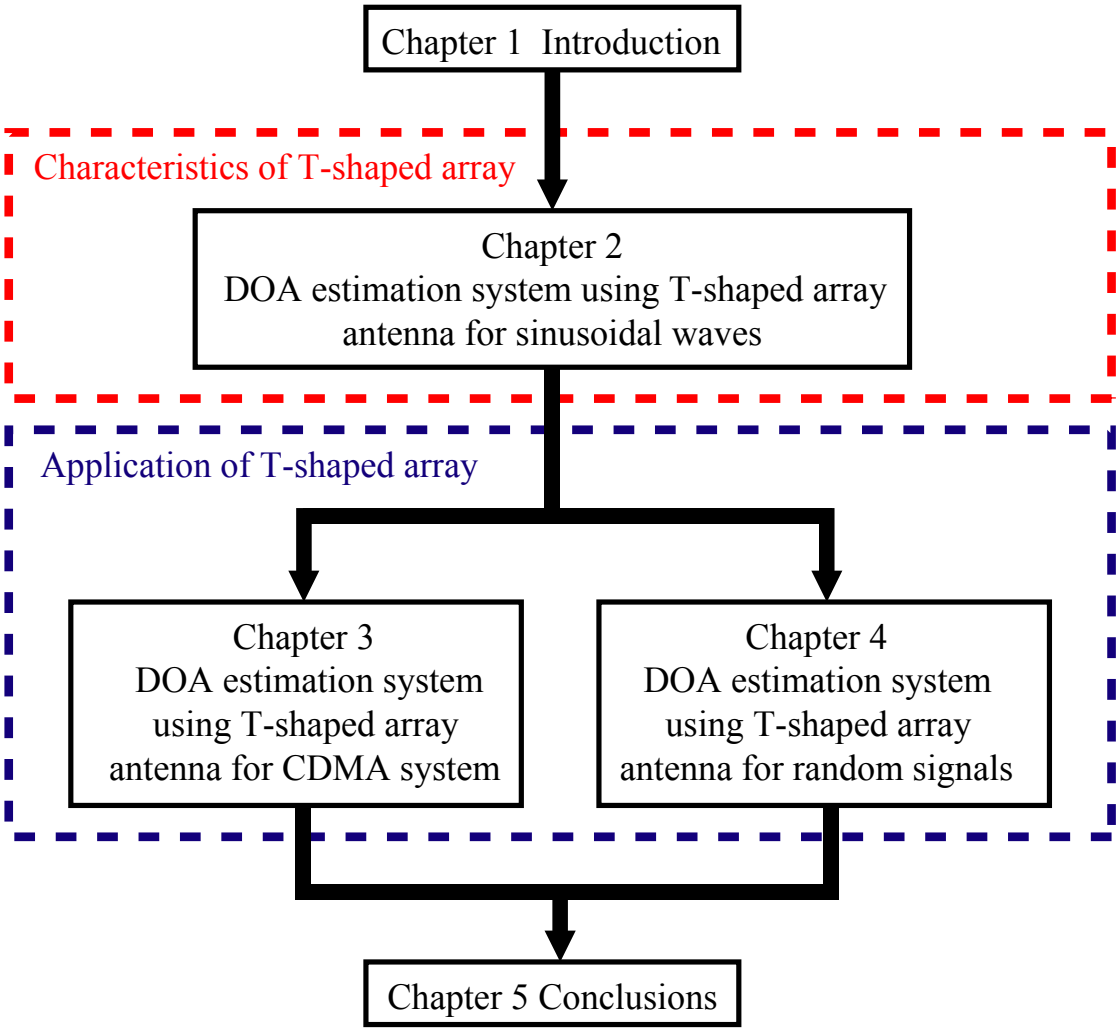

Fig. 1-11 Structure of dissertation

Chapter 2 Basic evaluation of DOA estimation system using T-shaped array antenna

2.1 Introduction

This chapter introduces the DOA estimation system with the virtual planar array antenna synthesized by the T-shaped array antenna. In the proposed method, arrival waves are received with shifting of the T-shaped array antenna. Data received by the virtual planar array antenna are synthesized correcting the different phases between linear arrays by comparison of overlapping elements, and the DOA are estimated using these data. In this chapter, it is assumed that arrival waves are sinusoidal waves only for basic evaluation of the proposed method, and the performance of the proposed method during DOA estimation is evaluated based on simulations and experiments in an anechoic chamber.

The method described here may not estimate DOA when radio waves representing different random data from several sources arrive and phases of the data received by the compared elements cannot be measured due to degradation of the signal to noise (SN) ratio by multipath fading. However, this method performs DOA estimation when arrival waves are sinusoidal or are phase-modulated by the same signals and it is possible to measure signal components in the two compared elements. Therefore, with the establishment of frame synchronization, this method can be applied to systems in which reference signals from several transmitters, which are the same waves phase-modulated in preamble or training, are received.

2.2 Method of synthesizing data of a virtual planar array antenna using T-shaped array antenna

This section describes the method used for synthesizing data received by a virtual planar array antenna. First, the DOA estimation method using a conventional planar array is explained, and

then the method for synthesizing data realized by moving the T-shaped array antenna is presented.

2.2.1 DOA estimation method using a planar array antenna

Antenna elements are arranged in an $M \times N$ planar array at regular intervals of Δx on the x-axis and Δy on the y-axis, as shown in Fig. 2-1. The arrival waves are incident on the array at an angle of θ_l, as shown in Fig. 2-2. In this case, the DOA can be estimated by applying MUSIC or ESPRIT. However, the receiver cost would increase as several elements are required to estimate the coherent waves. These problems will be resolved and accurate estimations will be possible if the data received by the planar array are realized with an array antenna, in which the number of antenna elements is small.

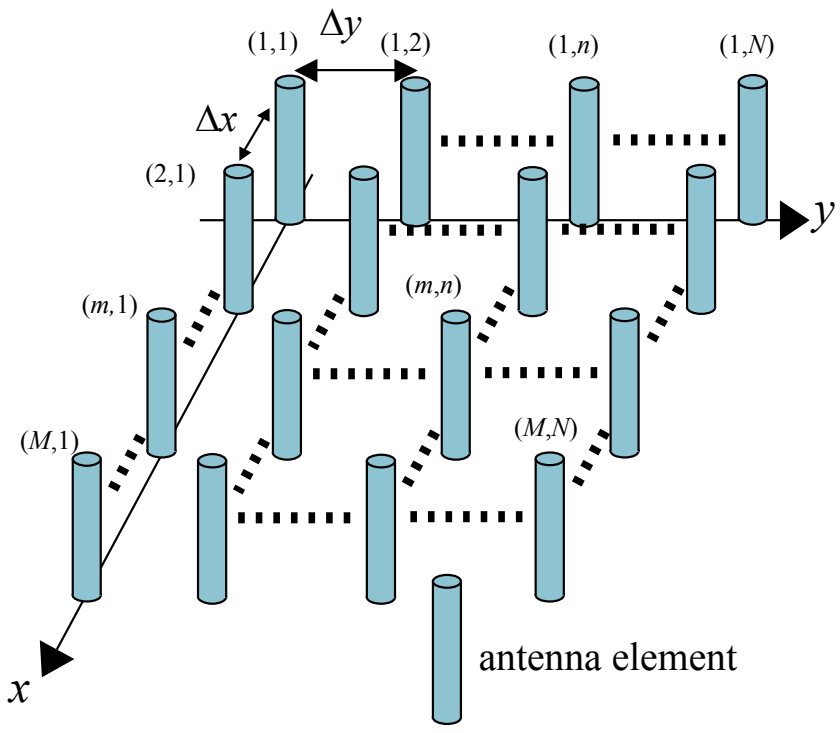

Fig. 2-1 Planar array antenna

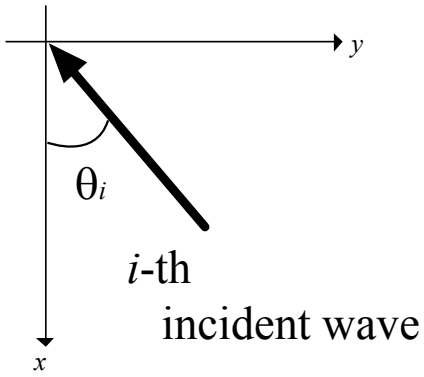

Fig. 2-2 DOA of incident wave

2.2.2 Method of synthesizing data received by a virtual planar array antenna

This subsection describes the method of synthesizing data received by a virtual planar array antenna to reduce system costs. This method uses base band signals, which are complex data received by the T-shaped array antennas and down-converted, when arrival waves are sinusoidal waves. These received data have periodic characteristics, as shown in Fig. 2-3, and it is possible to synthesize virtual data received by the planar array antenna using these characteristics. Synthesizing data received by a virtual planar array antenna implies that a real array antenna is used to receive the arrival waves, and the received data are used for realization the same as data received by the conventional planar array antenna.

Fig. 2-4 shows one method with an N linear array antenna for synthesizing data received by the virtual plane array. The arrival waves are measured by the linear array at a certain position when carrier synchronization between transmitters and the receiver is established. Then, arrival waves are measured by the linear array after shifting parallel only at element intervals. This operation is repeated M times, and measured data are synthesized, such as for the $M \times N$ planar array antenna. DOA can be estimated by applying these data to 2D discrete Fourier transform or the MUSIC method. When carrier synchronization between transmitters and receivers is not established, a received signal is measured at actual points because there is not a reference for the start of sampling although it must be sampled at ideal points for DOA estimation as shown in Fig. 2-3. Thus, DOA cannot usually be estimated by this system because it is not able to consider differences in timing at the start of sampling at each linear array in the case of data received over along period, although the time for obtaining all data is short enough to ignore differences in timing at each linear array.

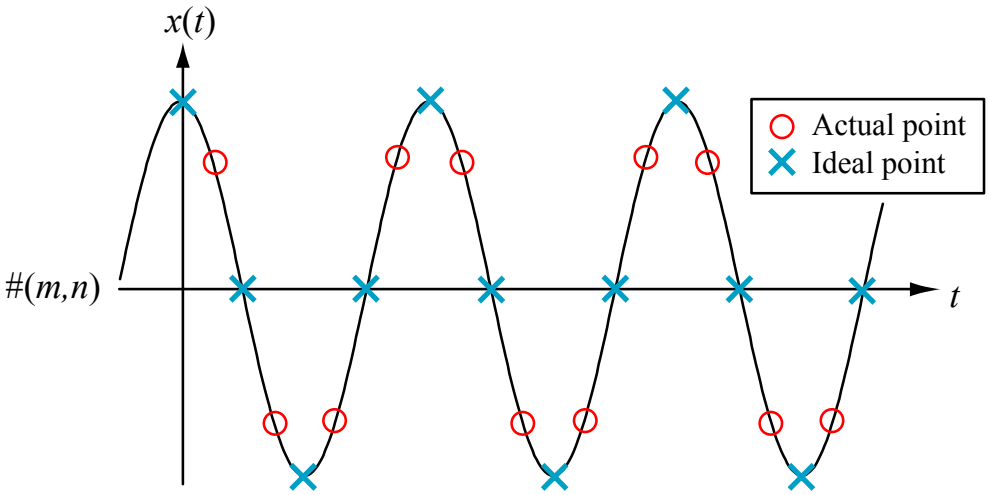

Fig. 2-3 Received signal

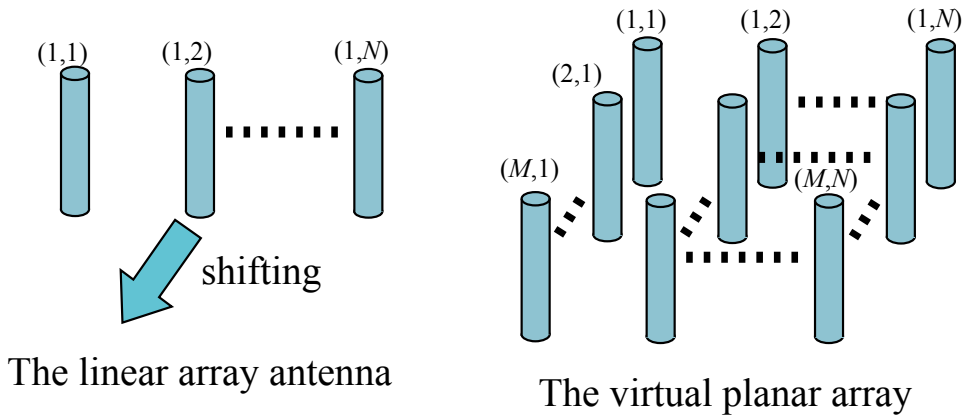

Fig. 2-4 The virtual planar array by the linear array antenna

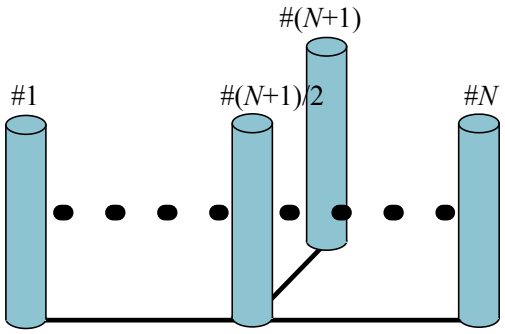

Fig. 2-5 The T-shaped array antenna

Thus, this dissertation proposes a method for synthesizing data received by the virtual planar array realized by shifting the (N + 1) T-shaped arrays as shown in Fig. 2-5. When N is even, the (N + 1)-th element is located at a position such that the (N + 1)/2-th element and the (N + 1)-th element after movement may overlap, as shown in Fig. 2-6.

$\mathbf{X}_1$ denotes data received by the T-shaped array antenna at a certain position, K is the number of samplings, and T is the sampling interval. $\mathbf{X}_1$ is given by:

$$\mathbf{X}_1 = \left[x_{11}, x_{12}, \cdots, x_{1,(N+1)} \right]$$

$$\mathbf{x}_{1n} = \left[x_{1n}(T), x_{1n}(2T), \cdots, x_{1n}(KT) \right]^T$$

where $\mathbf{x}_{1n}$ ($n = 1, \cdots, N+1$) is the measurement data of the n-th element and $x_{1n}(kT)$ ($k = 1, \cdots, K$) is the k-th data sampled at the n-th element. Then, the T-shaped array antenna is shifted parallel for a distance equal to the interval between elements (see Fig. 2-6), and $\mathbf{X}_2$ is the data received at the location, and is given by:

$$\mathbf{X}_2 = \left[x_{21}, x_{22}, \cdots, x_{2,(N+1)} \right]$$

$$\mathbf{x}_{2n} = \left[x_{2n}(T), x_{2n}(2T), \cdots, x_{2n}(KT) \right]^T$$

The measurement signals, which are $\mathbf{x}_{1,(N+1)/2}$ and $\mathbf{x}_{2,N+1}$, are approximately the same data-sequence because the positions of these data are the same and different phases between arrival waves are not changed. In this case, $\mathbf{x}_{2,N+1}$ have a different phase from $\mathbf{x}_{1,(N+1)/2}$ due to the difference in measurement times because of the time taken for the parallel shift of the T-shaped array (See Fig. 2-6). However, $\mathbf{X}_1$ and $\mathbf{X}_2$ are synthesized such that the difference in phase is corrected, synthesizing data received by a 2 × N virtual planar array antenna.

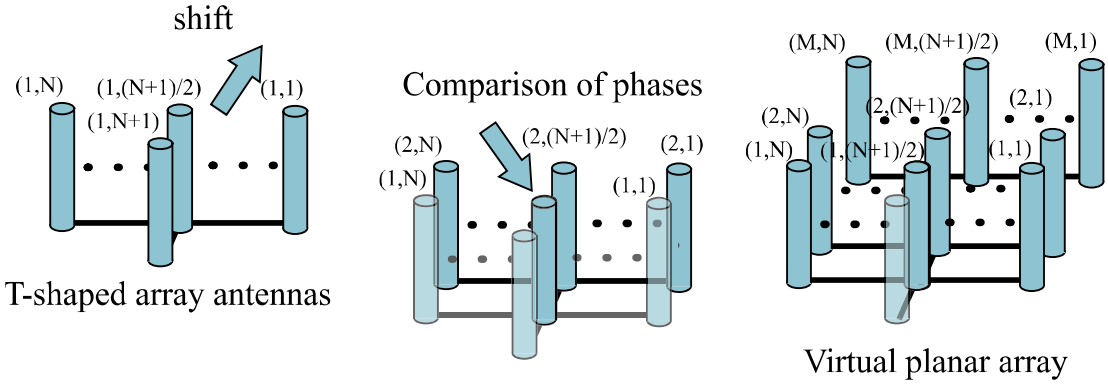

Fig. 2-6 The virtual planar array by the T-shaped array antenna

There are two methods for calibrating the different phases. First, the method in which cross-correlation values calculated with the two data-sequences are used for synthesizing data is described. The cross-correlation value of the two data-sequences, $\mathbf{x}_{1,(N+1)/2}$ and $\mathbf{x}_{2,N+1}$, is given by:

$$C(p)=\sum_{i=1}^{L} x_{1,(N+1)/2}((\hat{p}_{01}+i-1)T)\cdot x^{*}_{2,N+1}((p+i-1)T) \quad \textbf{(1)}$$

where $[\cdot]^{*}$ denotes a complex conjugate, $L\left(L\le K\right)$ is the number of data, and $\hat{p}_{01}$ is the number of the first line of $\mathbf{X}_1$ used for DOA estimation (usually 1). It is assumed that received data have periodicity in this method, and thus it is necessary that the number of data *K* is greater than two cycles of the sampled signal and the number of data for computing the cross-correlation value *p* is greater than one cycle of sampled signal. $\hat{p}_{12}$ is *p* that gives the maximum $C(p)$, the number of snapshot is $Y\left(Y\le K\right)$. $\dot{\mathbf{X}}_1$ and $\dot{\mathbf{X}}_2$ used for DOA estimation are extracted from $\mathbf{X}_1$ and $\mathbf{X}_2$ as follows:

$$\dot{\mathbf{X}}_1=\left[\hat{\mathbf{x}}_{11},\hat{\mathbf{x}}_{12},\cdots,\hat{\mathbf{x}}_{1N}\right]$$
$$=\begin{bmatrix} x_{11}\left(\hat{p}_{01}T\right) & x_{12}\left(\hat{p}_{01}T\right) & \cdots & x_{1N}\left(\hat{p}_{01}T\right) \\ x_{11}\left(\left(\hat{p}_{01}+1\right)T\right) & x_{12}\left(\left(\hat{p}_{01}+1\right)T\right) & \cdots & x_{1N}\left(\left(\hat{p}_{01}+1\right)T\right) \\ \vdots & \vdots & \ddots & \vdots \\ x_{11}\left(\left(\hat{p}_{01}+Y-1\right)T\right) & x_{12}\left(\left(\hat{p}_{01}+Y-1\right)T\right) & \cdots & x_{1N}\left(\left(\hat{p}_{01}+Y-1\right)T\right) \end{bmatrix}\in\mathbf{R}^{Y\times N}$$

$$\dot{\mathbf{X}}_2=\left[\hat{\mathbf{x}}_{21},\hat{\mathbf{x}}_{22},\cdots,\hat{\mathbf{x}}_{2N}\right]$$
$$=\begin{bmatrix} x_{21}\left(\hat{p}_{12}T\right) & x_{22}\left(\hat{p}_{12}T\right) & \cdots & x_{2N}\left(\hat{p}_{12}T\right) \\ x_{21}\left(\left(\hat{p}_{12}+1\right)T\right) & x_{22}\left(\left(\hat{p}_{12}+1\right)T\right) & \cdots & x_{2N}\left(\left(\hat{p}_{12}+1\right)T\right) \\ \vdots & \vdots & \ddots & \vdots \\ x_{21}\left(\left(\hat{p}_{12}+Y-1\right)T\right) & x_{22}\left(\left(\hat{p}_{12}+Y-1\right)T\right) & \cdots & x_{2N}\left(\left(\hat{p}_{12}+Y-1\right)T\right) \end{bmatrix}\in\mathbf{R}^{Y\times N}$$

where $\mathbf{R}^{Y\times N}$ denotes a set of $Y \times N$ real number matrices. By repeating the above procedure, $\hat{p}_{(m-1),m}$ is calculated for each data sampled at overlapping elements, and data received by the virtual planar array antenna are synthesized as follows:

$$\mathbf{X}_{M1} = \left[\dot{\mathbf{X}}_1, \dot{\mathbf{X}}_2, \cdots, \dot{\mathbf{X}}_M\right] \in \mathbf{R}^{Y\times MN}$$
$$= \left[\hat{\mathbf{x}}_{11}, \cdots, \hat{\mathbf{x}}_{1N}, \hat{\mathbf{x}}_{21}, \cdots, \hat{\mathbf{x}}_{2N}, \cdots, \hat{\mathbf{x}}_{M1}, \cdots, \hat{\mathbf{x}}_{MN}\right]$$
$$\dot{\mathbf{X}}_m = \begin{bmatrix} x_{m1}\left(\hat{p}_{(m-1),m}T\right) & x_{m2}\left(\hat{p}_{(m-1),m}T\right) & \cdots & x_{mN}\left(\hat{p}_{(m-1),m}T\right) \\ x_{m1}\left(\left(\hat{p}_{(m-1),m}+1\right)T\right) & x_{m2}\left(\left(\hat{p}_{(m-1),m}+1\right)T\right) & \cdots & x_{mN}\left(\left(\hat{p}_{(m-1),m}+1\right)T\right) \\ \vdots & \vdots & \ddots & \vdots \\ x_{m1}\left(\left(\hat{p}_{(m-1),m}+Y-1\right)T\right) & x_{m2}\left(\left(\hat{p}_{(m-1),m}+Y-1\right)T\right) & \cdots & x_{mN}\left(\left(\hat{p}_{(m-1),m}+Y-1\right)T\right) \end{bmatrix}$$

where $\mathbf{R}^{Y\times MN}$ denotes a set of $Y \times MN$ real number matrices. This method is defined as the method using the cross-correlation value.

Next, the other method for synthesizing data is explained. The received signals are sinusoidal waves with the same frequencies, and thus data-sequences $\mathbf{x}_{1,(N+1)/2}$ and $\mathbf{x}_{2,N+1}$ are sinusoidal waves with a certain constant phase difference. To reduce the influence of thermal noise, this method calculates the average phase difference between $\mathbf{x}_{1,(N+1)/2}$ and $\mathbf{x}_{2,N+1}$, which is given by:

$$-\phi'_{12} = \arg\left(\frac{1}{K}\sum_{k=1}^{K}\frac{x_{2(N+1)}}{x_{1,(N+1)/2}}\right)$$

Using ϕ'_{12} to calibrate the phase difference due to the differences in measurement time, the data without the phase difference are given by:

$$\mathbf{X}'_2 = \mathbf{X}''_2 \times e^{j\phi'_{12}}$$
$$= \left[\mathbf{x}_{21}e^{j\phi'_{12}}, \mathbf{x}_{22}e^{j\phi'_{12}}, \cdots, \mathbf{x}_{2,N}e^{j\phi'_{12}}\right]$$
$$\mathbf{X}''_2 = \left[\mathbf{x}_{21}, \mathbf{x}_{22}, \cdots, \mathbf{x}_{2,N}\right]$$

By repeating the above procedures, the data without phase differences due to differences in measurement time can be obtained as follows:

$$\mathbf{X}'_{m'} = \mathbf{X}''_{m'} \cdot e^{j\phi_{m'-1,m'}}$$
$$= \left[\mathbf{x}_{m'1}e^{j\phi_{m'-1,m'}}, \mathbf{x}_{m'2}e^{j\phi_{m'-1,m'}}, \cdots, \mathbf{x}_{m',N}e^{j\phi_{m'-1,m'}}\right]$$
$$\mathbf{X}''_{m'} = \left[\mathbf{x}_{m'1}, \mathbf{x}_{m'2}, \cdots, \mathbf{x}_{m',N}\right] \quad \left(m' = 1, \cdots, M\right)$$

$$\begin{cases} \phi_{m'-1,m'} = 0 & (m' = 1) \\ \phi_{m'-1,m'} = \sum_{m''=1}^{m'} \phi'_{m''-1,m''} & (m' \geq 2) \end{cases} \quad \textbf{(2)}$$

$$-\phi'_{m''-1,m''} = \arg\left(\frac{1}{K} \sum_{k=1}^{K} \frac{x_{(m''),(N+1)}}{x_{(m''-1),(N+1)/2}} \right) \quad (m'' \geq 2)$$

The synthesizing data received by the virtual planar array are given by:

$$\mathbf{X}_{M2} = \left[\mathbf{X}'_1, \mathbf{X}'_2, \cdots, \mathbf{X}'_M \right]$$

This method is defined as the method calculating phase differences.

When each row of $\mathbf{X}_{M1}$ and $\mathbf{X}_{M2}$ are used as input vectors, DOA can be estimated by MUSIC or ESPRIT. Fig. 2-7 shows a flowchart of the proposed method. The proposed method assumes that positions of elements are the same by shifting parallel, and thus it is necessary to measure position information of the T-shaped array antenna correctly. A concrete method for these problems is described in Sec. 2.4. The proposed method is applicable to a linear array with a fixed element instead of a T-shaped array, as illustrated in Fig. 2-8.

The number of shifting operations is determined by the number of elements in the virtual planar array required for DOA estimations and the T-shaped array antenna. For example, when an $N \times N$ planar array is used for DOA estimation, the number of shifting operations is $N - 1$ times that of an $N + 1$ T-shaped array antenna. In fact, the proposed method can replace the $N \times N$ planar array with the $N + 1$ T-shaped array.

Although the proposed system requires a unit for array shifting, if the cost of the unit is the same as that of a receiver and an analog-digital converter (ADC), the cost of the proposed system is reduced when the number of shifts required becomes greater than or equal to three. The cost of the unit for the shifting of the array antenna for the experiments described here was practically less than 1/100 as compared with that of the receiver and the ADC. Therefore, the proposed method is effective in reducing the system cost. In urban areas, it is easier for individuals to measure the DOA while walking as the estimation system is small and lightweight.

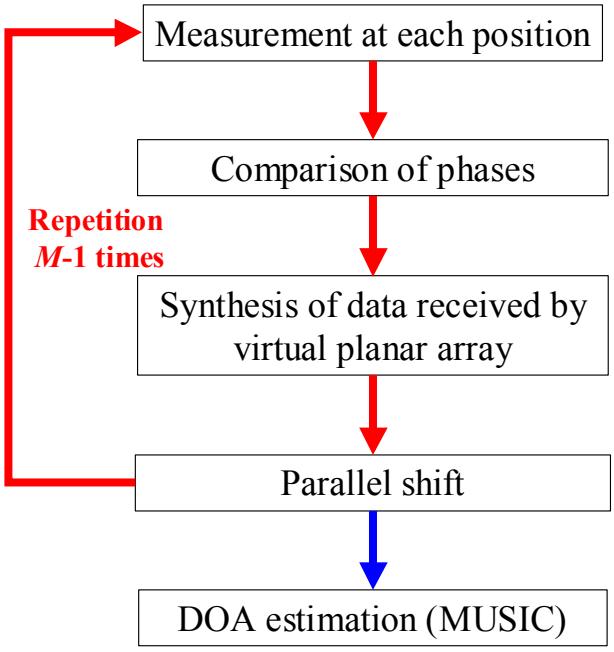

Fig. 2-7 Flowchart of the proposed method

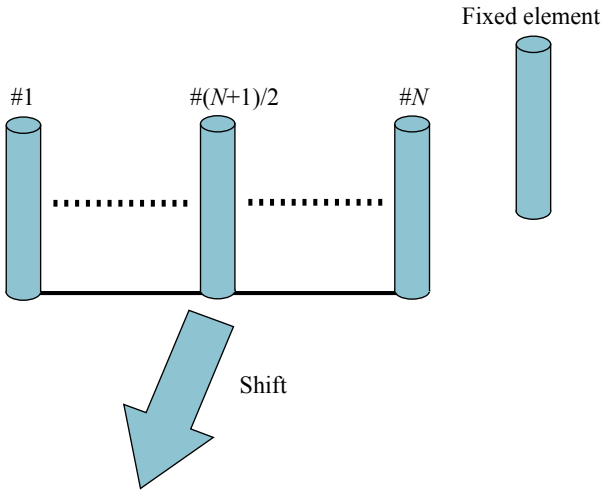

Fig. 2-8 Synthesis of virtual planar array with T-shaped array antenna

2.3 Characteristic evaluation by computer simulation

This section presents the results of the simulations performed to evaluate the effectiveness of the virtual planar arrays. First, the results of the method using Eq. (1) and its problems are

introduced, and a solution for the problems is presented. Next, the results of the method using Eq. (2) are shown, confirming the usefulness of the proposed method. In the proposed methods, the estimation accuracy is thought to be influenced by the synthetic accuracy of the data received by the virtual planar array antenna to use data with different measurement times. In addition, there is a possibility of position errors due to parallel shifting of the T-shaped array antenna. Therefore, the influences of SN ratio, frequency offset, frequency fluctuation, *etc,* on estimation errors were evaluated by carrying out simulations in each method.

2.3.1 Simulation of method using the cross-correlation

2.3.1.1 Comparison with linear array antenna

When virtual planar array antenna data are synthesized without carrier synchrony between transmitters and receivers, the method using a linear array antenna cannot estimate DOA due to differences in the sampling points. On the other hand, the proposed method can synthesize data of virtual planar array antenna with good accuracy. Therefore, a comparison with methods using the linear array and T-shaped array antennas was performed by simulations when MUSIC was used as the DOA estimation algorithm.

The number of elements in the linear array was 7, and the form of the virtual planar array was 7 × 4 with 3 parallel shifts. In a similar way, a 7 × 4 virtual planar array antenna was synthesized with 3 parallel shifts of a 7 + 1 T-shaped array antenna. When the interval between antenna elements is longer than a half wavelength, imaging peaks in angles without incident waves exist in the MUSIC spectrum because the mode vector of an angle is equal to the mode vectors of the other angles, and thus DOA cannot be estimated. Thus, for accurate DOA estimation, it is necessary for the intervals between antenna elements to be less than a half wavelength. However, the accuracy of DOA estimation decreases due to the influence of mutual couplings, when the interval between antenna elements is short. Thus, the interval between antenna elements was set as 0.4 wavelengths. Table 2-1 shows the simulation specifications. The frequency of received data was 1 MHz because the chip rate for spreading codes is 1 Mcps in systems providing services in actual use. The sampling number was 500, snapshot number was 300, and the data number used to calculate the cross-correlation value was 300. Sampling frequency was 40 MHz. It was assumed that carrier synchrony was not established between transmitters and receivers, and sampling frequency was 5 MHz. The number of arrival waves was 6. The amplitudes of arrival waves were equal, and MUSIC was used as the DOA estimation algorithm. The method for synthesizing data received by the virtual planar array was that using the cross-correlation value. The time from measurement at a certain position to the next measurement by parallel shifting of the T-shaped array was 1 second. In this simulation,

SNR was defined as follows:

$$\mathrm{SNR} = 10\log\frac{\text{Total Electric Power}}{\text{Noise Power}}$$

The simulation result in the case of synchrony error was 1×10^{-6} MHz as shown in Fig. 2-9. Fig. 2-9 shows that the system with a linear array cannot estimate DOA, while the proposed system could estimate DOA. This was because errors in sampling points can be corrected by using Eq. (1). The results of these simulations confirmed the effectiveness of the proposed system.

Table 2-1 Simulation Specifications

Array form	The T-shaped array antenna (7+1 elements) The linear array antenna
Number of elements of virtual planar array	7 × 4 elements (28 elements)
Number of element of subarray	3 × 3 elements (9 elements)
Interval between elements	0.4 wavelength
Number of arrival waves	6 (–140°, –40°, –10°, 70°, 100°, 160°)
SN ratio	10 dB
Sampling number	500 times
Number of data compared	300
Snapshot number	300 times

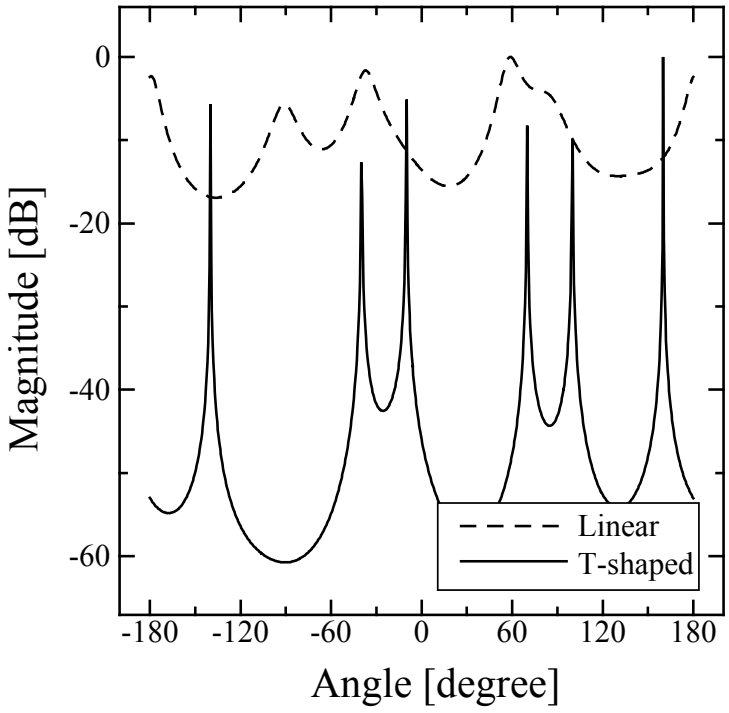

Fig. 2-9 Comparison of linear and T-shaped arrays

2.3.1.2 Comparison with real planar array antenna

The performance of the proposed system during DOA estimation was evaluated by comparison with the conventional method using a real planar array. The form of the real array is a 7 × 4 planar array antenna, and the subarray is a 3 × 3 planar array. Oversampling rate is 40 times, and the other specifications are the same as described in Sec. 2.3.1.1.

Fig. 2-10 shows the MUSIC spectra of the simulations. It was confirmed that the proposed method can estimate DOA with the same accuracy as the real planar array. However, the MUSIC spectrum of the virtual planar array showed degradation due to errors in sampling points without establishing carrier synchrony and the influence of thermal noise. On the other hand, the differences in estimation results regarding electrical power from the real planar array were about 3 %. Thus, the accuracy of the proposed method with regard to electrical power estimation was the same as that of the real planar array.

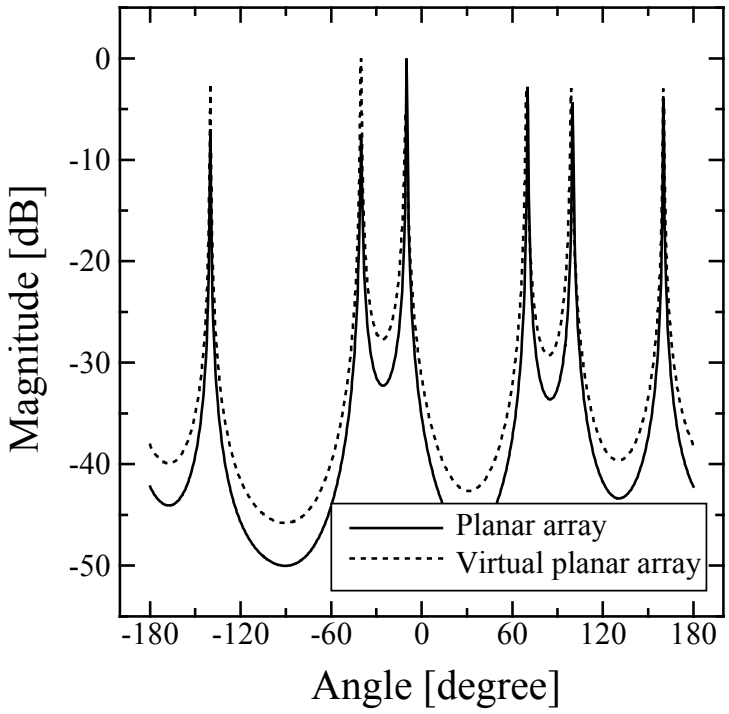

Fig. 2-10 MUSIC spectrum (SNR = 10 [dB])

2.3.1.3 Influence of SN ratio

The performance of the proposed system during DOA estimation was evaluated by changing the SN ratio. In this simulation, the SN ratio was varied, while the other specifications were the same as described in Sec. 2.3.1.1.

Fig. 2-11 shows the MUSIC spectrum of the proposed method with varying SNR. When the SR ratio was small, the dynamic range of the MUSIC spectrum and accuracy with regard to DOA estimation were degraded as errors in synthesizing data increased due to noise.

These results showed that the proposed method can estimate DOA with the same accuracy as the real planar array, although the proposed method is influenced by the SN ratio. The degradation regarding DOA estimation and dynamic range of the MUSIC spectrum can be improved by increasing the sampling rate and interpolating data. However, the computational cost then increases by N^2 times because the received data are increased by N times when the sampling rate is increased by N times.

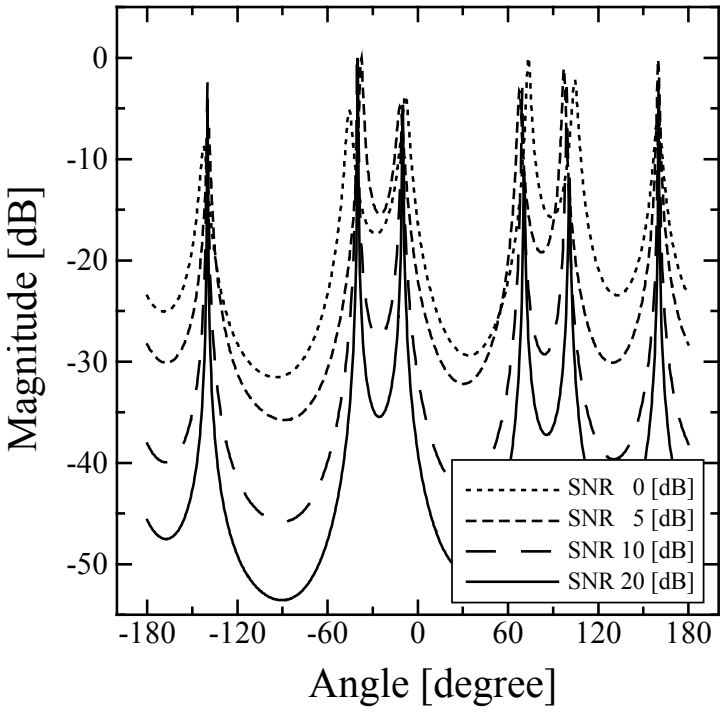

Fig. 2-11 MUSIC spectrum of virtual planar arrays

2.3.1.4 Influence of frequency offset

In the proposed method, the limit of correction of differences in synchrony, such as that shown in Fig. 2-3, may be determined by the sampling frequency. Therefore, the performance of the relationship between the differences in synchrony and sampling frequency can be evaluated by performing simulations. The differences in sampling points between linear arrays due to differences in synchrony and parallel shifts are provided by the initial phase at each row given by uniform random numbers. The number of trials was 1000. When estimation errors at each arrival wave were more than 15°, these results were ignored as unable to be used to estimate DOA. The other specifications of the simulations were the same as in Sec. 2.3.1.1. The estimation error Θ is defined as follows:

$$\Theta = \frac{1}{KL}\sum_{k=1}^{K}\sum_{l=1}^{L}\left|\theta_l - \hat{\theta}_l\right| \qquad \textbf{(3)}$$

where L is the number of arrival waves, K is the number of trials, θ_l is the direction of the *l*-th arrival wave, and $\hat{\theta}_l$ is the estimation result of the *l*-th arrival wave.

Fig. 2-12 shows the simulation results. DOA can be estimated within the estimation error of

1°, when oversampling rate is more than 40 times. The estimation error may be decreased by interpolating data, such as virtually increasing the sampling rate when the oversampling rate is low. Thus, simulations in which oversampling rate is lower than 100 times oversampling are virtually increased by spline interpolation, such as 100 times.

Fig. 2-13 shows the simulation results. When oversampling was lower than 40 times, the success rate and the estimation accuracies were improved by spline interpolation. However, the computation cost of Eq. (1) became A^2 times in the case that oversampling increased by A times.

These results can be summarized as follows. For accuracy estimation, it is necessary that oversampling is more than 40 times without spline interpolation, or 4 times with spline interpolation. For example, it is necessary for estimation accuracy that the frequency of sampled data be lower than 25 and 2.5 MHz with or without spline interpolation, respectively. The radio frequency evaluated here was the 900 MHz band, and thus it is possible that the difference in frequency between transmitters and receivers was within 2.5 MHz without establishing carrier synchrony.

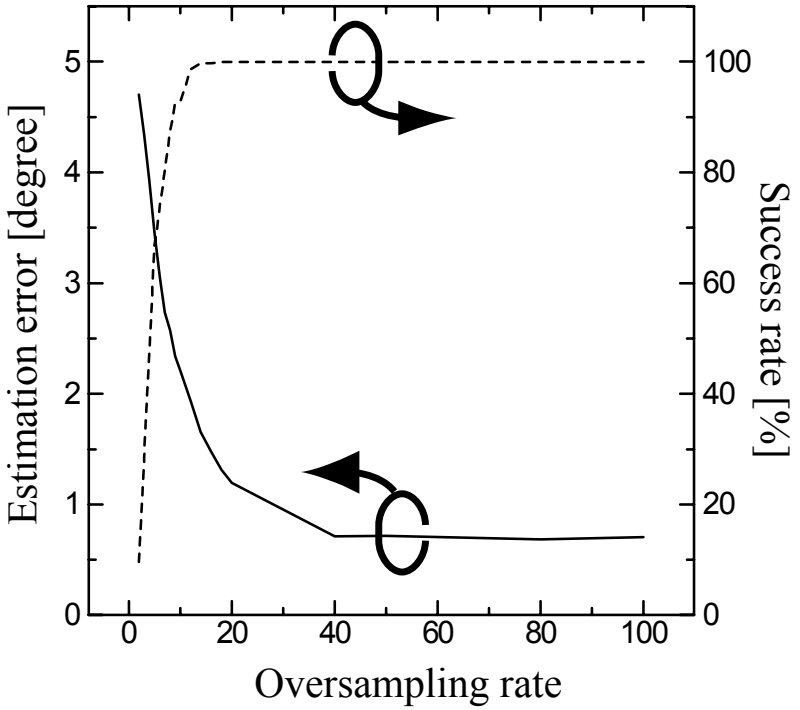

Fig. 2-12 Influence of step-out

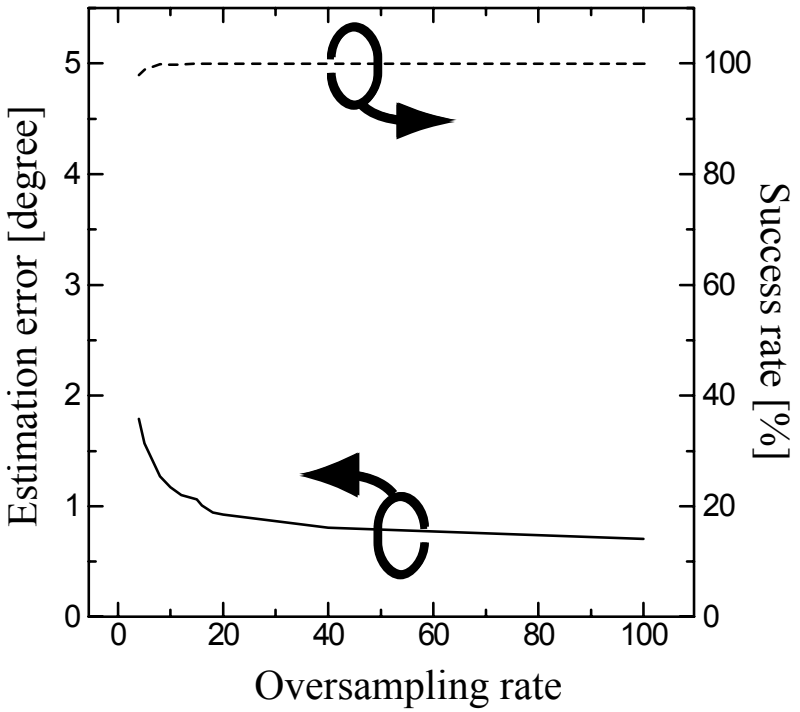

Fig. 2-13 Influence of step-out with spline interpolation

2.3.1.5 Influence of frequency fluctuation

The proposed system used data measured with shifting a T-shaped array. Thus, the times of measurements at each position were different, and the frequencies of the received data at each row were changed because oscillators in transmitters and the receiver varied at different times. The influence of these errors during DOA estimation can be evaluated by performing simulations. Frequency fluctuation is defined as follows:

$$\text{Frequency fluctuation} = \frac{\text{Maximum frequency} - \text{Minimum frequency}}{\text{Center frequency}} \qquad \textbf{(4)}$$

where the maximum frequency, minimum frequency, and the center frequency imply the highest, lowest, and center frequency in the data of the linear array, respectively. The oversampling rate was 40 times. The other simulation specifications were the same as in Sec. 2.3.1.1. Then, simulations with a large number of shifts were performed, because this case may be affected more strongly by the frequency fluctuation; the number of shifts was 99 times in this case. It was assumed that frequency fluctuations do not occur within the terms of measurements. The definition of the estimation error is given by Eq. (3).

Fig. 2-14 and Fig. 2-15 show the simulation results for cases with 3 and 99 shifts, respectively. As shown in Fig. 2-14, there was no influence of frequency fluctuations within about 1×10^{2}. On the other hand, DOA could be estimated within about 1×10^{2} in frequency fluctuation when the number of shifts increased. These results confirmed that DOA can be estimated with

accuracy with 40 times oversampling over the range of frequency fluctuation of about 1×10^{2}.

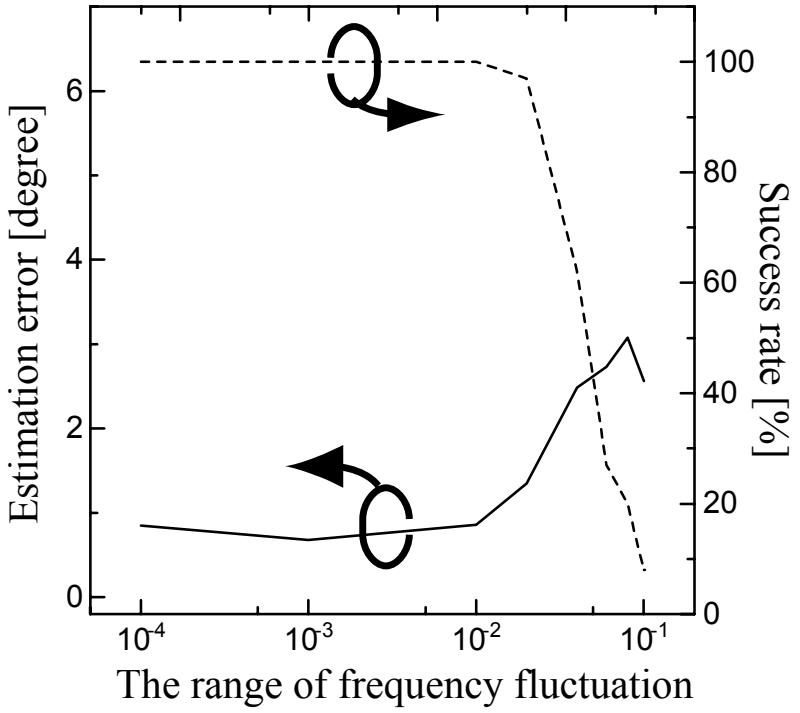

Fig. 2-14 Influence of frequency fluctuation (7×4 virtual planar array)

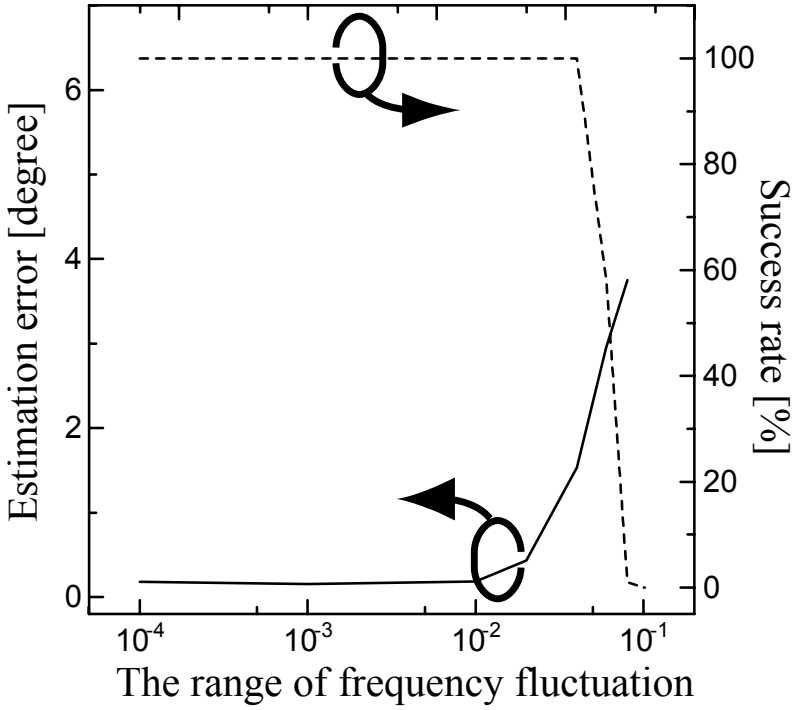

Fig. 2-15 Influence of frequency fluctuation (7×100 virtual planar array)

2.3.1.6 Influence of sequential measurements

Although the proposed method assumes that arrival waves are measured when the T-shaped array has stopped, this subsection considers arrival waves measured while the T-shaped array is moving. The speed of movement of the T-shaped array was 40 km/h (about 11.1 m/s), sampling frequency was 40 MHz, and the sampling number was 1000. In this case, the time for one measurement is given by:

$$\frac{1}{40\times10^{6}}\times1000 = 2.5\times10^{5} \ \text{[sec]}$$

The distance moved by the T-shaped array is given by:

$$1.11\times2.5\times10^{5} = 2.775\times10^{-1} \ \text{[mm]}$$

This length is 0.2% of the interval between elements. Simulations of these influences were performed. The frequency of measured data was 1 MHz. The other simulation specifications were the same as in Sec. 2.3.1.1. The information of positions was obtained with good accuracy.

Fig. 2-16 shows the simulation results, which confirmed that the proposed system can estimate DOA with accuracy. This result indicated that this system can estimate DOA when the system is installed in a car and arrival waves are measured while moving.

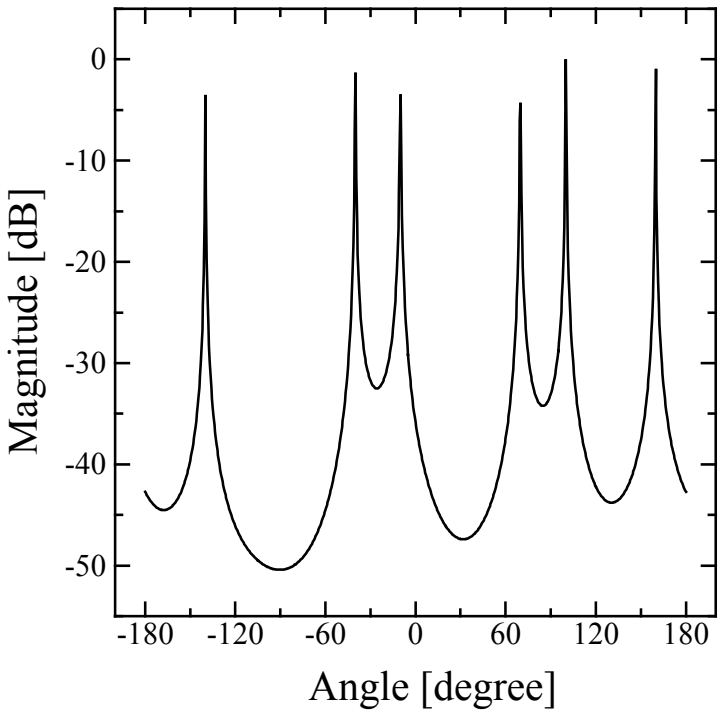

Fig. 2-16 MUSIC spectrum (Speed = 40 km/h)

2.3.2 Simulation of method by calculating difference phases

2.3.2.1 Relationship between number of snapshots and SN ratio

The proposed method calibrates the phase difference due to a parallel shift of the T-shaped antenna, and estimates DOA of arrival waves using the data. Thus, it is possible that the estimation errors increase when the SN ratio or the number of samplings is small. In the method involving calculation of phase differences, the characteristics of these influences are evaluated by performing simulations. Table 2-2 shows the simulation specifications. Averages of estimation errors were evaluated when the number of samplings and SN ratio were changed. The trial number was 500. The definition of the estimation error is given by Eq. (3).

Fig. 2-17 shows the MUSIC spectrum of the proposed method with varying SN ratio. DOA could not be estimated at the SN ratio of 0 dB as the information of phases at overlapping elements could not be obtained due to the noise. The success rates in case of SN ratio = 0 dB was about 30% for all snapshot numbers. Thus, the case where the SN ratio is 0 dB was not considered in the following simulation. Fig. 2-18 shows the results of the simulations. With small SN ratio, DOA could be estimated correctly. These results confirmed that the proposed system can estimate DOA with accuracy by increasing the number of samplings when the SN ratio is small.

Table 2-2 Simulation specifications (Method by calculating phase differences)

Array form	The T-shaped array antenna (7+1 elements)
Number of shifting operations	3
Number of elements of virtual planar array	7 × 4 elements (28 elements)
Number of element of sub array	3 × 3 elements (9 elements)
Interval between elements	0.4 wavelength
Number of arrival waves	6 (–140°, –40°, –10°, 70°, 100°, 160°)
Sampling number	2000 times

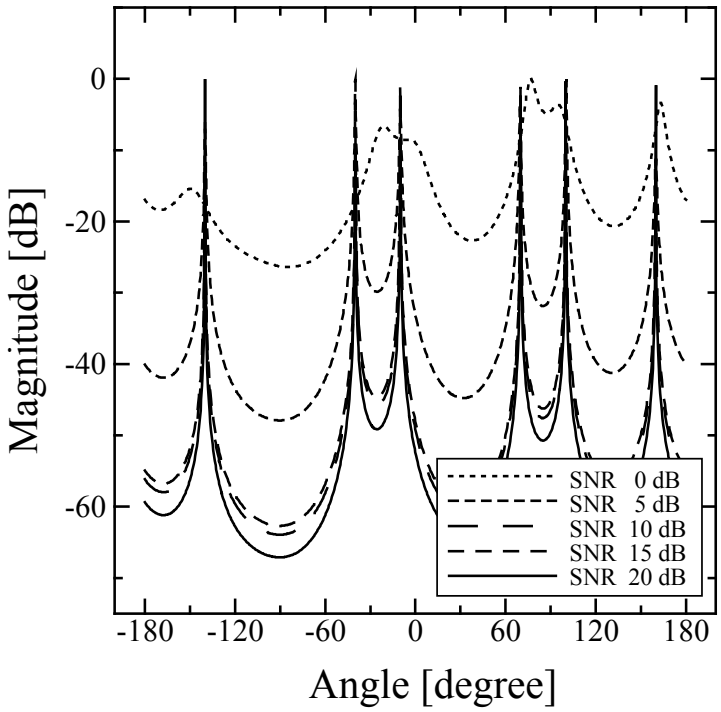

Fig. 2-17 MUSIC spectrum (Method of calculating phase)

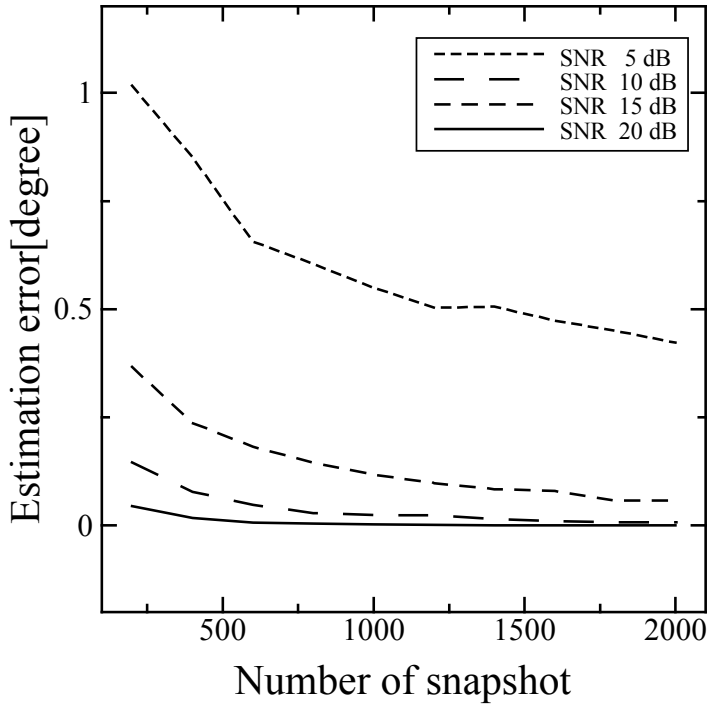

Fig. 2-18 Estimation errors (Changing number of snapshots)

2.3.2.2 Influence of position errors

The influence of position errors was evaluated by performing simulations of methods calculating difference phases. Position errors at each position were given by uniform random numbers. Simulations were conducted with varying the range of position errors. The other specifications of the simulation were the same as in Sec. 2.3.2.1. The definition of the estimation error is given by Eq. (3). Fig. 2-19 shows the results of the simulations. In the case where the range of errors was small, DOA could be estimated correctly. Ranges of errors were within 0.02 wavelengths for estimation errors that had accuracy greater than 1°. A distance of 0.02 wavelengths is about 6 mm at 900 MHz. It is easy to fabricate the DOA estimation system such that position errors are within 6 mm, and thus high-precision equipment is not required for shifting the T-shaped array. Therefore, the proposed system is uncomplicated and can be implemented at low cost.

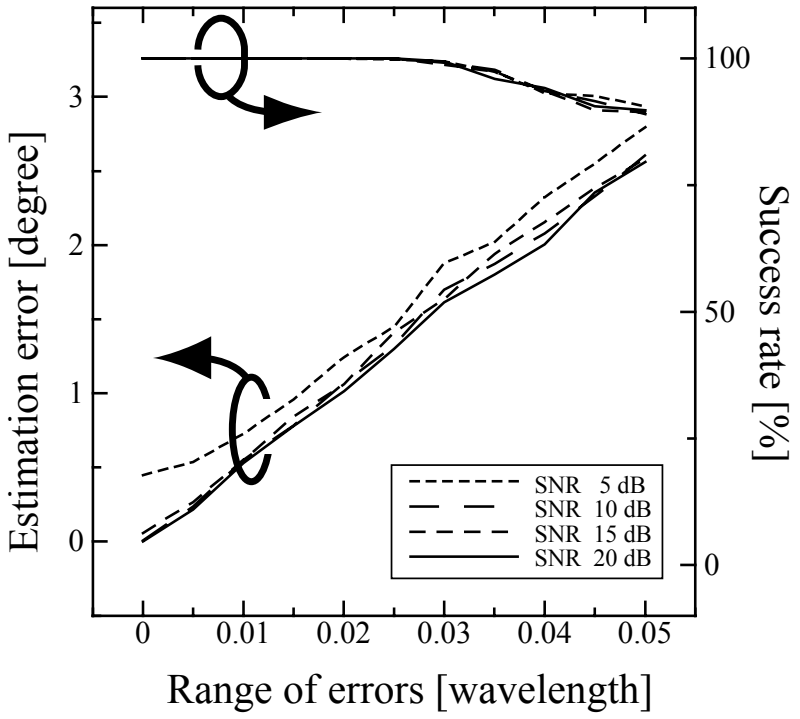

Fig. 2-19 Influence of position errors (Method of calculating phase differences)

2.3.2.3 Relation between number of shifting operations and SN ratio

The relationship between number of shifting operations and SN ratio was evaluated by performing simulations of methods calculating difference phases. Specifications of the simulation were the same as in Sec. 2.3.2.1 except for the number of shifting operations. The

definition of the estimation error is given by Eq. (3). Fig. 2-20 shows the results of the simulations. When SN ratio was 5 dB, although estimation errors increased with increasing number of shifting operations, errors converged more than 10 times. On the other hand, the estimation errors converged to a value when the SN ratio increased although it increased only once. With SN ratio of 20 dB, DOA could be estimated correctly. These results confirmed that the proposed system can estimate DOA with accuracy by increasing the number of samplings when SN ratio is small.

2.3.2.4 Relationship between frequency fluctuation and SN ratio

The influence of frequency fluctuations that occurred while shifting the array was evaluated by performing simulations. Specifications of the simulation were the same as in Sec. 2.3.2.1 except for SN ratio and frequency fluctuations as shown in Eq. (4). The definition of the estimation error is given by Eq. (3). Fig. 2-21 shows the results of the simulations. DOA could be estimated correctly when the range of frequency fluctuation was within 10^{-2}. It is possible that a stability of the oscillator in receivers and transmitters is within 10^{-2}, and thus the proposed method is not influenced by frequency fluctuations in real systems.

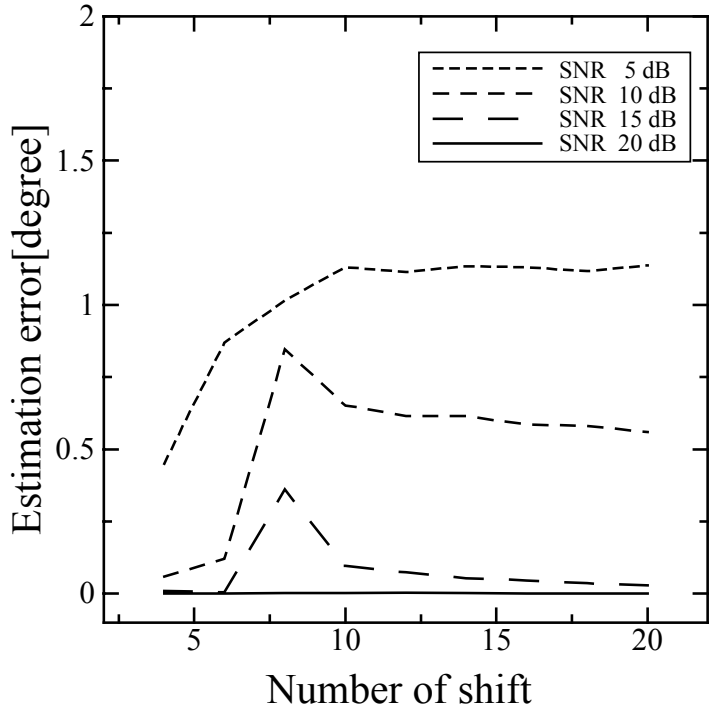

Fig. 2-20 Influence of number of shifting operations (Method of calculating phase differences)

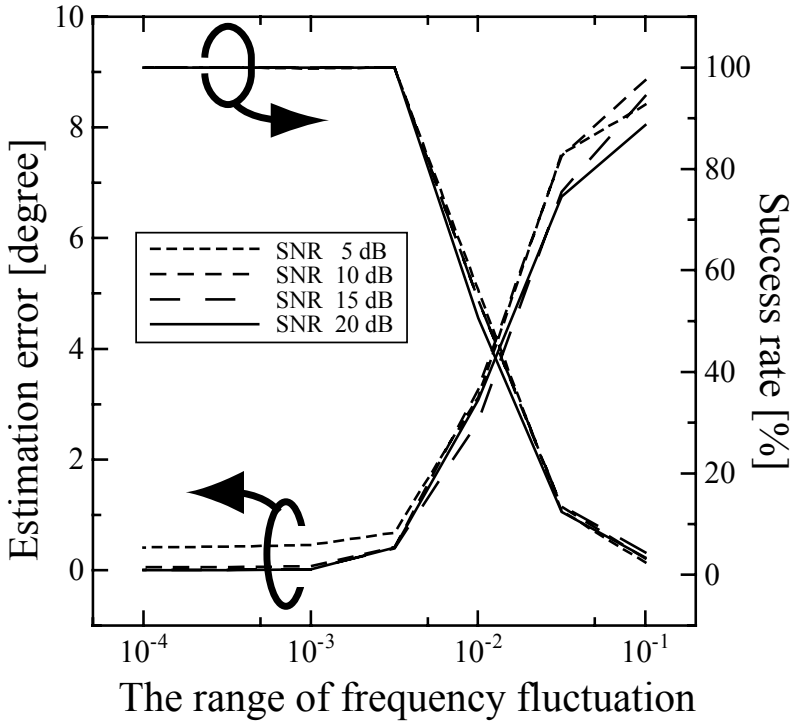

Fig. 2-21 Influence of frequency fluctuation (Method of calculating phase differences)

2.3.2.5 Characteristics regarding incident angles

The characteristics regarding incident angles were evaluated by performing simulations of methods calculating difference phases. The number of arrival waves was 1, the array form was a 3 + 1 T-shaped array, and the data received by a 3 × 3 virtual planar array was synthesized by shifting the T-shaped array twice. When DOA was changed from –180° to 180°, DOA was estimated at each angle. SN ratio was 10 dB, and the range of position error was changed from 0 to 0.05 wavelengths. The number of trials was 50 at each angle. In this simulation, estimation errors were 0° all angles at all position errors. These results confirmed that the proposed system does not have characteristics regarding incident angle, and can estimate DOA at all angles correctly.

2.4 Measurements in anechoic chamber

Experiments in an anechoic chamber were conducted for confirming the effective and limited characteristics of the proposed method. First, the experiment in one arrival wave was carried out for basic consideration. Then, the experiment in two arrival waves was conducted for

confirming DOA estimation when several waves arrive.

2.4.1 Experiments for the case of one arrival wave

The performance of the proposed system during DOA estimation was evaluated by experiments in the case of one arrival wave in an anechoic chamber. The radio frequency was 900 MHz band, and the wave was sinusoidal. The frequency of base band signals was 1 MHz. The SN ratio was about 20 dB, and was calculated by Fourier transformer of outputs of ADC. Although carrier synchrony between the transmitter and receiver was established, it may have no influence because the stability of the transmitter was 5×10^{-10}/day and the time between each measurement of the arrival wave was about 1 minute. The experiment is shown schematically in Fig. 2-22. The array form was a 3 + 1 T-shaped array antenna, and a 3 × 4 virtual planar array was synthesized by shifting 3 times. Measurement errors increased due to the influence of twisted cables and the short distance between the transmit antenna and receiving antenna with the parallel shifted of the T-shaped array antenna. Thus, in this experiment the T-shaped array antenna was moved to reduce measurement errors, as shown in Fig. 2-22. In this experiment, shifting distance $\Delta\hat{x}$ was defined by the following equation, such that the distance was equal to the theory described in Sec. 2.2.2:

$$\Delta\hat{x} = \Delta x \times \cos\theta$$

where Δx is the interval between elements. The subarray was a 3 × 3 planar array, and the system estimated DOA using MUSIC with the F/B spatial smoothing procedure. Based on the results shown in Sec. 2.3.1.4, the probability of successful DOA estimation was about 65% because the oversampling of ADC was about 5 times. Thus, the number of measurements at each position was 10, and the virtual planar array was synthesized according to each data set, and that with the best accuracy was assumed to be a result. If this method is not used, it is necessary to use spline interpolation, ADC with higher sampling frequency, such as 40 MHz, or the second method.

Fig. 2-23 shows the experiments results, which confirmed that DOA could be estimated with accuracy and the dynamic range of the MUSIC spectrum was obtained. Fig. 2-24 shows the estimation errors in all directions. The average estimation error was 2.06°, indicating the effectiveness of the proposed method.

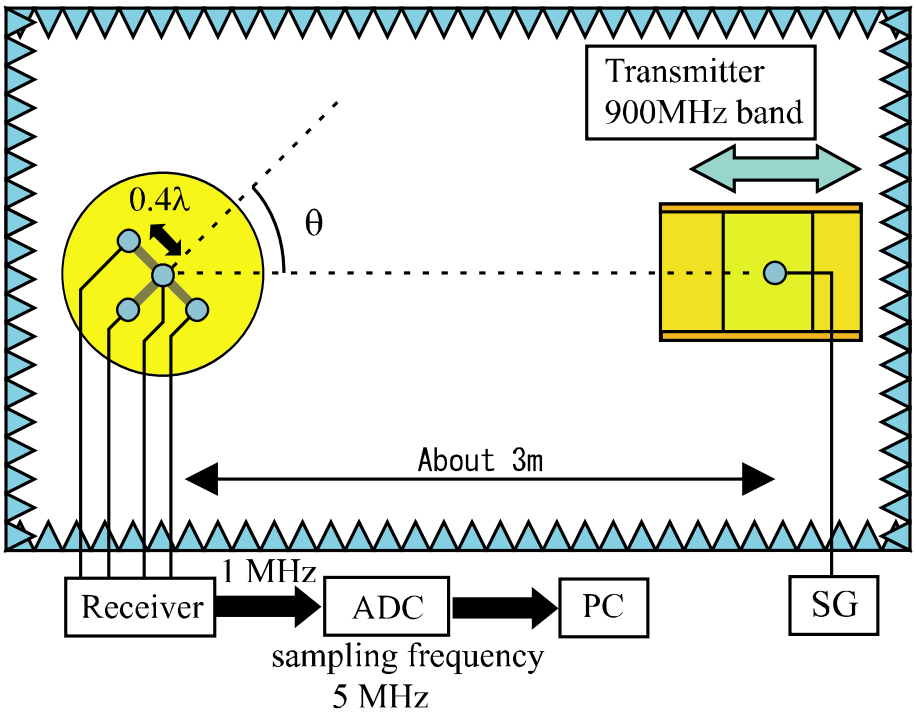

Fig. 2-22 Experimental situation (one wave)

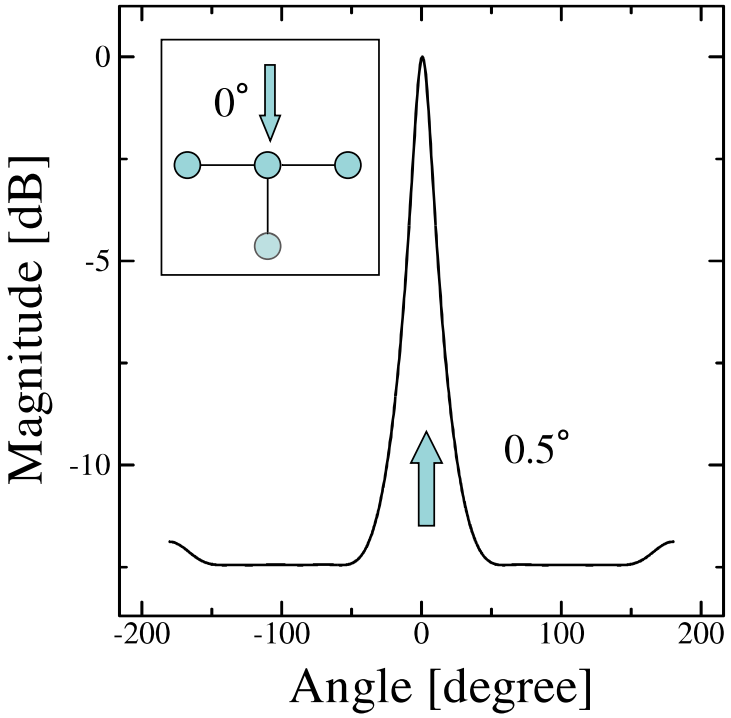

Fig. 2-23 Results of DOA estimation (DOA = 0 [deg.])

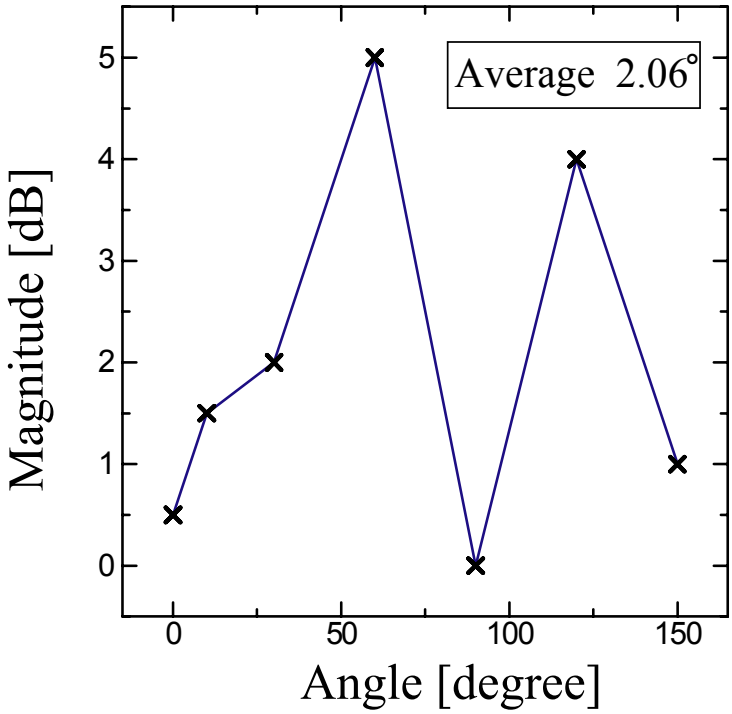

Fig. 2-24 Estimation errors (one arrival wave)

2.4.2 Experiments for the case of two arrival waves

The performance of the proposed system during DOA estimation was evaluated by experiment in the case of two coherent arrival waves.Fig. 2-25 shows a schematic view of the experiment. The radio frequency was the 900 MHz band, and two coherent waves, which were sinusoidal waves, were transmitted. The frequency of the transmitter was adjusted such that the output of the receiver was about 1 MHz. The power of the transmitter was –15 dBm. The SN ratio calculated using Fourier transform of output data at ADC was about 20 dB. The array form was a 5 + 1 T-shaped array, and the data received by a 5 × 4 virtual planar array was synthesized by shifting 4 times. The ADC in this experiment had 8 channels, and thus I- and Q-components of six elements were not measured simultaneously. However, the Q-components could be calculated from I-components using an all-path filter because arrival waves were sinusoidal. Thus, I-components of the six elements were measured by ADC, Q-components were obtained using the all-pass filter on a PC, and DOA were estimated using the calculated data. The transfer function was given by:

$$H(z) = \frac{1 + \alpha z^{-1}}{\alpha + z^{-1}}$$

where α is defined as:

$$\angle H(z) = -\omega_0 T + 2\tan^{-1}\left(\frac{\alpha \sin \omega_0 T}{1+\alpha \cos \omega_0 T}\right) = \frac{\pi}{2}$$

where ω_0 is the center frequency, and T is the sampling interval. Although the antenna side of the transmitter was shifted to reduce the measurement errors in the case of one arrival wave, the antenna side of the receiver was shifted because of problems in setting up the trial apparatus. The other experimental specifications were the same as in the case of one arrival wave. Fig. 2-26 and Fig. 2-27 show the experiment results, which confirmed the estimations of two arrival elements.

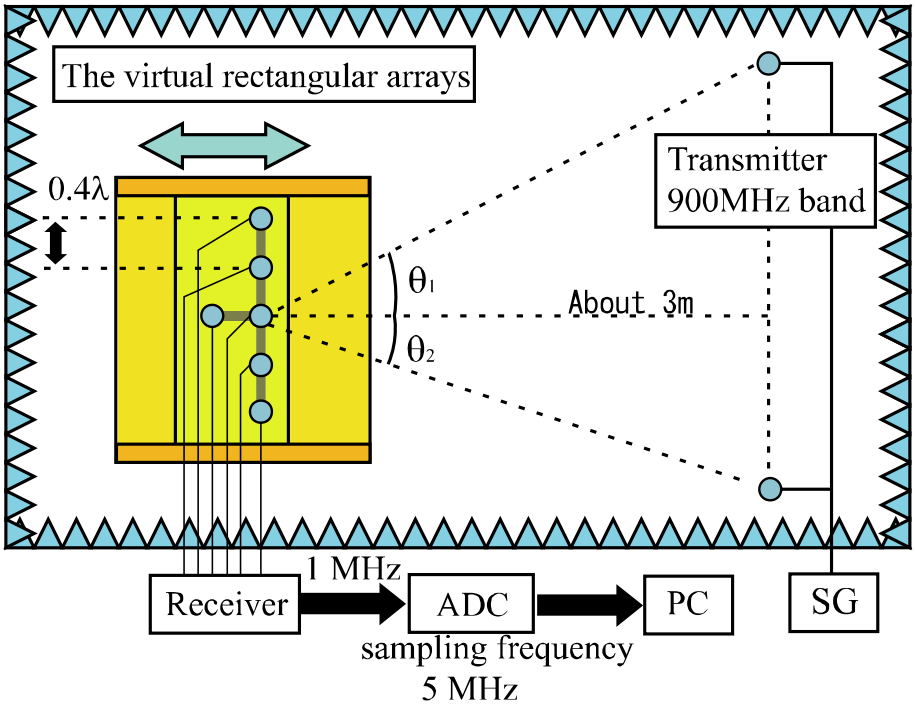

Fig. 2-25 Schematic view of experiment (two arrival waves)

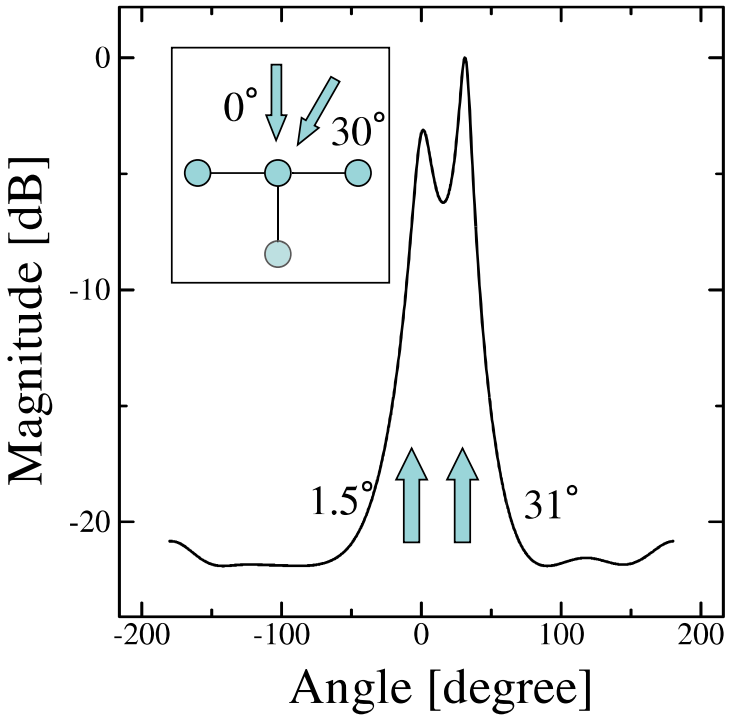

Fig. 2-26 Results of DOA experiments (DOA = 0, 30 [deg.])

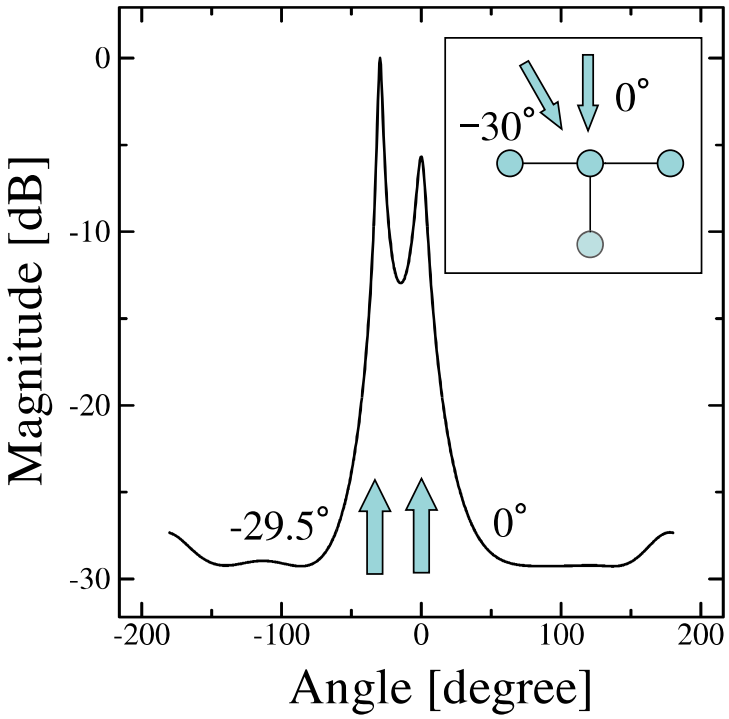

Fig. 2-27 Results of DOA estimation (DOA = –30, 0 [deg.])

2.5 Summary

This chapter introduced the DOA estimation system with a virtual planar array antenna synthesized by a T-shaped array antenna assuming arrival waves are sinusoidal waves only, and described simulations and experiments performed as basic evaluations of the proposed method.

Simulation results indicated the effectiveness of the proposed method although the dynamic range of the MUSIC spectrum was degraded. Moreover, the average estimation errors was within 3° when the SN ratio was within 5 dB in the presence of influences, such as position errors, frequency fluctuation, *etc*. Then, the proposed system was built, and used for experiments in cases of one and two arrival waves. In the case of one arrival wave, the average estimation error was 2.06°. On the other hand, two waves could be distinguished accurately. These results confirmed that the proposed method provides an effective DOA estimation.

On the other hand, when the arrival waves are modulated by random signals, the method using the virtual planar array introduced by this chapter cannot estimate the DOA. The shift in phase cannot be determined since the phases of the received waves change randomly. Thus, it is impossible to calibrate the phase differences because the measurements at each position are performed at different times. For these problem, the development of the proposed method is described, along with its application to DOA estimation when arrival waves are waves in a CDMA system or random signals, such as noise in Chapters 3 and 4.

Chapter 3 DOA estimation system using T-shaped array antenna for CDMA system

3.1 Introduction

Based on the assumption that the arrival waves are sinusoidal and information on precise positions can be obtained, we have proposed a method in which the DOA can be estimated by adding an element used for correcting different phases. Further, we confirmed the basic characteristics and effectiveness of this method by performing simulations and experiments in Chapter 2. The advantages of this method include low cost because of the reduction in the number of receivers, weight saving, *etc*. On the other hand, when the arrival waves are modulated by random signals, the method using the virtual planar array cannot estimate the DOA. The shift in phase cannot be determined since the phases of the received waves change randomly. Thus, it is impossible to calibrate the phase differences because the measurements at each position are performed at different times. However, it is assumed that the arrival waves are only emitted by the transmitters of CDMA systems such as IS-95 and CDMA2000. Pilot signals for the synchronization of spreading codes are always included in the arrival waves and in identical repeated signals. Therefore, the pilot signals can only be obtained by despreading the received signals. Moreover, it is possible to calculate the phase differences at each position by despreading these signals.

Based on the above considerations, we developed the method described in Chapter 2, and proposed a method for the DOA estimation with a synthesized virtual planar array using pilot signals of the CDMA systems. The proposed method offers the advantages of low cost due to the reduction in the number of receivers, weight saving, and the estimation of the arrival waves that are random signals including pilot signals. In other words, the proposed method can reduce the system cost and determine the arrival waves in outdoor environments more easily than methods using real planar arrays. Moreover, it can estimate the arrival waves, which cannot be estimated by the methods in Chapter 2, transmitted by the CDMA systems such as IS-95 and CDMA2000. This chapter has demonstrated the utility of the proposed method by simulations and experiments in an anechoic chamber and in an outdoor environment. The proposed method can be applied to superior resolution methods such as MUSIC and ESPRIT. In this study, the

MUSIC method was used as the DOA estimation algorithm.

3.2 Method of synthesizing data of a virtual planar array antenna using pilot signals

This chapter assumed that the arrival waves are transmitted from the base stations of the CDMA systems such as IS-95 and CDMA2000 that use the pilot signals. The proposed method adopts a novel approach to solve the problem of data acquisition. Instead of a conventional planar array antenna, this approach uses a T-shaped array antenna shifted in parallel for estimating DOA. In this subsection, it was assumed that there was only one base station, one pilot signal, and N was odd.

It is described that the method for synthesizing the data received by the virtual planar array that is realized by shifting the (N + 1) T-shaped arrays, as shown in Fig. 3-1. When N is even, element N + 1 is located at a position shifted from Fig. 3-1 such that the antenna of the elements from 1 to N and the N+1 element after movement may overlap.

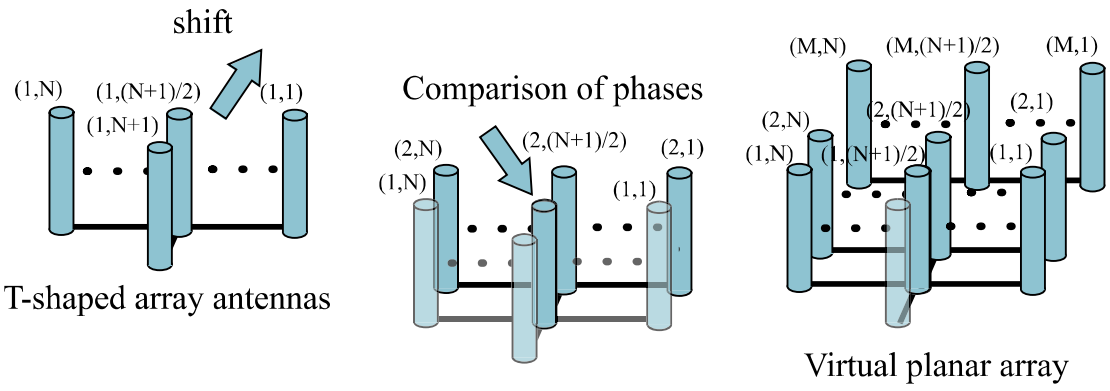

Fig. 3-1 Synthesis of virtual planar array with T-shaped array antenna

The data $\mathbf{X}_1$ received by the T-shaped array antenna at its first position are given by:

$$\mathbf{X}_1 = \left[\mathbf{x}_{11}, \mathbf{x}_{12}, \cdots, \mathbf{x}_{1(N+1)}\right]$$

$$\mathbf{x}_{1n} = \left[x_{1n}(T_s), x_{1n}(2T_s), \cdots, x_{1n}(KT_s)\right]^T$$

where the superscript ^{T} denotes transposition, K is the number of data samples, T_s is the

sampling time, and $\mathbf{x}_{1n}(n=1,\cdots,N+1)$ are data received by the *n*-th element. The variable $x_{1n}(kT_s)(k=1,\cdots,K)$ is the *k*-th data at the n-th element and can be expanded as follows:

$$x_{1n}(kT) = \sum_{l=1}^{L} \sqrt{P_l} W(kT_s) c(kT_s) d(kT_s) e^{j\phi_{1n}(\theta_l)} + n_{1n}(kT_s)$$

where $W(kT_s)$ is the Walsh code for channel separation, $c(kT_s)$ is the spreading sequence for the separation of base stations, $d(kT_s)$ is the pilot data, $e^{j\phi_{1n}(\theta_l)}$ is the phase difference introduced by the angle of the DOA, θ_1, L is the number of arrival waves from a base station, and $n_{1n}(kT_s)$ is the additive white Gaussian noise (AWGN). It is assumed that the arrival signals are only pilot signals, $W(kT_s)$ and $d(kT_s)$ are always equal to one, and $c(kT_s)$ is a periodic pseudo random noise code (PN) sequence. By assuming that the chip signals are synchronized, the despread data can be expanded as follows:

$$\mathbf{Y}_1 = \left[y_{11}, y_{12}, \cdots, y_{1(N+1)} \right]$$

$$\begin{aligned} y_{1n} &= \frac{1}{K} \sum_{k=1}^{K} x_{1n}(kT_s) W^*(kT_s) c^*(kT_s) \\ &= \frac{1}{K} \sum_{k=1}^{K} \sum_{l=1}^{L} \sqrt{P_l} W(kT_s) c(kT_s) d(kT_s) W^*(kT_s) c^*(kT_s) e^{j\phi_{1n}(\theta_l)} \\ &\qquad + \frac{1}{K} \sum_{k=1}^{K} n_{1n}(kT_s) W^*(kT_s) c^*(kT_s) \end{aligned} \quad \textbf{(5)}$$

Since the number of samples *K* is sufficiently large, Eq. (5) can be approximated by Eq. (6), because the second term on its right hand side remains in the spread data and can be neglected.

$$y_{1n} \cong \frac{1}{K} \sum_{k=1}^{K} \sum_{l=1}^{L} \sqrt{P_l} W(kT_s) c(kT_s) d(kT_s) W^*(kT_s) c^*(kT_s) e^{j\phi_{1n}(\theta_l)} \quad \textbf{(6)}$$

The T-shaped array antenna is shifted parallel by a distance equal to an element interval (see Fig. 3-1), and $\mathbf{X}_2$ is the data received at a location; it is given by:

$$\mathbf{X}_2 = \left[\mathbf{x}_{21}, \mathbf{x}_{22}, \cdots, \mathbf{x}_{2(N+1)} \right]$$

$$\mathbf{x}_{2n} = \left[x_{2n}(T_s + t_2), x_{2n}(2T + t_{2s}), \cdots, x_{2n}(KT_s + t_2) \right]^T$$

$$x_{2n}(kT + t_2) = \sum_{l=1}^{L} \sqrt{P_l} W(kT_s + t_2) c(kT_s + t_2) d(kT_s + t_2) e^{-j\phi_{2n}(\theta_l)} e^{-j\psi_{12}} + n_{2n}(kT_s + t_2)$$

where t_2 is the time between the beginning of the first measurement and the beginning of the measurement after shifting, and $e^{-j\psi_{12}}$ is the phase difference between $\mathbf{X}_1$ and $\mathbf{X}_2$ due to an error in sampling points caused by shifting t_2. The despread signal Y_2 is expressed in the

same manner as Y_1:

$$\mathbf{Y}_2 = \left[y_{21}, y_{22}, \cdots, y_{2(N+1)} \right]$$

$$\begin{aligned} y_{2n} &= \frac{1}{K}\sum_{k=1}^{K} x_{2n}(kT_s + t_2)W^*(kT_s + t_2)c^*(kT_s + t_2) \\ &= \frac{1}{K}\sum_{k=1}^{K}\sum_{l=1}^{L}\sqrt{P_l}W(kT_s + t_2)c(kT_s + t_2)d(kT_s + t_2)W^*(kT_s + t_2)c^*(kT_s + t_2) \\ &\quad \times e^{-j\phi_{2n}(\theta_l)}e^{-j\psi_{12}} + \frac{1}{K}\sum_{k=1}^{K} n_{2n}(kT_s + t_2)W^*(kT_s + t_2)c^*(kT_s + t_2) \end{aligned} \quad \textbf{(7)}$$

The above equation is approximated similar to Eq. :

$$\begin{aligned} y_{2n} \cong \frac{1}{K}\sum_{k=1}^{K}\sum_{l=1}^{L}\sqrt{P_l}W(kT_s + t_2)c(kT_s + t_2)d(kT_s + t_2) \\ \times W^*(kT_s + t_2)c^*(kT_s + t_2)e^{-j\phi_{2n}(\theta_l)}e^{-j\psi_{12}} \end{aligned} \quad \textbf{(8)}$$

The measurement signals $y_{1,(N+1)/2}$ and $y_{2,(N+1)}$ are the despread signals of data sampled by elements $(N + 1)/2$ and $(N + 1)$ that are located at the same positions at two different times before and after shifting the T-shaped antenna, respectively. The positions at which they receive the signal are the same, and the phase difference between the arrival waves does not change. Hence, they are two data-sequence elements that differ from each other only by a phase difference of $e^{-j\psi_{12}}$ and AWGN. Since K is sufficiently large, $e^{-j\psi_{12}}$ can be approximated by following Eqs. (6) and (8):

$$e^{-j\psi_{12}} \cong \frac{y_{2(N+1)}}{y_{1(N+1)/2}}$$

If $\hat{\mathbf{Y}}_2$ denotes the corrected despread data for the phase difference due to the difference in sample time, it can be expressed by multiplying Y_2 with $e^{j\psi_{12}}$:

$$\hat{\mathbf{Y}}_2 = e^{j\psi_{12}}\mathbf{Y}_2 \quad \textbf{(9)}$$

By repeating the above procedure $(M - 1)$ times and synthesizing them as shown in Eq. (10), we can define a despread data sequence $\mathbf{Y}$ that represents the virtual data received by an $M \times N$ planar array antenna with the spread data obtained by a parallel shift of the T-shaped antenna:

$$\begin{aligned} \mathbf{Y} &= \left[\mathbf{Y}_1, \hat{\mathbf{Y}}_2, \cdots, \hat{\mathbf{Y}}_M \right] \\ &= \left[\mathbf{Y}_1, e^{j\psi_{12}}\mathbf{Y}_2, \cdots, e^{j(\psi_{12}+\cdots+\psi_{(M-1)M})}\mathbf{Y}_M \right] \end{aligned} \quad \textbf{(10)}$$

Using $\mathbf{Y}$ as an input vector, we can perform an analysis of the DOA estimation by MUSIC

and ESPRIT. In the proposed method, it is not required to calculate the average of the correlation matrices to decrease the influence of AWGN because $\mathbf{Y}$ is the despread data in which the noise is decreased by using equivalent time-averaged data.

The proposed method is applicable to a linear array with a fixed element instead of a T-shaped array, as illustrated in Fig. 3-2. In this case, the phase difference $e^{-j\psi_{12}}$ generated by different sampling start times can be estimated using the data of the fixed element at each position of the linear antenna in the same manner as in Eq. (10). Therefore, we can obtain the despread data $\mathbf{Y}$ that virtually represents the data received by the $M \times N$ planar array antenna.

In fact, the radio waves transmitted from a base station include not only the pilot signals but also other channel data. However, all signals excluding the pilot signals are spread even after despreading. Hence, the proposed method can be applied because these spread signals are included in the second terms on the right hand sides of Eqs. (5) and (7).

When the arrival waves transmitted from several base stations and repeaters are combined, the waves with the synchronized pilot signal can be estimated. However, other waves with a non-synchronized pilot signal cannot be estimated because they are not despread and are included in the second terms on the right hand sides of Eqs. (5) and (7). Therefore, all the waves cannot be estimated simultaneously by the proposed method. Therefore, to estimate such combined arrival waves transmitted from several base stations, this method performs synchronization, despreads each arrival wave, synthesizes the virtual planar array data, and adds these data to enable their application as input vectors for the MUSIC method. Fig. 3-3 shows a flowchart of the proposed method using pilot signals.

The number of shifting operations is decided by the number of elements in the virtual planar array required for the DOA estimations and T-shaped array antenna. For example, when an N × N planar array is used for the DOA estimation, the number of shifting operations is $N - 1$ times those of an $N + 1$ T-shaped array antenna. In fact, the proposed method can replace the $N \times N$ planar array with the $N + 1$ T-shaped array.

The proposed method can be applied to the CDMA system including pilot signals. The array shifting speed is arbitrary if DOA does not change and sufficient received signals are obtained to despread the pilot signals, because the phase difference due to errors in the sampling points caused by shifting time can be calibrated by Eq. (10). Although the proposed system requires a unit for array shifting, if the cost of the unit is the same as that of a receiver and an analog-digital converter (ADC), the cost of the proposed system reduces when the number of shifts required becomes greater than or equal to three. The cost of the unit for the shifting of the array antenna for the experiments described here was practically less than 1/100 as compared with that of the receiver and the ADC. Therefore, the proposed method is effective in reducing

the system cost. In urban districts, it is easier for individuals to measure the DOA while walking since the estimation system is small and lightweight.

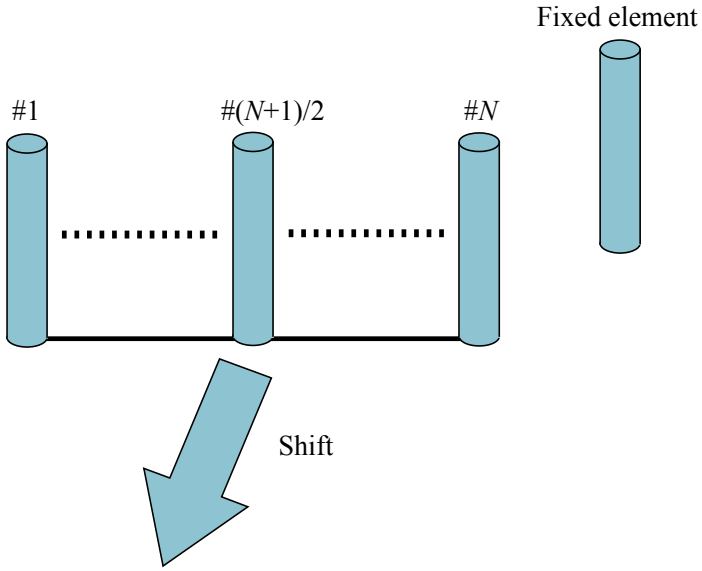

Fig. 3-2 Method with linear array antennas

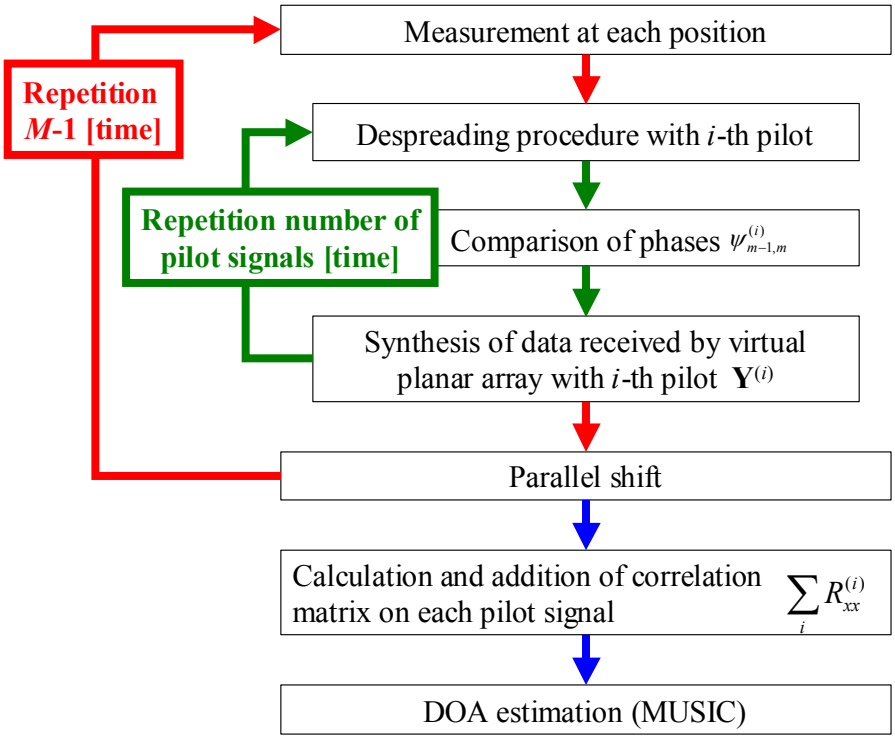

Fig. 3-3 Flowchart of the proposed method uesing pilot signals

3.3 Characteristic evaluation by computer simulation

In this section, it is presented that the results of the simulations performed for evaluating the effectiveness of the virtual planar arrays. In the proposed methods, the estimation accuracy is thought to be influenced by the synthetic accuracy of the data received by the virtual planar array antenna to use data with different measurement times. In addition, there is a possibility of position errors due to parallel shifting of the T-shaped array antenna. Therefore, the influences of SN ratio, frequency offset, frequency fluctuation, *etc,* on estimation errors were evaluated by carrying out simulations. First, the proposed method was compared with the conventional method using the planar array. Next, the relationships between the SN ratio, position errors, and estimation errors were determined.

3.3.1 Comparison between the virtual and real planar array

The performance of the proposed system during the DOA estimation was evaluated by a comparison with the conventional method using a real planar array. Table 3-1 lists the specifications of the simulation. It is considered that six arrival waves are with the same power level. Three arrival waves—#1–#3—included the same pilot signal (PN sequence 1), while the remaining three—#4–#6—included another pilot signal (PN sequence 2). The virtual planar array included 28 (7 × 4) elements, and the subarrays were 3 × 3 planar arrays for spatial smoothing. The interval between the elements was 0.4 wavelengths. The chip rate was 1.23 Mcps, sampling frequency of the ADC was 5 MHz, and sampling number was 2000. The number of other channels—the number of forward traffic signals such as sync signals and paging signals—was 10. In these simulations, the other channels are random signals whose power levels are the same as that of the pilot signal. Fig. 3-4 shows a schematic view of the virtual array antenna and arrival waves. The MUSIC method was employed as the DOA estimation algorithm.

Fig. 3-5 shows the results for the real and virtual planar arrays. When data were synthesized using only PN sequence 1, arrival waves #1–#3 could be estimated, whereas arrival waves #4–#6 could not. This was because arrival waves #4–#6 could not be despread using PN sequence 1, and the data of these waves were calculated as noise. Similarly, when data were synthesized using only PN sequence 2, arrival waves #4–#6 could be estimated, whereas arrival waves #1–#3 could not. The addition of data despread using PN sequence 1 with those despread

using PN sequence 2 resulted in the accurate estimation of the six waves.

The averages of the estimation errors of the planar and virtual planar arrays were 0 and 0.58 degrees, respectively. These results indicate that the virtual planar array of the proposed system can estimate the DOA with almost the same accuracy as that of the real planar array. On the other hand, the dynamic range of the virtual planar array was less than that of the real planar array (See Fig. 3-5). This may be due to AWGN and the errors caused by the presence of other signals during synthesis. The results of these simulations confirmed the effectiveness of the proposed system.

Table 3-1 Simulation specifications

Array from	T-shaped array antenna (7 + 1 elements)
Number of shifting operations	3
Number of virtual planar array elements	7 × 4 (28 elements)
Number of subarray antenna elements	3 × 3 (9 elements)
Interval between elements	0.4 wavelengths
Number of arrival waves	6 (–140°, –40°, –10°, 70°, 100°, 160°)
SN ratio	10 dB
Pilot signal for waves #1–#3	PN sequence 1
Pilot signal for waves #4–#6	PN sequence 2
Number of other channels	10

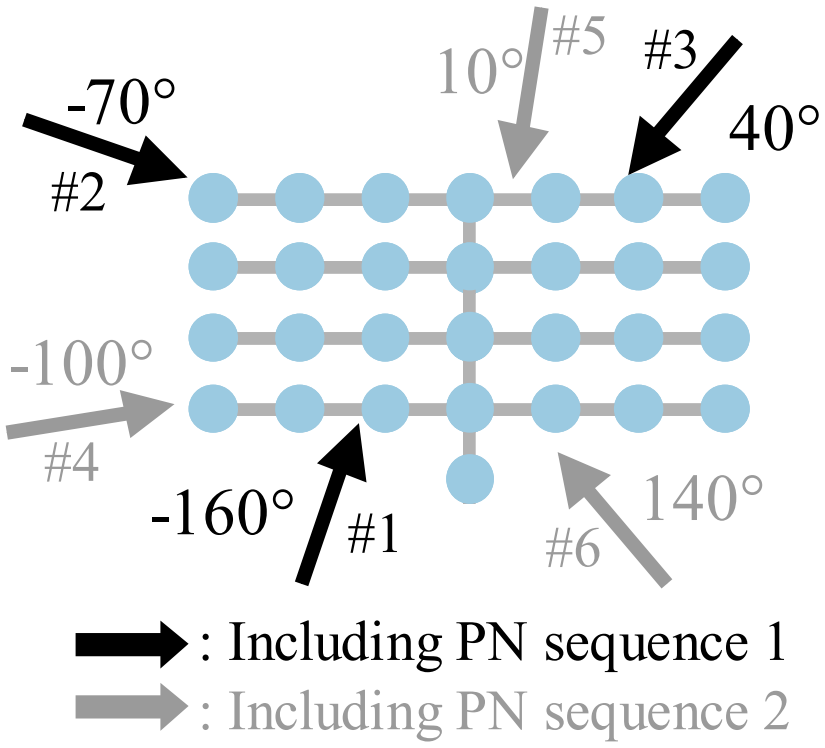

Fig. 3-4 Schematic view of virtual array antenna and incident wave

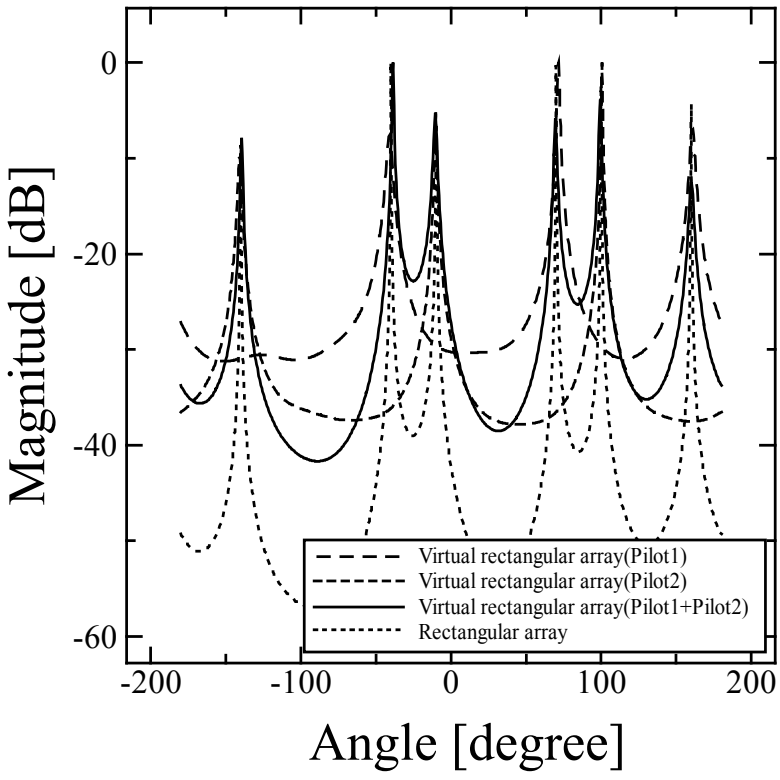

Fig. 3-5 Simulation results of MUSIC spectrum

3.3.2 Relationship between SN ratio and number of samplings

The proposed method calibrated the phase difference with Eq. (10) by a parallel shift of the T-shaped antenna and estimated the DOA of the arrival waves using the data obtained. Thus, it is possible that the estimation errors will increase when the SN ratio or the number of samplings is small. Therefore, the characteristics of these influences were evaluated by performing simulations.

The specifications of the simulation were the same as those in Sec. 3.3.1 with the exception of the SN ratio and the number of samplings. All the arrival waves (i.e., the six waves) were estimated using PN sequences 1 and 2, and their estimation errors were computed. The averages of the estimation errors were evaluated by changing the number of samplings and SN ratio; the number of trials was 50. An estimation error Θ is defined as follows:

$$\Theta = \frac{1}{KL}\left(\sum_{k=1}^{K} \sum_{l=1}^{L} \left| \theta_l - \hat{\theta}_l \right| \right) \quad \textbf{(11)}$$

where L is the number of arrival waves, K is the number of trials, θ_l is the direction of the *l*-th arrival wave, and $\hat{\theta}_l$ is the estimation result of the *l*-th arrival wave.

Fig. 3-6 shows the simulation results. When the SN ratio was small, the DOA was estimated with 1500 or more samplings. These results confirmed that the proposed system can estimate the DOA accurately by increasing the number of samplings when the SN ratio is small.

3.3.3 Relationship between position errors and estimation errors

The influences of the position errors that occurred while shifting the array were evaluated by performing simulations. The specifications of the simulations were the same as those described in Sec. 3.3.1. All the arrival waves (i.e., the six waves) were estimated using PN sequences 1 and 2, and their estimation errors were computed. The averages of the estimation errors were evaluated by changing the ranges of the position errors; the number of trials was 50. The definition of the estimation error is given by Eq. (11).

Fig. 3-7 shows the simulation results. The DOA could be estimated accurately when the range of the position errors was smaller than 0.01 wavelengths. These results indicate that high-precision equipment is not required for shifting the T-shaped array; therefore, the proposed system is uncomplicated and can be implemented at low cost.

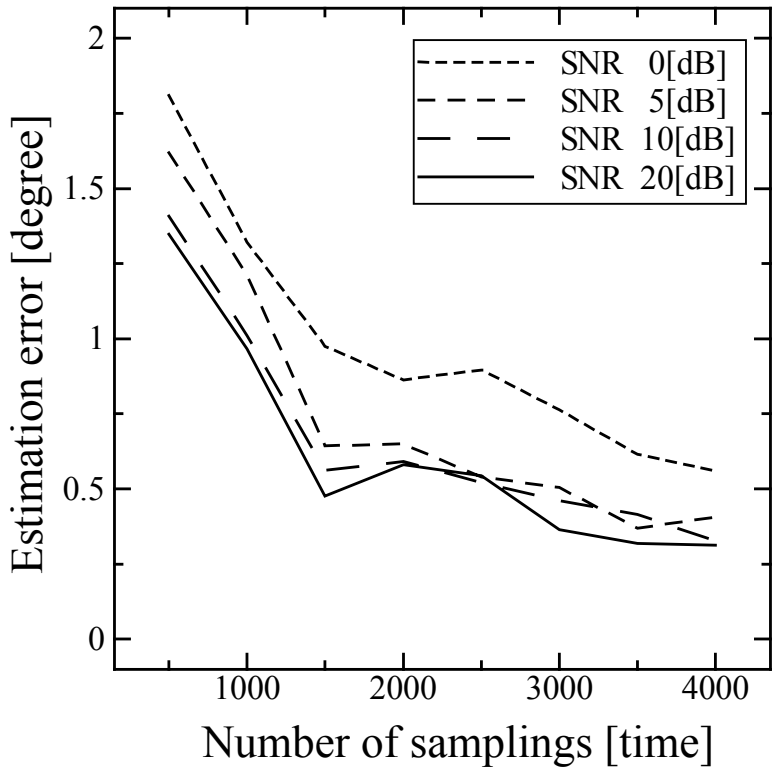

Fig. 3-6 Influence of SN ratio

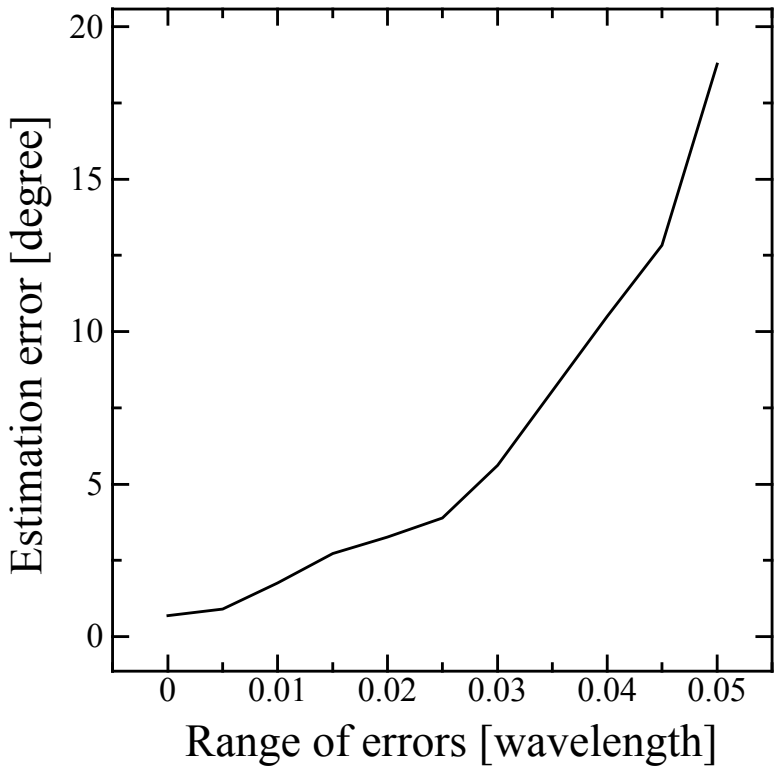

Fig. 3-7 Influence of position errors

3.3.4 Relationship between the number of shifting operations and estimation error

The relationship between the number of shifting operations and the estimation error was evaluated by performing simulations. Table 3-2 lists the simulation specifications. Six arrival waves with the same power level were considered. All the arrival waves—#1–#6—included the same pilot signal (i.e., all the arrival waves were correlation waves). When the number of shifting operations is 0 (T-shaped array) and 1 (5 × 2 virtual planar array), all the arrival waves cannot be estimated theoretically. The array should be shifted two times or more to estimate the DOA. Thus, we consider a case in which the number of shifting operations is greater than or equal to two. In general, the number of shifting operations is decided by the number of arrival waves and of the elements in the T-shaped array. The number of subarray antenna elements was 3 × 3 (9 elements). The chip rate was 1.23 Mcps, sampling frequency of the ADC was 5 MHz, and sampling number was 2000. The number of other channels was 10. The averages of the estimation errors were evaluated by changing the number of shifting operations; the number of trials was 50. The definition of the estimation error is given by Eq. (11).

Table 3-2 Simulation specifications

Array from	T-shaped array antenna (5 + 1 elements)
Number of subarray antenna elements	3 × 3 (9 elements)
Interval between elements	0.4 wavelengths
Number of arrival waves	6 (–140°, –40°, –10°, 70°, 100°, 160°)
SN ratio	10 dB
Pilot signal for waves #1–#6	PN sequence 1
Number of other channels	10

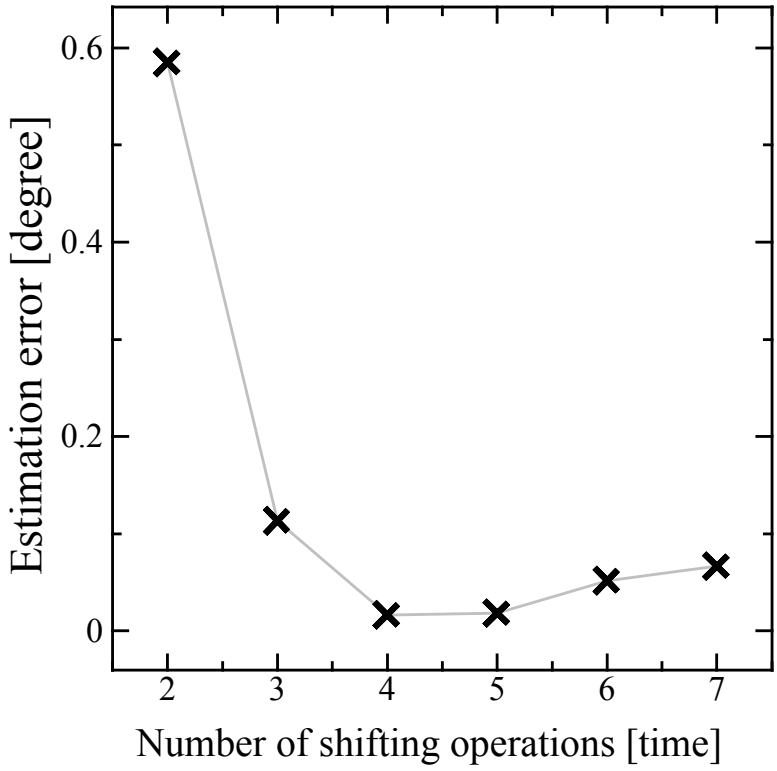

Fig. 3-8 Relationship between number of shifting operations and estimation error

Fig. 3-8 shows the simulation results. A 5 × 3 (=15) array antenna is required for the DOA estimation with MUSIC and forward/backward spatial smoothing method in the case of the conventional planar array. On the other hand, a 5 + 1 (=6) T-shaped array antenna and three shifting operations are required for the proposed method. In fact, the cost, size, and weight of the system can be reduced by using the proposed system. Additionally, an improvement in the estimation error is expected by increasing the number of shifting operations by four times. The estimation errors worsened moderately due to the errors of synthesizing data of T-shaped arrays when the number of shifting operations was greater than or equal to five. The solution to this problem is a part of future work. The results of these simulations confirmed the effectiveness of the proposed system.

3.4 Experiments in anechoic chamber

Experiments in an anechoic chamber were conducted for confirming the effective and limited characteristics of the proposed method. First, the experiment in case of one arrival wave was carried out for basic consideration. Then, the experiment in case of two arrival waves was

conducted for confirming DOA estimation when several waves arrive.

3.4.1 Experiments for the case of one arrival wave

The performance of the proposed system during the DOA estimation was evaluated by several experiments. First, we conducted experiments in an anechoic chamber, as shown in Fig. 3-9. Table 3-3 shows the specifications of the experiments in which the number of arrival waves was equal to one. A transmitting antenna was shifted to decrease the estimation errors caused by the influence of cable twisting. The area swept by shifting the T-shaped receiving antenna is equivalent to the size of a planar antenna with 5 × 4 elements, which is equal to the size of the virtual planar array. The distance moved, $\Delta\hat{x}$, was defined by Eq. (11) such that it became equivalent to the theory presented in Sec. 3.2:

$$\Delta\hat{x} = \Delta x \times \cos\theta \quad \textbf{(12)}$$

where Δx is the interval between the elements. A 3 × 3 planar array was used as a subarray for spatial smoothing. The radio frequency varied over a 900 MHz band, the chip rate was 1.23 Mcps, sampling frequency of the ADC was 5 MHz, number of samplings was 2000, and MUSIC was used for the DOA estimation. The estimation errors are summarized in Fig. 3-10. It shows that the DOA was estimated accurately.

Table 3-3 Experimental specifications (one arrival wave)

Array form	T-shaped array antenna (5 + 1 elements)
Number of shifting operations	3
Number of virtual planar array elements	5 × 4 (20 elements)
Number of subarray antenna elements	3 × 3 (9 elements)
Interval between elements	0.4 wavelengths
Radio frequency	900 MHz band
Chip rate	1.23 Mcps
Sampling frequency of ADC	5 MHz

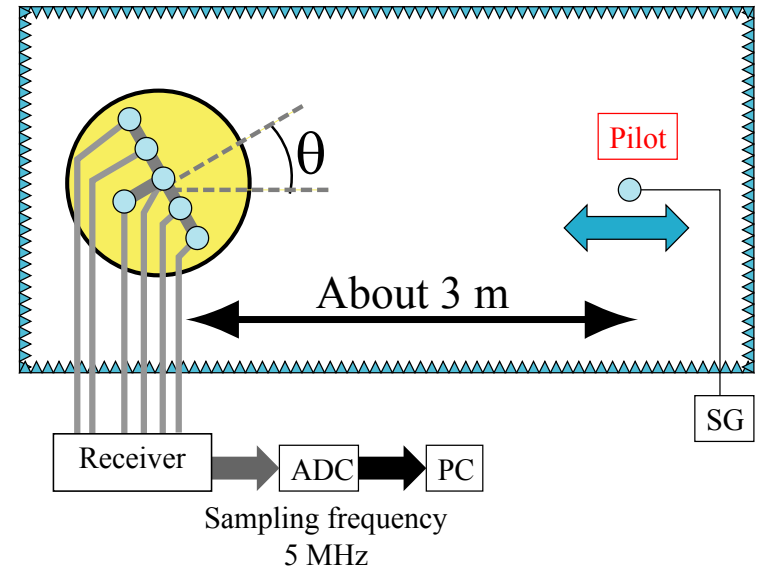

Fig. 3-9 Schematic view of experiments (one arrival wave)

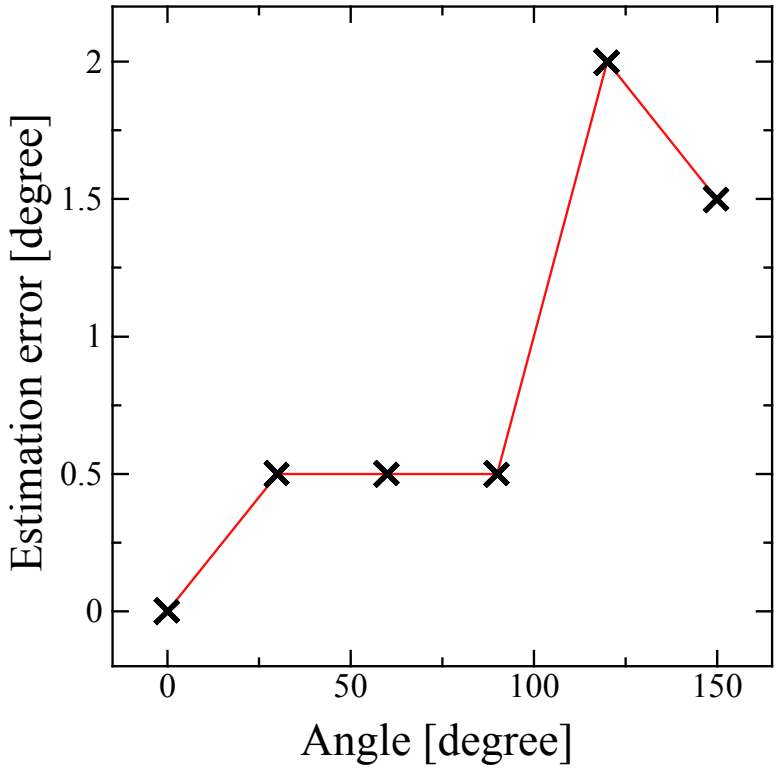

Fig. 3-10 Estimation errors of experimental results (one arrival wave)

3.4.2 Experiments for the case of two arrival waves

We conducted experiments for the case of two arrival waves in the anechoic chamber, as shown in Fig. 3-11. Table 3-4 lists the experimental specifications. In contrast to the previous experiment, the 5 × 4 virtual planar array was obtained by shifting the 5 + 1 T-shaped array antenna. One of the waves was a pilot signal and the other was a sinusoidal wave; their transmitting powers were identical. The radio frequency varied over a 900 MHz band, chip rate of the pilot signal was 1.23 Mcps, number of samplings was 2000, and MUSIC was used for the DOA estimation.

Fig. 3-12 shows the MUSIC spectrum. As shown in this figure, the direction of the pilot signal was estimated accurately because the sinusoidal wave was spread and equated with noise. Since the transmitting powers of the two waves including the pilot signals were the same, they can be estimated by the proposed method. This result confirmed that the proposed method was effective for the DOA estimation.

Table 3-4 Experimental specifications (two waves)

Array type	T-shaped array antenna (5 + 1 elements)
Number of shifting operations	3
Number of virtual planar array elements	5 × 4 (28 elements)
Number of subarray antenna elements	3 × 3 (9 elements)
Interval between elements	0.4 wavelengths
Radio frequency	900 MHz
Chip rate	1.23 Mcps
Sampling frequency of ADC	5 MHz
Signals	Sinusoidal wave, Pilot signal

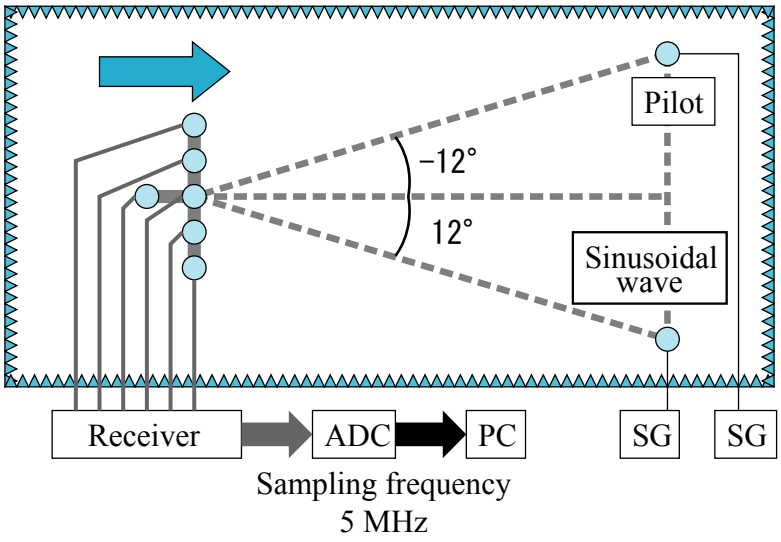

Fig. 3-11 Schematic view of experiment (two arrival waves)

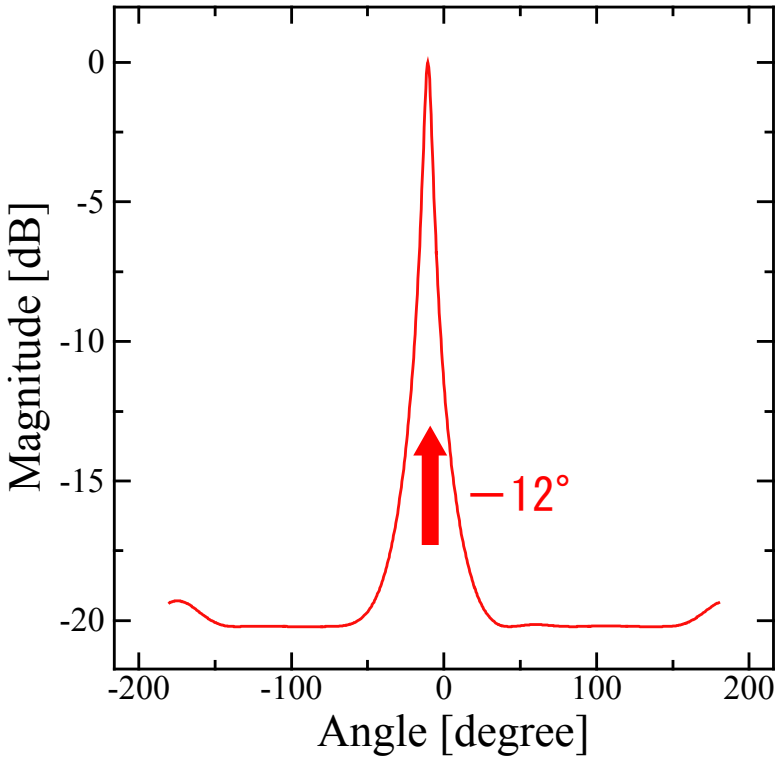

Fig. 3-12 Results of DOA estimation (two arrival waves)

3.5 Outdoor experiments

Experiments in outdoor environments were conducted for confirming a possibility of DOA

estimation by the proposed method in actual environments. First, the experiment at the line-of-sight was carried out, then the experiment at the non-line-of-sight was conducted.

3.5.1 Experiments at Line of sight

We conducted an experiment for the line-of-sight case in an outdoor environment and measured the arrival waves transmitted from base stations currently used in cellular systems. Fig. 3-13 shows a schematic view of the experiment. The specifications of the receiver were the same as those described in subsection 3.4.2: the number of elements was six (5 + 1 T-shaped array), and the number of shifting operations was three. As evident from the results of the pilot signal analysis, a wave of approximately 12 dB, which is stronger than those transmitted from other base stations, was transmitted from a base station in the vicinity of the measurement point. At this point, the base station was located at an angle of –88°. Figure Fig. 3-14 shows the experimental results that confirmed that the DOA estimation results were accurate.

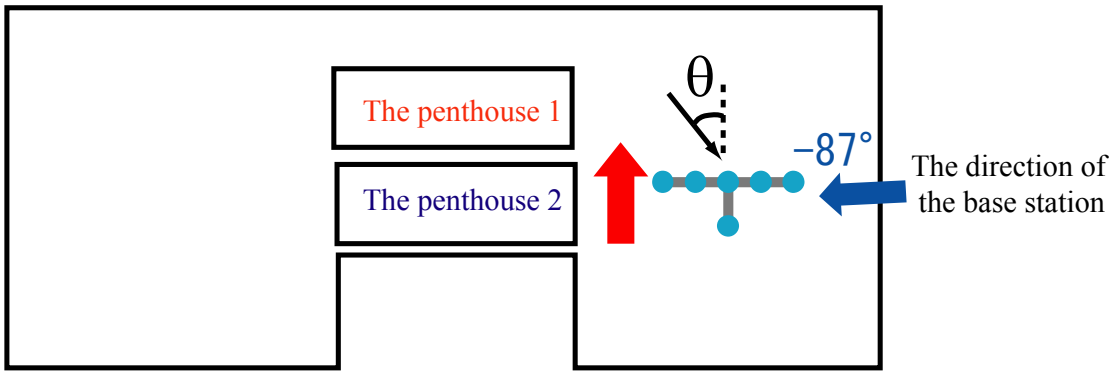

(a) The situation (Line-of-sight)

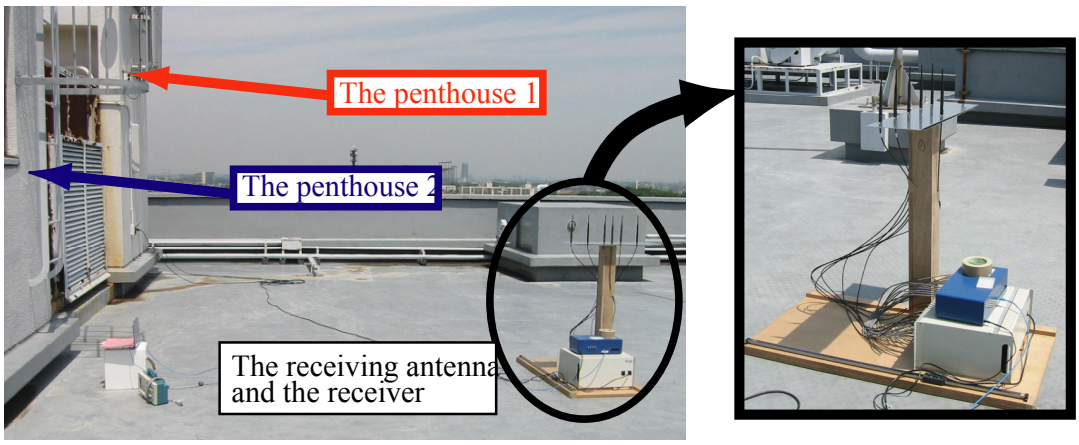

(b) The photograph (Line-of-sight)

Fig. 3-13 Schematic view of outdoor experiment (Line of sight)

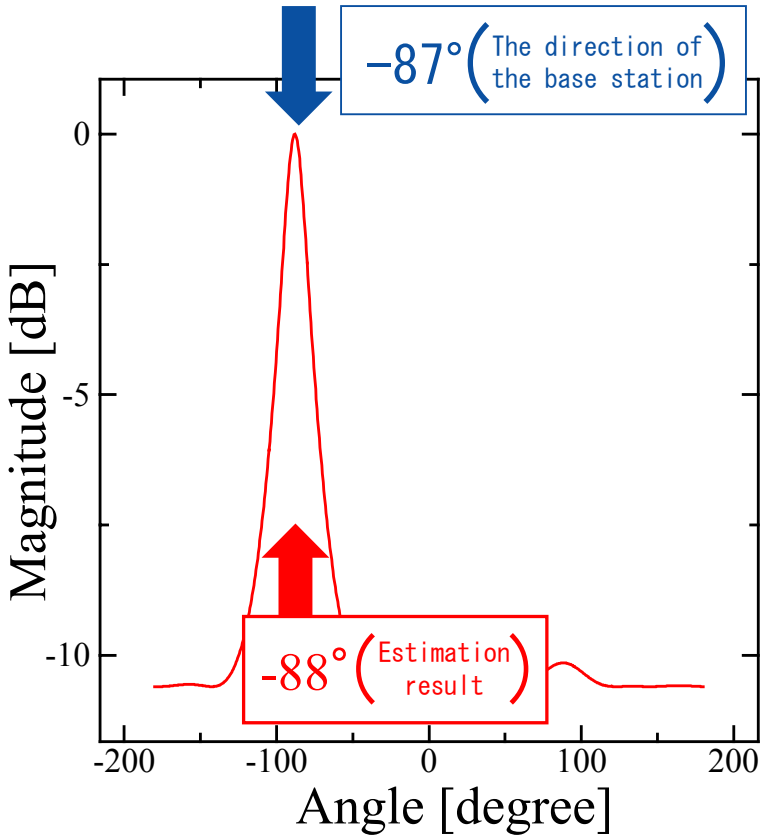

Fig. 3-14 Results of DOA estimation (Line of sight)

3.5.2 Experiments at Non-line-of-sight

We conducted an experiment for the non-line-of-sight case in an outdoor environment and measured the arrival waves from base stations currently used in cellular systems. The propagation environment is shown in Fig. 3-15(a). It is impossible to accurately determine the DOA from base stations. Therefore, we examined the accuracy of the results by changing the direction of shift of the T-shaped array, as shown in Fig. 3-15 (b) and (c). The specifications of the receiver were the same as those described in subsection 3.4.2: the number of elements was six (5 + 1 T-shaped array) and the number of shifting operations was three.

The experimental results are shown in Fig. 3-16. The estimation error was approximately 9 ° since the SN ratio was smaller than that in the line-of-sight case because the base stations were not along the line of sight. However, the DOA was estimated in almost the same direction. In order to reduce the estimation error, it was essential to increase the sampling number, as described in subsection 3.3.2. Experiments with greater sampling numbers will be performed in future studies. These results confirmed the performance of the proposed method in DOA estimation experimentally.

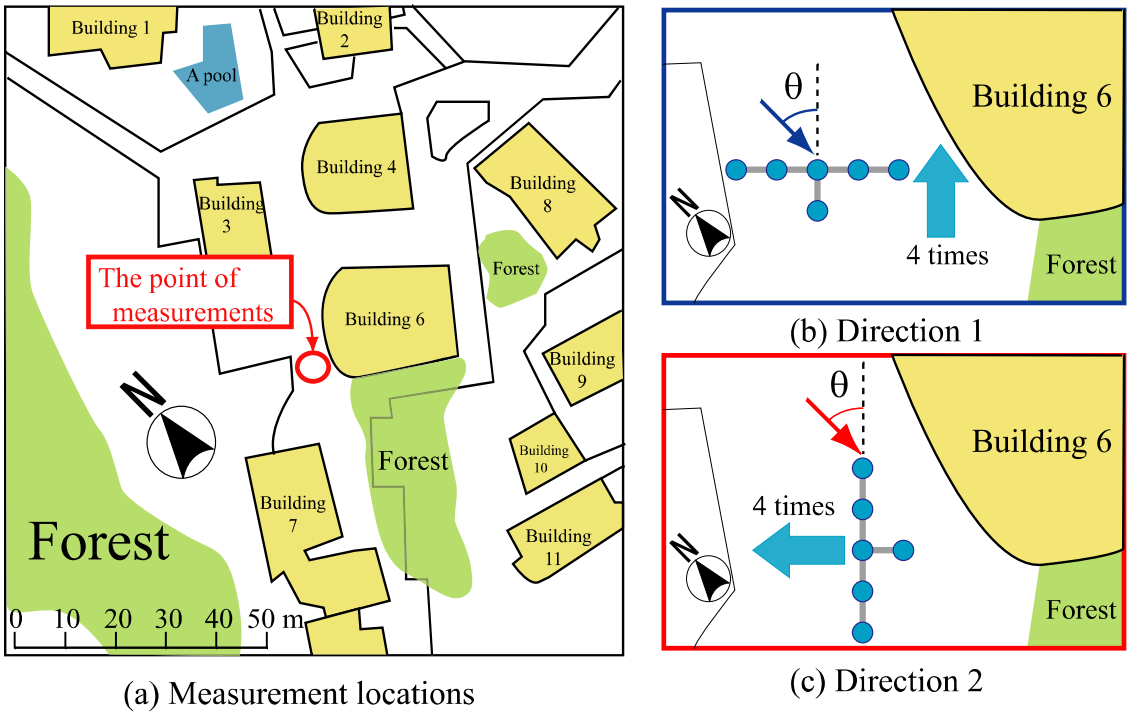

Fig. 3-15 Schematic view of outdoor experiment (Non-line-of-sight case)

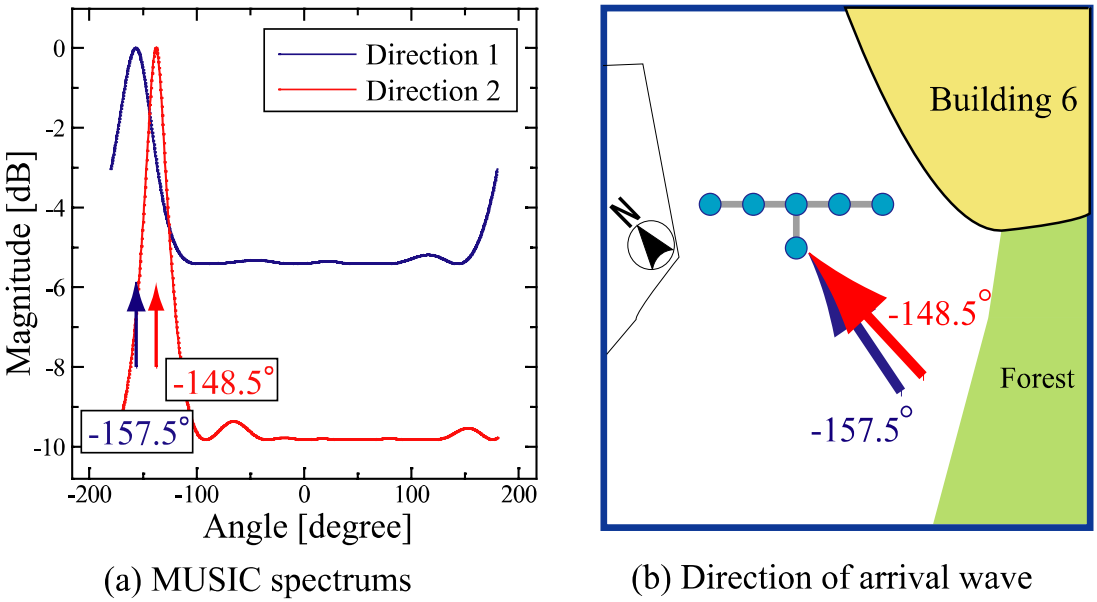

Fig. 3-16 Experimental results of DOA estimation (Non-line-of-sight case)

3.6 Summary

In this chapter, we proposed a method for estimating the DOA using pilot signals in the CDMA system. when the arrival waves are modulated by random signals, the method in Chapter 2 cannot estimate the DOA. However, it is assumed that the arrival waves are only emitted by the transmitters of CDMA systems such as IS-95 and CDMA2000, we developed the method described in Chapter 2, and proposed a method for the DOA estimation with a synthesized virtual planar array using pilot signals of the CDMA systems.

We evaluated the proposed method by performing simulations and experiments in an anechoic chamber and outdoor environment. In the simulations, the DOA was estimated accurately, and the effectiveness of the proposed method was confirmed. Moreover, we evaluated the average estimation errors to be approximately 1° in the anechoic chamber, and found that arrival waves from base stations could be estimated in the outdoor environment. These results confirmed that the proposed method provides an effective DOA estimation. Further studies are required to improve the accuracy of DOA estimation and estimate the arrival waves simultaneously from certain base stations.

Chapter 4 DOA estimation system using T-shaped array antenna for random signals

4.1 Introduction

Chapter 2 presented the method for synthesizing data received by the virtual planar array antenna, and discussed demonstration of the utility of the proposed method by simulations and experiments in an anechoic chamber assuming that arrival waves are only sinusoidal waves. Then, **Chapter 3** introduced the method for synthesizing data received by the virtual planar array antenna using pilot signals, and discussed the effectiveness of the proposed method demonstrated by simulations and experiments in an anechoic chamber and in an outdoor environment, assuming that arrival waves included pilot signals. These methods use the known signals in arrival waves, and thus these methods cannot estimate DOA when unknown signals arrive. Although it is important for area designs in urban areas to discover illegal repeaters that transmit interference waves, and the waves from the illegal repeaters are sinusoidal due to oscillation or wide band signals without pilot signals. In fact, these methods cannot distinguish the illegal repeaters.

To address these problems, this chapter describes a method of synthesizing data received by the virtual planar array using eigenvectors of correlation matrices. This method uses the characteristic that eigenvectors of correlation matrices have phase information of mode vectors corresponding to DOA. Thus, this method can estimate DOA when arrival waves are random signals. This chapter describes the utility of the proposed method demonstrated by simulations and experiments in an anechoic chamber. The proposed method can be applied to superior resolution methods, such as MUSIC and ESPRIT. In the present study, the MUSIC method was used as the DOA estimation algorithm. On the other hand, this method cannot estimate DOA when arriving waves include non-coherent waves. This problem remains to be addressed in future studies.

4.2 Method of synthesizing data of the virtual planar array antenna using eigenvectors

In this section, we describe the method of synthesizing data of the virtual planar array antenna using eigenvectors. It is assumed that arrival waves are random and coherent waves. The proposed method adopts a novel approach to solve the problem of data acquisition; this approach uses the T-shaped array antenna shifted parallel, instead of a conventional planar array antenna to estimate DOA. Synthesizing data received by the virtual planar array antenna imply that the T-shaped array antenna is used to receive arrival waves, and the received data are used to realize the same data as those received by the conventional planar array antenna by synthesizing the received data. To provide a brief description in this subsection, it is assumed that the number of arrival waves is only one and that N is odd.

We describe the method of synthesizing data received by the virtual planar array and realized by shifting the (N+1) T-shaped arrays as shown in Fig. 4-5.

The data $\mathbf{X}_1$ received by a T-shaped array antenna at its first position are given by:

$$\begin{aligned}\mathbf{X}_1(t) &= \left[x_{11}(t), x_{12}(t), \cdots, x_{1(N+1)}(t) \right]^T \\ &= \mathbf{A}_1(\theta) F(t) + \mathbf{N}_1(t)\end{aligned}$$

where the superscript ^{T} denotes a transposition, t is time, θ is DOA, $F(t)$ is a random signal of a base point, and $\mathbf{A}_1(\theta)$ and $\mathbf{N}_1(t)$ can be expanded as:

$$\mathbf{A}_1(\theta) = [e^{j\phi_{11}(\theta)}, e^{j\phi_{12}(\theta)}, \cdots, e^{j\phi_{1N+1}(\theta)}]^T$$

$$\mathbf{N}_1(t) = [n_{11}(t), n_{12}(t), \cdots, n_{1N+1}(t)]^T$$

where $\phi_{1n}(\theta)(n = 1, 2, \cdots, N+1)$ is a phase difference introduced by θ to a base element, and $n_{1n}(t)$ is thermal noise. A correlation matrix $\mathbf{R}_1$ of $\mathbf{X}_1(t)$ is given by:

$$\mathbf{R}_1 = E[\mathbf{X}_1(t)\mathbf{X}_1^H(t)]$$

where the superscripts $E[\bullet]$ and ^{H} denote an ensemble average and a conjugate transposition, respectively. Eigenvalues λ_{1n} of $\mathbf{R}_1$ and the eigenvectors $\mathbf{e}_{1n}$ to the eigenvalues can be calculated. When the number of arrival waves is 1, the relationships between eigenvalues are given by:

$$\lambda_{11} > \lambda_{12} = \cdots = \lambda_{1N+1}$$

and the eigenvector of $\mathbf{e}_{11}$ is expressed by:

$$\mathbf{e}_{11} = \alpha_1 \mathbf{A}_1(\theta) = \left[\alpha_1 e^{j\phi_{11}(\theta)}, \alpha_1 e^{j\phi_{12}(\theta)}, \cdots, \alpha_1 e^{j\phi_{1,N+1}(\theta)} \right]^T \quad \textbf{(13)}$$

where α_1 is a constant.

The T-shaped array antenna is shifted parallel by the distance of the element interval (see Fig. 4-1), and an eigenvector $\mathbf{e}_{21}$ can be obtained from data at the position as well as by the above procedures:

$$\mathbf{e}_{21} = \alpha_2 \mathbf{A}_2(\theta) = \left[\alpha_2 e^{j\phi_{21}(\theta)}, \alpha_2 e^{j\phi_{22}(\theta)}, \cdots, \alpha_2 e^{j\phi_{2,N+1}(\theta)} \right]^T \quad \textbf{(14)}$$

The elements of the eigenvectors $e^{j\phi_{1,(N+1)/2}}$ and $e^{j\phi_{2,N+1}}$ are the same data, because the elements of $e^{j\phi_{1,(N+1)/2}}$ and $e^{j\phi_{2,N+1}}$ are located at the same position at two different times before and after shifting of the T-shaped antenna, respectively. Hence, by comparing $\alpha_1 e^{j\phi_{1,(N+1)/2}}$ with $\alpha_2 e^{j\phi_{2,N+1}}$, it is possible to obtain the different phases ψ_{12} between first and second positions as follows:

$$\psi_{12} = \frac{\alpha_1 e^{j\phi_{1,(N+1)/2}}}{\alpha_2 e^{j\phi_{2,N+1}}} = \frac{\alpha_1}{\alpha_2}$$

Therefore, the different phases between first and second positions can be calibrated and data of a 2 × N virtual planar array can be synthesized as follows:

$$\begin{aligned}
\mathbf{Y}_{2\times N} &= \begin{bmatrix} \mathbf{e}_{11} \\ \psi_{12}\hat{\mathbf{e}}_{21} \end{bmatrix} \\
&= [\alpha_1 e^{j\phi_{11}(\theta)}, \alpha_1 e^{j\phi_{12}(\theta)}, \cdots, \alpha_1 e^{j\phi_{1N}(\theta)}, \psi_{12}\alpha_2 e^{j\phi_{21}(\theta)}, \cdots, \psi_{12}\alpha_2 e^{j\phi_{2N}(\theta)}]^T \\
&= \alpha_1 [e^{j\phi_{11}(\theta)}, e^{j\phi_{12}(\theta)}, \cdots, e^{j\phi_{1N}(\theta)}, e^{j\phi_{21}(\theta)}, \cdots, e^{j\phi_{2N}(\theta)}]^T
\end{aligned}$$

$$\hat{\mathbf{e}}_{21} = [\alpha_2 e^{j\phi_{21}(\theta)}, \cdots, \alpha_2 e^{j\phi_{2N}(\theta)}]^T$$

By repeating the above procedures (M–1) times, virtual data $\mathbf{Y}_{M\times N}$ received by an M × N planar array antenna by a parallel shift of the T-shaped antenna can be synthesized as follows:

$$\begin{aligned}
\mathbf{Y}_{M\times N} &= \begin{bmatrix} \mathbf{e}_{11} \\ \psi_{12}\hat{\mathbf{e}}_{21} \\ \vdots \\ \psi_{(M-1),M}\hat{\mathbf{e}}_{M1} \end{bmatrix} \\
&= [\alpha_1 e^{j\phi_{11}(\theta)}, \alpha_1 e^{j\phi_{12}(\theta)}, \cdots, \alpha_1 e^{j\phi_{1N}(\theta)}, \psi_{12}\alpha_2 e^{j\phi_{21}(\theta)}, \cdots, \psi_{(M-1),M}\alpha_M e^{j\phi_{MN}(\theta)}]^T \quad \textbf{(15)} \\
&= \alpha_1 [e^{j\phi_{11}(\theta)}, e^{j\phi_{12}(\theta)}, \cdots, e^{j\phi_{1N}(\theta)}, e^{j\phi_{21}(\theta)}, \cdots, e^{j\phi_{MN}(\theta)}]^T
\end{aligned}$$

$$\psi_{(M-1)M} = \sum_{m=2}^{M} \frac{\alpha_{(m-1)} e^{j\phi_{(m-1),(N+1)/2}}}{\alpha_m e^{j\phi_{m,N+1}}} = \sum_{m=2}^{M} \frac{\alpha_{(m-1)}}{\alpha_m}$$

Using $\mathbf{Y}_{M\times N}$ as an input vector, we can perform analysis of DOA estimation by the MUSIC and ESPRIT methods. In fact, there are several correlated waves transmitted from a base station, and thus the eigenvectors at each position become degenerate. However, data at each position can be synthesized as well as by Eq. (15), and the proposed method can estimate DOA using F/B spatial smoothing. Fig. 4-2 shows a flowchart of the proposed method using eigenvectors.

The number of shifting operations is decided by the number of elements in the virtual planar array required for the DOA estimations and T-shaped array antenna. For example, when an N × N planar array is used for the DOA estimation, the number of shifting operations is N – 1 times those of an N + 1 T-shaped array antenna. In fact, the proposed method can replace the $N \times N$ planar array with the N + 1 T-shaped array.

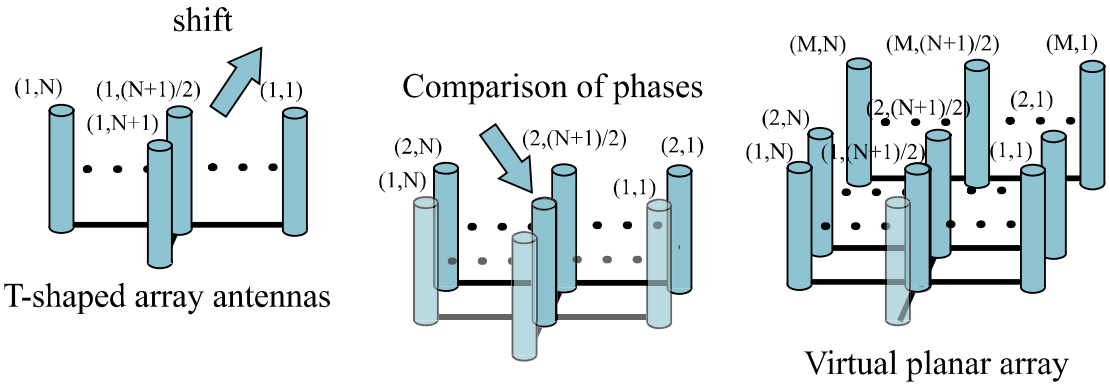

Fig. 4-1 Synthesis of the virtual planar array

The proposed method is applicable to a linear array with a fixed element instead of a T-shaped array, as illustrated in Fig. 4-3. In this case, the phase difference $e^{-j\psi_{12}}$ generated by different sampling start times can be estimated using the data of the fixed element at each position of the linear antenna in the same manner as in Eq. (15). Therefore, we can obtain the despread data $\mathbf{Y}_{M\times N}$ that virtually represents the data received by the $M \times N$ planar array antenna.

The array shifting speed is arbitrary if DOA does not change and sufficient received signals are obtained to despread the pilot signals, because the phase difference due to errors in the sampling points caused by shifting time can be calibrated by Eq. (15). Although the proposed system requires a unit for array shifting, if the cost of the unit is the same as that of a receiver and an ADC, the cost of the proposed system reduces when the number of shifts required

becomes greater than or equal to three. The unit for the shifting of the array antenna for the experiments described here was practically >100. Therefore, the proposed method is effective in reducing the system cost. In urban districts, it is easier for individuals to measure the DOA while walking since the estimation system is small and lightweight.

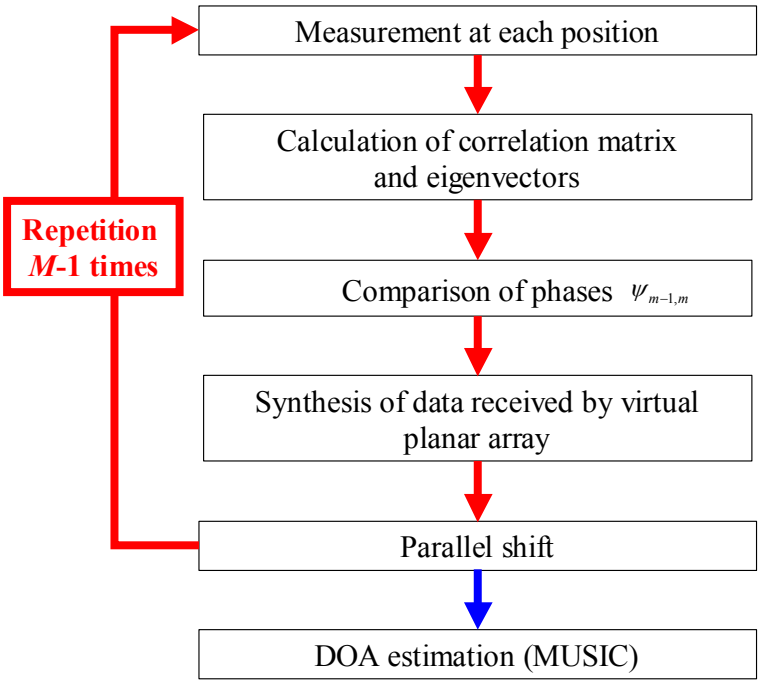

Fig. 4-2 Flowchart of the proposed method using eigenvectors

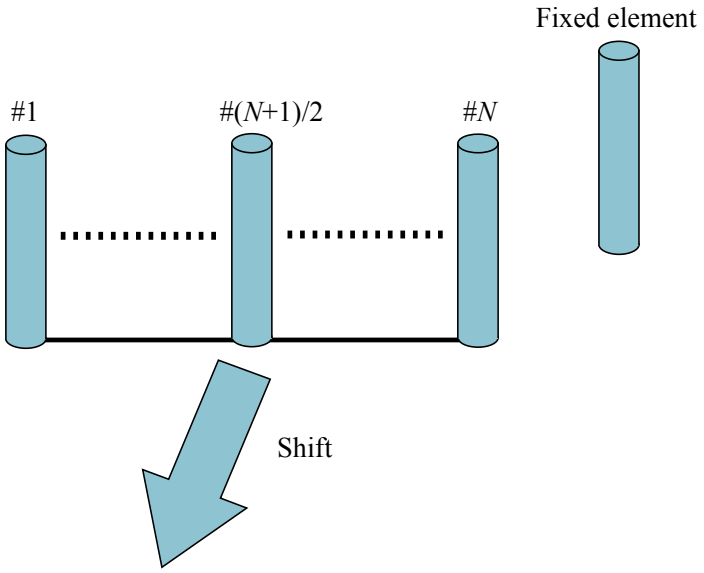

Fig. 4-3 Method using linear array antenna

4.3 Characteristic evaluation by computer simulation

In this section, it is presented that the results of the simulations performed for evaluating the effectiveness of the virtual planar arrays. In the proposed methods, the estimation accuracy is thought to be influenced by the synthetic accuracy of the data received by the virtual planar array antenna to use data with different measurement times. In addition, there is a possibility of position errors due to parallel shifting of the T-shaped array antenna. Therefore, the influences of SN ratio, position errors, *etc,* on estimation errors were evaluated by carrying out simulations. First, the proposed method was compared with the conventional method using the planar array. Next, the relationships between the SN ratio, position errors, and estimation errors were determined.

4.3.1 Comparison of the virtual planar array with the real planar array

The performance of the proposed system in DOA estimation was evaluated by comparison with the conventional method using the planar array. Table 4-1 shows the specifications of the simulation. There were 6 arrival waves, all of which had the same power level. All arrival waves were correlation waves. Twenty-eight (7 × 4) elements were included in the virtual planar array, and the subarrays were 3 × 3 planar arrays for spatial smoothing. The interval between the elements was 0.4 wavelengths. The number of sampling times was 2000. We used the MUSIC method as the DOA estimation algorithm.

Fig. 4-4 shows the results for the real and virtual planar arrays. The average estimation errors of both the planar array and the virtual planar array were 0°. Based on the results of these simulations, it was evident that the virtual planar array of the proposed system could estimate the DOA with almost the same accuracy as the real planar array.

Table 4-1 Simulation specifications

Array form	The T-shaped array antenna (7+1 elements)
Number of shifting operations	3
Number of virtual planar array elements	7 × 4 (28 elements)
Number of subarray antenna elements	3 × 3 (9 elements)
Interval between elements	0.4 wavelength
Number of arrival waves	6 (–140°, –40°, –10°, 70°, 100°, 160°)
SN ratio	10 dB

4.3.2 Relationship between SN ratio and number of samplings

The proposed method calibrates the phase difference due to a parallel shift of a T-shaped antenna, and estimates DOA of arrival waves using the data thus obtained. Thus, it is possible that the estimation errors increases when the SN ratio or number of samplings is small. This subsection discusses the characteristics of these influences evaluated by performing simulations.

Specifications of the simulation were the same as in Sec. 4.3.1 except for SN ratio and the number of samplings. Averages of estimation errors were evaluated when the number of samplings and SN ratio were changed. The number of trials was 500. The estimation error Θ is defined as follows:

$$\Theta = \frac{1}{KL}\left(\sum_{k=1}^{K} \sum_{l=1}^{L} \left| \theta_l - \hat{\theta}_l \right| \right) \quad \textbf{(16)}$$

where L is the number of arrival waves, K is the number of trials, θ_l is the direction of the *l*-th arrival wave, and $\hat{\theta}_l$ is the estimation result of the *l*-th arrival wave.

Fig. 4-5 shows the results of simulations. When SN ratio was small, DOA could be estimated correctly. These results confirmed that the proposed system can estimate DOA with accuracy by increasing the number of samplings when SN ratio is small.

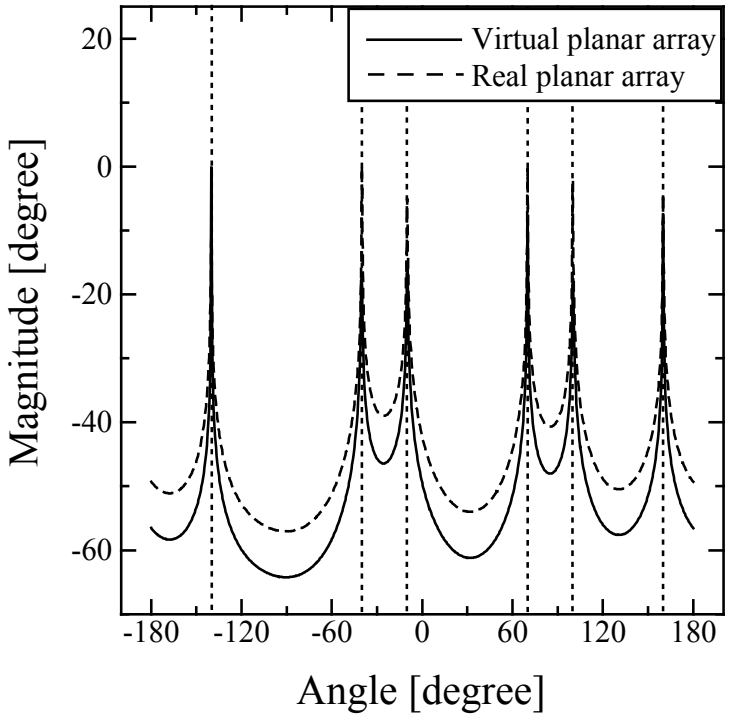

Fig. 4-4 Comparison with real planar array

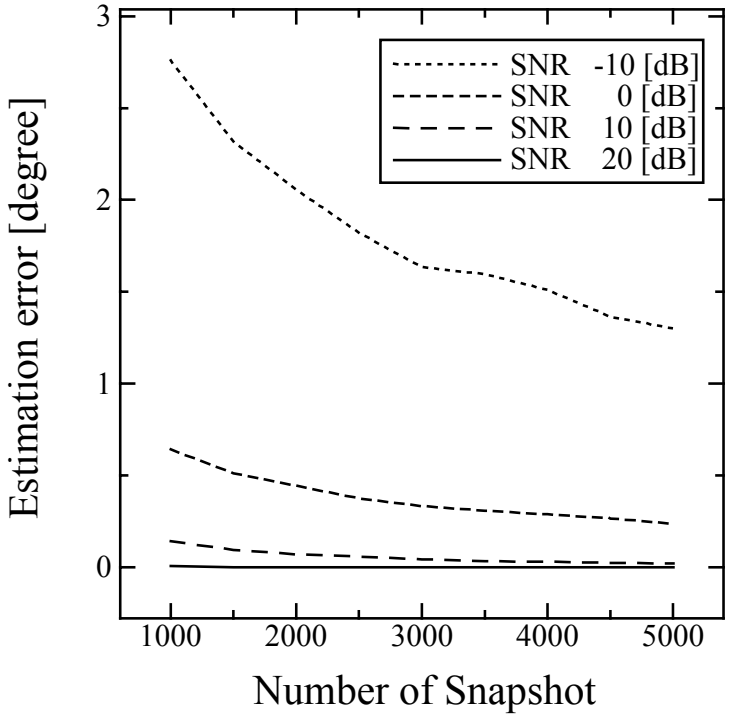

Fig. 4-5 The influence of SN ratio

4.3.3 Influence of position errors at each position

The influence of position errors was evaluated by performing simulations of methods using eigenvectors. Position errors at each position were given by uniform random numbers. Simulations were conducted while the ranges of position errors were varied. The other specifications of the simulation were the same as in Sec. 4.3.1. The definition of the estimation error is given by Eq. (16).

Fig. 4-6 shows the results of the simulations. When the range of errors was small, DOA could be estimated correctly. On the other hand, DOA estimation error was within 3° when the range of position errors was large. These results confirmed that the method using eigenvectors is much less sensitive to position errors than that assuming that arrival waves are sinusoidal waves. These results indicate that high-precision equipment is not required for shifting the T-shaped array; therefore, the proposed system is uncomplicated and can be implemented at low cost.

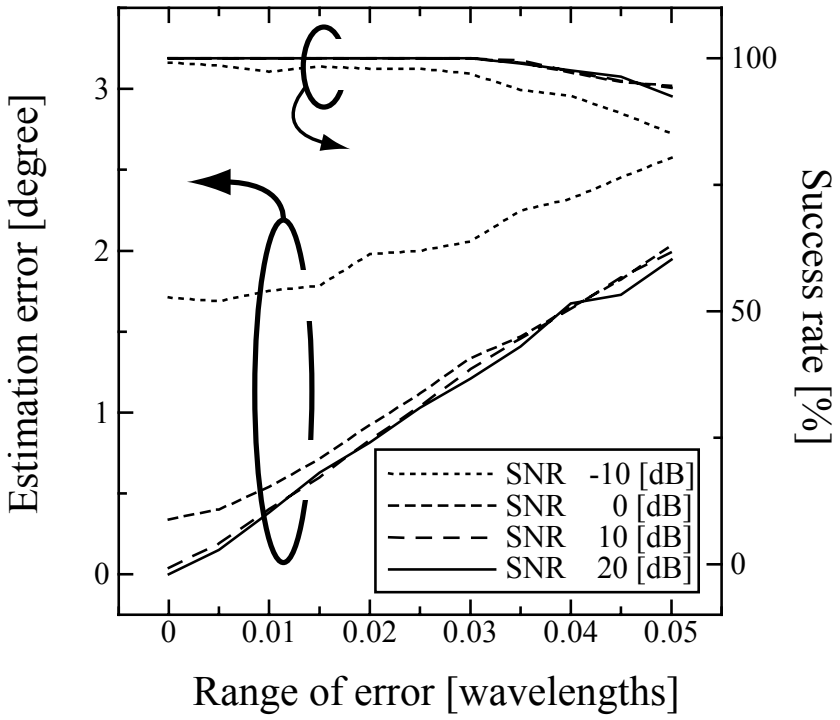

Fig. 4-6 Influence of position errors

4.3.4 Relationship between number of shifting operations and estimation errors

The relationship between the number of shifting operations and the estimation errors was evaluated by performing simulations. The averages of the estimation errors were evaluated by changing the number of shifting operations. The other simulation specifications were the same as in Sec. 4.3.1.

Fig. 4-7 shows the simulation results. DOA estimations degraded when SN ratio was poor, although the estimation error was within 3°. These results confirmed that the proposed system can estimate DOA with accuracy when the number of shifting operations increases.

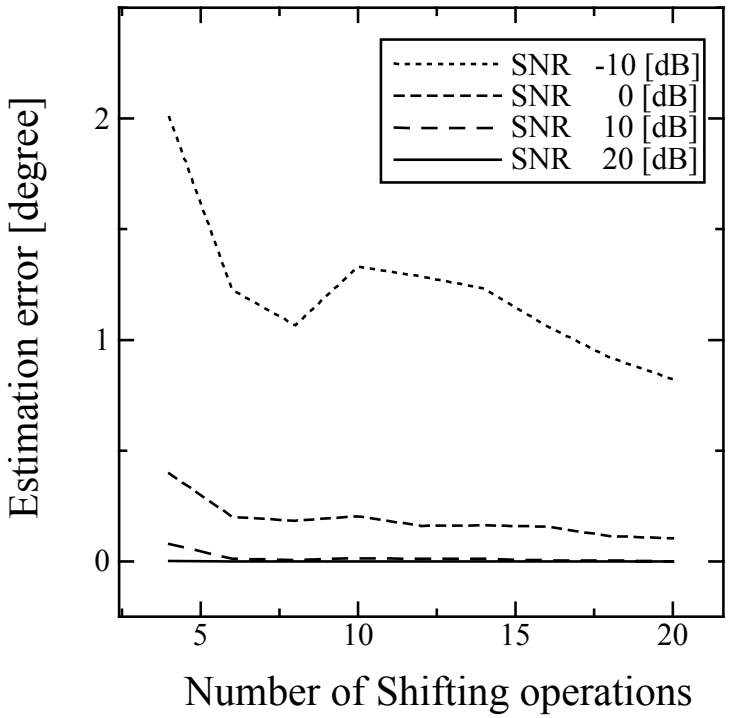

Fig. 4-7 Relationship between number of shifting operations and estimation error

4.4 Measurements in anechoic chamber

Experiments in an anechoic chamber were conducted for confirming the effective and limited characteristics of the proposed method. First, the experiment in one arrival wave was carried out for basic consideration. Then, the experiment in two arrival waves was conducted for confirming DOA estimation when several waves arrive.

4.4.1 Experiments with one arrival wave in an anechoic chamber

The performance of the proposed system in DOA estimation was evaluated by experiment. First, we conducted experiments in an anechoic chamber as shown in Fig. 4-8. Table 4-2 shows the specifications of the experiment, in which a transmitting antenna was shifted to decrease estimation errors caused by the influence of cable twist. The area swept out by shifting the T-shaped receiving antenna was equivalent to the size of a 5 × 4-element planar antenna, which was the size of the virtual planar array. The distance moved $\Delta\hat{x}$ is defined by Eq. (17) such that it becomes equivalent to the theory presented in Sec. 4.2:

$$\Delta\hat{x} = \Delta x \times \cos\theta \quad \textbf{(17)}$$

where Δx is the interval between elements. The subarray for spatial smoothing was a 3 × 3 planar array. The radio frequency was 900 MHz band, the transmitted signal was random modulated with the QPSK method, the sampling frequency of ADC was 40 MHz, the number of samplings was 2000, and the method used for DOA estimation was MUSIC.

The average of DOA estimation error was 0.5°. The estimation errors are summarized in Fig. 4-9, which shows that DOA was estimated accurately.

Table 4-2 Specifications of experiments (one arrival wave)

Array form	The T-shaped array antenna (5+1 elements)
Number of shifting operations	3
Number of virtual planar array elements	5 × 4 (20 elements)
Number of subarray antenna elements	3 × 3 (9 elements)
Interval between elements	0.4 wavelength
Radio frequency	900 MHz band
Chip rate	1.23 Mcps
Sampling frequency of ADC	40 MHz

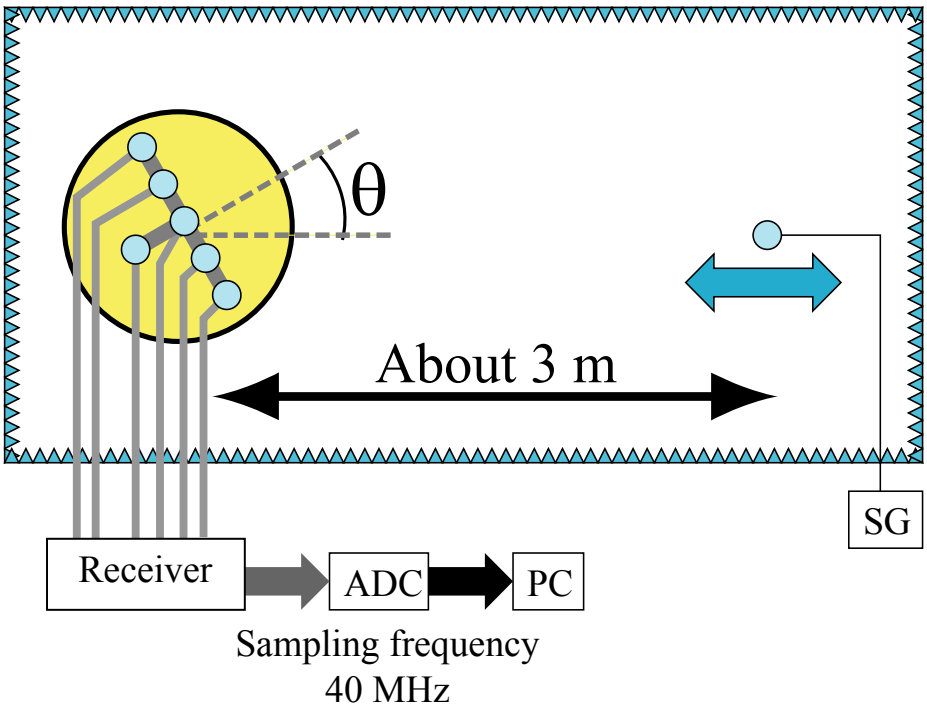

Fig. 4-8 Schematic view of experiment (Case of 1 arrival wave)

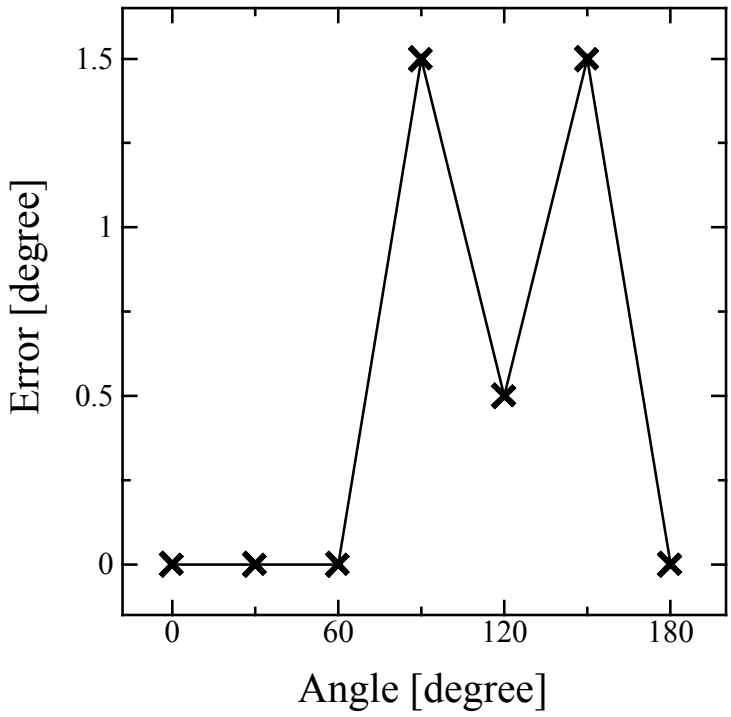

Fig. 4-9 Estimation errors of experimental results (Case of 1 arrival wave)

4.4.2 Experiments with two arrival waves in an anechoic chamber

The experiment with two arrival waves was carried out in anechoic chamber. In the experiment, a T-shaped array antenna was shifted parallel to allow synthesis o the virtual planar array, because transmitters cannot be moved in the manner described in the experiment with one arrival wave. The difference in direction was 30°. The other specifications of number of arrival waves were the same as in the case of one arrival wave. Fig. 4-10 shows the MUSIC spectrum of the experiment results. The average of estimation errors was 1.25°, and DOA could be estimated with accuracy. These results confirmed that the proposed method using eigenvectors could estimate DOA correctly.

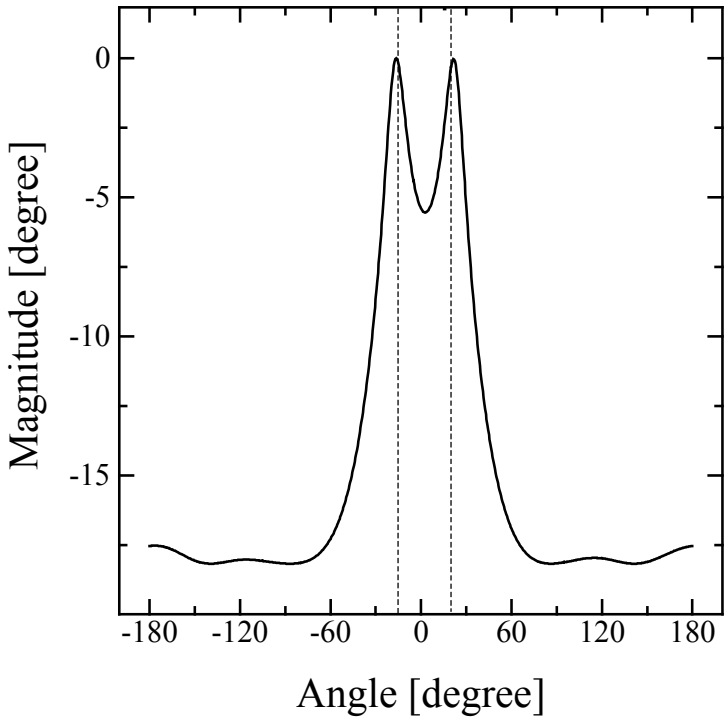

Fig. 4-10 MUSIC spectrum (two arrival waves)

4.5 Summary

In this chapter, we proposed a method of DOA estimation using eigenvectors and described evaluation of the proposed method by simulations and experiments in an anechoic chamber. The methods in **Chapter 2** and **Chapter 3** cannot estimate DOA when arrival waves are random signals without pilot signals. To address these problems, this chapter describes a method of synthesizing data received by the virtual planar array using eigenvectors of correlation matrices. This method uses the characteristic that eigenvectors of correlation matrices have phase information of mode vectors corresponding to DOA. Thus, this method can estimate DOA when arrival waves are random signals.

Simulation results indicated that DOA was estimated correctly within 3° despite the influence of position errors and the poor SN ratio. On the other hand, this method was confirmed to be much less sensitive to SN ratio than the other methods. The performance of the method was evaluated by performing experiments in an anechoic chamber, and the average of estimation errors was about 1.4°. The proposed method could estimate DOA of two arrival waves. These results confirmed that the proposed method is effective for DOA estimation. Further studies are to estimate DOA when arrival waves are non-coherence waves with accuracy.

Chapter 5 Conclusions

This dissertation presented a method for estimating DOA with a virtual planar array synthesized by shifting the T-shaped array antenna. The advantages of this method are low cost because of the reduction in number of receivers and antennas required, reduction of mutual coupling between elements, and weight saving. In the proposed system, it is important to synthesize the data of the virtual planar array by shifting the T-shaped array. Thus, this dissertation proposed three methods for synthesizing the data received by the virtual planar array. The results of simulations and experiments confirmed that the proposed methods were effective for DOA estimation.

Chapter 2 introduced the method for synthesizing virtual planar arrays and base characteristics of the virtual planar array by shifting the T-shaped array antenna in DOA estimations, when it was assumed that arrival waves were sinusoidal. In simulations, the average of estimation errors was within 3° when the SN ratio was within 5 dB when there were influences, such as position errors, frequency fluctuations, *etc*. Then, DOA estimation error was 2.06° in the experiments with one arrival wave, and the proposed method could estimate DOA of two arrival waves in the anechoic chamber. These basic evaluations confirmed the effectiveness of the system using data received by the virtual planar array.

Chapter 3 described a method for estimating the DOA using pilot signals in the CDMA system. We evaluated the proposed method by performing simulations and experiments in an anechoic chamber and outdoor environment. In the simulations, the DOA was estimated accurately, and the effectiveness of the proposed method was confirmed. Moreover, we evaluated the average estimation errors to be approximately 1° in the anechoic chamber, and found that arrival waves from base stations could be estimated in the outdoor environment. These results confirmed that the proposed method provides an effective means of DOA estimation.

Chapter 4 proposed a method of DOA estimation using eigenvectors and discussed evaluation of the proposed method by simulations and experiments performed in an anechoic chamber. Simulation results indicated that DOA was estimated correctly within 3° despite the influence of position errors and the poor SN ratio. On the other hand, this method was confirmed to be much less sensitive to SN ratio than the other methods. The performance of the method was evaluated by performing experiments in an anechoic chamber, and the average of estimation errors was about 1.4°. The proposed method could estimate DOA of two arrival waves. These results confirmed that the proposed method is effective for DOA estimation.

Appendix A Modified Calibration method for planar array antenna

A.1 Introduction

Radio waves from base stations in urban areas arrive from several directions in the horizontal plane. Further, the directions of arrival of these waves may be proximate. Therefore, systems based on super-resolution methods, such as MUSIC and ESPRIT, using the array antenna are useful for measurement of multipath propagation. In this case, there are mutual couplings between antenna elements and differences in phase and amplitude between channels in radio frequency (RF) parts. Therefore, the accuracy of DOA estimation is reduced. To resolve this problem, calibration methods for RF parts have been proposed [139]–[148]. A method was proposed previously in which measured mode vectors are applied to MUSIC for calibration of RF parts [139]. Although this method can correctly calibrate RF parts because the influences of mutual coupling and phase differences between channels can be considered, it has a number of faults, such as the requirement for the mode vector to be measured in all directions, and the non-applicability to ESPRIT. Moreover, this method cannot estimate DOA of coherent waves because the forward/backward spatial smoothing method cannot be applied. On the other hand, another method to estimate mutual coupling and fluctuations between elements by known sources has been proposed [140][141]. This method calibrates received data without mutual couplings by applying reverse specifications to received data, assuming that antennas have a single mode. This method can estimate DOA with F/B spatial smoothing, MUSIC, and ESPRIT. However, this method cannot consider influences, such as fabrication errors, position errors of antenna elements, and infinite ground plane. Therefore, DOA cannot be estimated correctly due to defective calibrations. A method was reported in which the calibration is carried out using mutual impedance measured with a network analyzer [142][143]. This method is not better than that using known sources, although it can be applied to the F/B spatial smoothing method [144]. A method using the moment method has been proposed, which can calibrate errors in the case of multimode antennas and with influence from the infinite and reflector planes [145]–[148]. Although this method can calibrate array antennas with arbitrary geometry, estimating coherent waves is difficult because the F/B spatial smoothing method cannot be applied.

To address these problems, this appendix introduces a modified calibration method that is more accurate than the conventional methods. The results of simulations and experiments

carried out to confirm efficiency are described. The proposed method uses the method with known sources [140][141] to obtain calibrated data, which are applied to mode vectors. This method can calibrate errors that cannot be calibrated by the method using known sources, and can estimate DOA with accuracy. This method can be applied to the F/B spatial smoothing method with consideration of the influence of reflector and infinite planes because it is equivalent to using measured mode vectors, and thus coherent waves can be estimated. On the other hand, although arrival waves with low elevation are considered in the conventional system, arrival waves with high elevation cannot be ignored because of the recent development of microcellular systems. Further, DOA estimation is carried out around base stations that are set up on the rooftops of buildings to find wave sources. Arrival waves at high elevation and depression angles cannot be estimated with accuracy because antenna patterns in the horizontal plane are different at different elevations and depression angles. Thus, accurate DOA estimation at high elevations and depression angles may be carried out with application of calibration tables measured at each elevation angle.

In this appendix, the theory of the proposed method for calibration of RF parts is introduced, and the effectiveness of the proposed method confirmed by simulations and experiments is described.

A.2 Improved calibration method for planar array antenna

In this section, a modified calibration method for the MUSIC method with a rectangular array is described. The method using known sources was combined with the mode vector measured in the proposed method. This method improves errors, which cannot be calibrated by the method using known sources, due to the use of measured mode vectors. The accuracy of DOA estimation is increased because of the use of more orthogonal mode vectors to the subspace correlation matrix, obtained from measured data.

A.2.1 Modeling of mutual coupling between antenna elements

The reasons for DOA estimation errors are the differences in phase and amplitude between channels in a receiver, fabrication and position errors of antennas, and mutual coupling between antenna elements. The mutual couplings may change because they are defined by the shapes and positions of antennas. It is assumed that the characteristics of the receiver, such as phase and amplitude, do not change at the time points of measuring data for calibration and DOA estimations, although these characteristics may change over long periods.

The shape of the array antenna is an M × N planar array, as shown in Fig. A-1. It is assumed that the number of arrival waves is one, and the direction from each arrival wave is $\theta_l (l = 1, \cdots, L)$. In this case, the received data are given by:

$$\hat{\mathbf{x}}_l(t) = \mathbf{C}\boldsymbol{\Gamma}\mathbf{a}(\theta_l)\mathbf{s}_l(t) + \mathbf{n}(t) \tag{18}$$

$$\mathbf{C} = \begin{bmatrix} c_{1,1} & c_{1,2} & \cdots & c_{1,MN} \\ c_{2,1} & c_{2,1} & \cdots & c_{2,MN} \\ \vdots & \vdots & \ddots & \vdots \\ c_{MN,1} & c_{MN,2} & \cdots & c_{MN,MN} \end{bmatrix}$$

$$\boldsymbol{\Gamma} = diag\left\{\gamma_1, \gamma_2, \cdots, \gamma_{MN}\right\}$$

$$\mathbf{a}(\theta_l) = \left[\varphi_{11}(\theta_l), \varphi_{12}(\theta_l), \cdots, \varphi_{1N}(\theta_l), \varphi_{21}(\theta_l), \varphi_{22}(\theta_l), \cdots, \varphi_{MN}(\theta_l)\right]^T$$

$$\varphi_{mn}(\theta_l) = e^{j\frac{2\pi}{\lambda}\{\Delta y(n-1)\sin\theta_l + \Delta x(m-1)\cos\theta_l\}} \qquad (m = 1, 2, \cdots, M, n = 1, 2, \cdots, N)$$

where the superscript ^{T} denotes transposition, $\mathbf{s}_l(t)$ is the complex amplitude of the *l*-th incident wave, $\mathbf{C}$ and $\boldsymbol{\Gamma}$ express mutual couplings and differences in amplitude and phase of channels, respectively, $\mathbf{a}(\theta_l)$ is a mode vector, and $\varphi_{mn}(\theta_l)$ is the phase difference relative to a base point. If $\mathbf{C}, \boldsymbol{\Gamma}$ are calculated by a given method, the received data can be calibrated as follows.

$$\mathbf{x}_l(t) = \left(\mathbf{C}\boldsymbol{\Gamma}\right)^{-1}\hat{\mathbf{x}}_l(t) \tag{19}$$

In the method using known sources, $\mathbf{C}, \boldsymbol{\Gamma}$ are computed using orthogonal eigenvectors of the correlation matrix in the noise subspace and mode vectors, and the received data are calibrated as shown in Eq. (19).

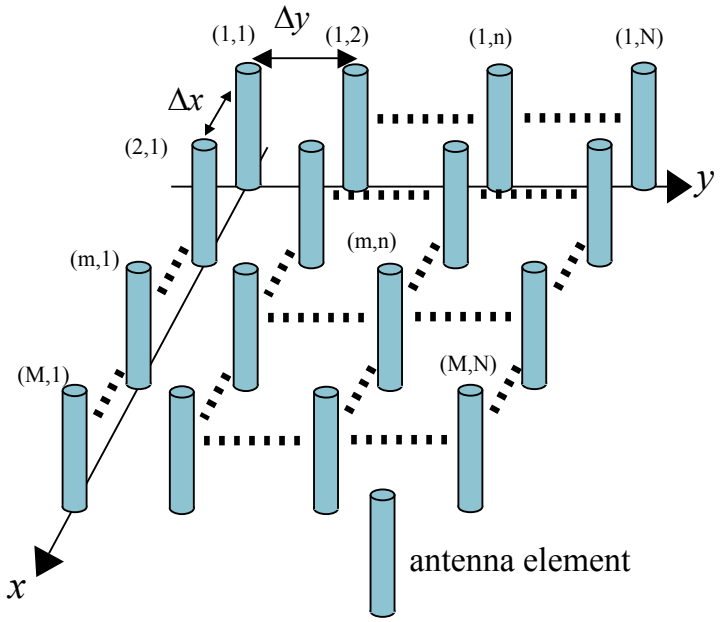

Fig. A-1 Planar array antenna

A.2.2 Modified calibration method for MUSIC method

Although mutual couplings are calculated by modeling, *e.g.*, by the equation in the method using known sources, there are errors due to the influence of scattering from the edges of the infinite plane and actual antenna elements without omni-pattern. Thus, the accuracy of DOA estimation is degraded because these errors are not modeled in the method using known sources and calibrated correctly. On the other hand, the method using measured mode vectors can calibrate these errors. However, this method cannot be applied to the F/B spatial smoothing procedure, and therefore DOA cannot be estimated. This chapter proposes a modified calibration method to resolve these problems. The proposed method uses the method with known sources to obtain calibrated data, and these calibrated data are used as mode vectors. The proposed method computes more orthogonal mode vectors to noise eigenvectors of the correlation matrix than the method using known sources, and thus the accuracy of DOA is improved. Moreover, the proposed method can use the F/B spatial smoothing method.

In the method using known sources, $\mathbf{C}$ and $\mathbf{\Gamma}$ are computed from data received from several known sources. Then, data in DOA estimation are multiplied by the inverse characteristics of $\mathbf{C}$ and $\mathbf{\Gamma}$, and DOA can be estimated assuming that mode vectors $\mathbf{a}(\theta)$ are ideal. On the other hand, this method uses mode vectors $\mathbf{a}(\theta)$, which are computed as follows.

$\mathbf{C}$ and $\mathbf{\Gamma}$ are estimated by the method using known sources. These matrices are expressed as

$\hat{\mathbf{C}}$ and $\hat{\mathbf{\Gamma}}$, respectively. $\hat{\mathbf{C}}\hat{\mathbf{\Gamma}}$ is not equal to $\mathbf{C\Gamma}$, because of the influences of irregular antenna patterns and scattering from the edges of the infinite plane. It is assumed that the number of arrival waves is one, using the same data when $\hat{\mathbf{C}}\hat{\mathbf{\Gamma}}$ is calculated, and the correlation matrix **R** is given by:

$$\mathbf{R}_l = E\left[\mathbf{x}_l(t)\mathbf{x}_l^H(t)\right] = E\left[\left(\hat{\mathbf{C}}\hat{\mathbf{\Gamma}}\right)^{-1}\hat{\mathbf{x}}_l(t)\hat{\mathbf{x}}_l^H(t)\left(\left(\hat{\mathbf{C}}\hat{\mathbf{\Gamma}}\right)^{-1}\right)^H\right]$$

$$\mathbf{x}_l(t) = \left(\hat{\mathbf{C}}\hat{\mathbf{\Gamma}}\right)^{-1}\hat{\mathbf{x}}_l(t)$$

where the superscript ^{H} denotes conjugate transposition. The eigenvector corresponding to the maximal value of the correlation matrix is $\hat{\mathbf{e}}_1^{(l)}$, the and other eigenvectors are $\hat{\mathbf{e}}_n^{(l)}$. In this case, the relationship between $\hat{\mathbf{e}}_1^{(l)}$ and $\hat{\mathbf{e}}_n^{(l)}$ is as follows:

$$\left\{\hat{\mathbf{e}}_1^{(l)}\right\} \perp \left\{\hat{\mathbf{e}}_2^{(l)}, \cdots, \hat{\mathbf{e}}_N^{(l)}\right\}$$

From these specifications, $\hat{\mathbf{e}}_1^{(l)}$ is used as a calibration table as shown in Eq. (3) when MUSIC spectra $\hat{P}_{MU}(\theta_l)$ are calculated. This improves the orthogonality of noise eigenvectors obtained to use the eigenvector $\hat{\mathbf{e}}_1^{(l)}$ and DOA is estimated more accurately:

$$\hat{P}_{MU}(\theta_l) = \frac{\hat{\mathbf{a}}^H(\theta_l)\hat{\mathbf{a}}(\theta_l)}{\hat{\mathbf{a}}^H(\theta_l)\mathbf{E}_N\mathbf{E}_N^H\hat{\mathbf{a}}(\theta_l)} \quad \textbf{(20)}$$

$$\hat{\mathbf{a}}(\theta_l) = \hat{\mathbf{e}}_1^{(l)}$$

where $\mathbf{E}_N$ is a matrix composed of eigenvectors in the noise subspace of the correlation matrix, which is computed from the data calibrated using the inverse matrix of $\hat{\mathbf{C}}\hat{\mathbf{\Gamma}}$. Therefore, further orthogonal mode vectors to noise subspace calculated from the measured data are applied to estimate DOA because the mode vectors include errors that cannot be calibrated, and the accuracy of DOA can be estimated in advance. When the number of known sources is insufficient in the required resolution of DOA estimation, mode vectors among the above mode vectors are subjected to spline interpolation, and the calibration table corresponding to the

necessary resolution is calculated.

When the F/B spatial smoothing procedure is applied to the proposed method, the correlation matrix for calculating mode vectors $\hat{\mathbf{a}}(\theta_l)$ is replaced with a correlation matrix with F/B spatial smoothing as follows. Subarray antennas are an $M' \times N'$ planar array antenna:

$$\mathbf{R}'_l = \sum_{k=1}^{K} \frac{\mathbf{R}'_{lk} + \mathbf{J}\mathbf{R}'_{lk}\mathbf{J}}{2}, \quad K = (M - M' + 1)(N - N' + 1) \tag{21}$$

$$(M' = 1, \cdots, M, N' = 1, \cdots, N, M' \times N' \geq 2)$$

$$\mathbf{R}'_{lk} = E\left[\mathbf{x}_{lk}(t)\mathbf{x}_{lk}^H(t)\right]$$

$$\mathbf{J} = \begin{bmatrix} 0 & \cdots & 0 & 1 \\ 0 & \cdots & 1 & 0 \\ \vdots & \iddots & \vdots & \vdots \\ 1 & \cdots & 0 & 0 \end{bmatrix}$$

$$\mathbf{x}_l(t) = \left(\hat{\mathbf{C}}\hat{\mathbf{\Gamma}}\right)^{-1} \hat{\mathbf{x}}_l(t)$$

where $\mathbf{x}_{lk}(t)$ is the received signal vector of the *k*-th subarray antenna. Eigenvalue decomposition of the correlation matrix $\mathbf{R}'_l$ is carried out, and a calibration table is computed with the eigenvectors corresponding to the maximal eigenvalues. Then, the received data for DOA estimation are applied to the F/B spatial smoothing procedure, and DOA is estimated by computing the MUSIC spectrum in the same way as described for the case without using the F/B spatial smoothing procedure. When the number of known sources is insufficient in the required resolution of DOA estimation, the same processing as described above is performed.

In urban areas, arrival waves have various elevation angles because the antennas of base stations and repeaters are set up on high buildings. In addition, arrival waves exit at a certain depression angle. The accuracy of DOA estimation may degrade when arrival waves have different elevations from the angle of measurements for the calibration table, because the antenna patterns of a DOA estimation system change at several elevations and depression angles. Therefore, these errors are reduced by preparing calibration tables computed at each elevation angle.

A.3 Numerical analysis of the improved calibration method

A.3.1 Comparisons with the conventional method

The performance of the proposed method during calibration was evaluated by comparison with the method using known sources. To determine the influences of mutual coupling, infinite plane, and different angles in elevation or depression, the received signal vectors were calculated using antenna patterns at each elevation that are the result of the method of moments. Antenna models were monopole antennas, the interval between elements was 0.45 wavelengths, the array form was a 2 × 2 planar array, and the size of the ground plane was 0.9 × 0.9 wavelengths. Fig. A-2 shows the radiation patterns of array antennas at elevations of 0° and 40° from the horizontal plane by MoM. If there is one element, the radiation pattern is omni. However, the radiation patterns are illegal due to mutual couplings and the influence of the infinite plane. In addition, the radiation patterns change due to differences in elevation angle, and thus the performance of DOA estimation may be degraded.

First, simulations with an elevation angle of arrival waves of 0° was carried out. Table A-1 shows the simulation specifications. SNR was 20 dB and the sampling number was 2000. The calibration table was computed by each method using the known sources at an elevation of 0°. The known sources incidence from all directions at intervals of 5°, and the number of known sources was 120. The resolution of MUSIC was 0.5°. In this simulation, RMSE was evaluated by:

$$RMSE = \sqrt{\frac{1}{N}\sum_{i=1}^{N}\left|\hat{\theta}_i - \theta_i\right|^2} \tag{22}$$

where N is the number of trials, $\hat{\theta}_i$ is the estimation result, and θ_i is the true value. The results obtained with the conventional method was 0.0053°, while that obtained with the proposed method was 0.046°. These results showed that the accuracy of the proposed method is the same as that of the conventional method.

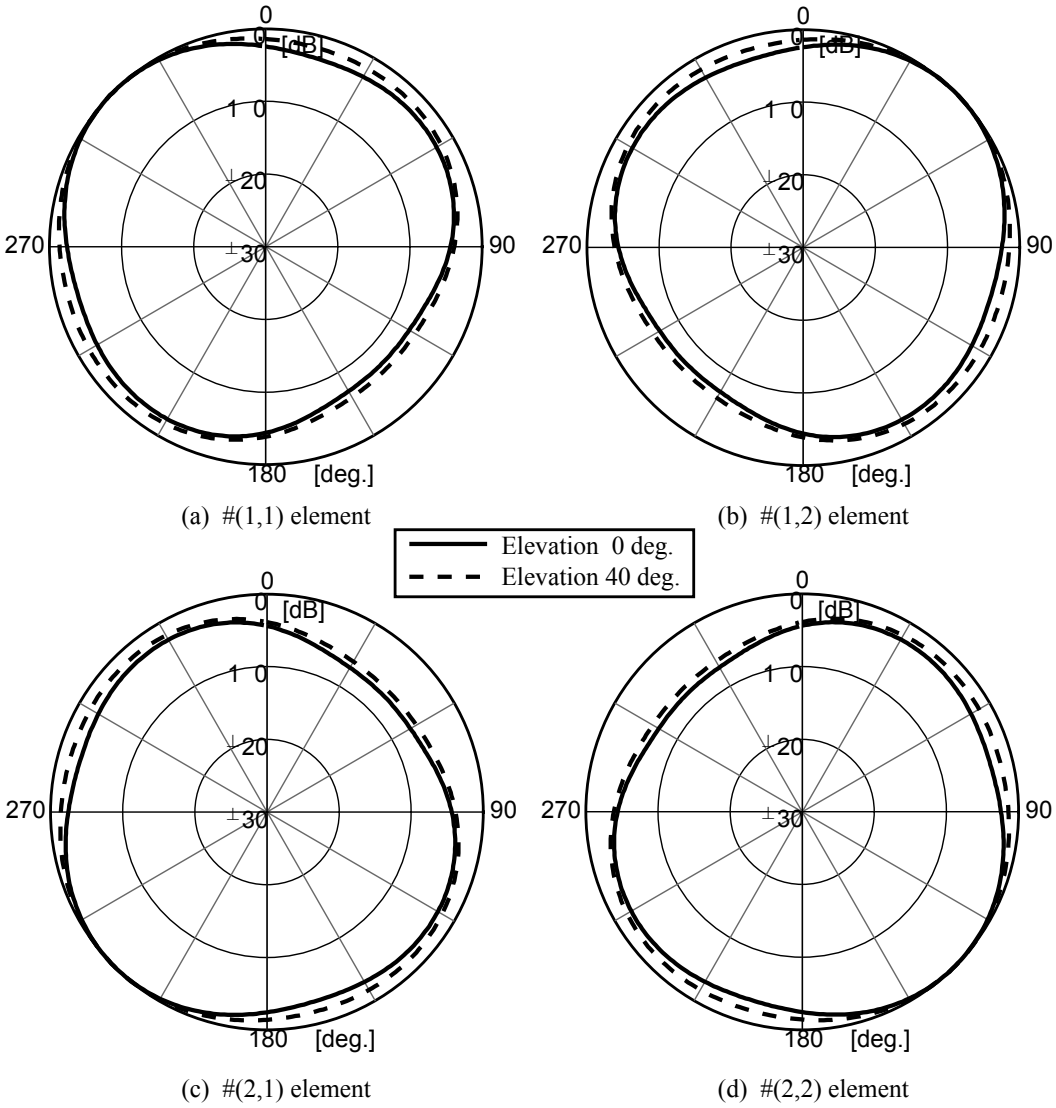

Fig. A-2 Radiation patterns (2 × 2 array antennas)

Table A-1 Simulation specifications

Array form	2×2 planar array
Interval between elements	0.45 wavelengths
Number of arrival waves	1
Sampling number	2000
SN ratio	20 dB

Then, the proposed method was evaluated by simulation with an elevation angle of arrival waves of 40°. The known waves incident with an elevation angle of 40° were used to calculate the calibration table. Parameters other than the elevation were the same. Fig. A-3 shows the results. RMSE for the conventional method was 2.00 and the accuracy of DOA estimation became poorer. On the other hand, the proposed method yielded a good estimate because RMSE was 0.05°. These results confirmed that the proposed method is effective for calibration when elevation angles are changed. In outdoor environments, the elevations of arrival waves are known. Thus, two or more calibration tables that change the elevation are prepared, and DOA is estimated by applying MUSIC to these calibration tables. For this method, DOA can be estimated with accuracy.

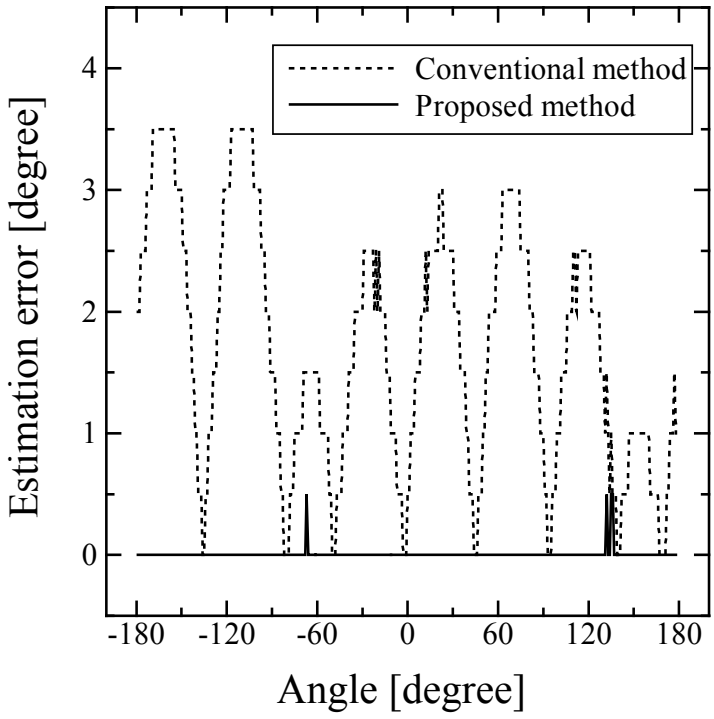

Fig. A-3 Estimation errors (elevation 40°)

A.3.2 Characteristics in the case of incoherent waves

The characteristics of the proposed method were evaluated by performing simulation in the case of 2 incoherent waves. RMSE was calculated by estimating DOA with changing angle from 0° to 360° where the difference between 2 incoherent waves with equal powers was fixed to 40°. The other simulation specifications were the same as in Sec. A.3. The results of the

MUSIC spectrum are shown in Fig. A-4. As shown in this figure, the proposed method was confirmed to be able to distinguish two waves with accuracy. RMSE was 0.28°. These results indicated that the proposed method can estimate DOA in the case of two incoherent waves.

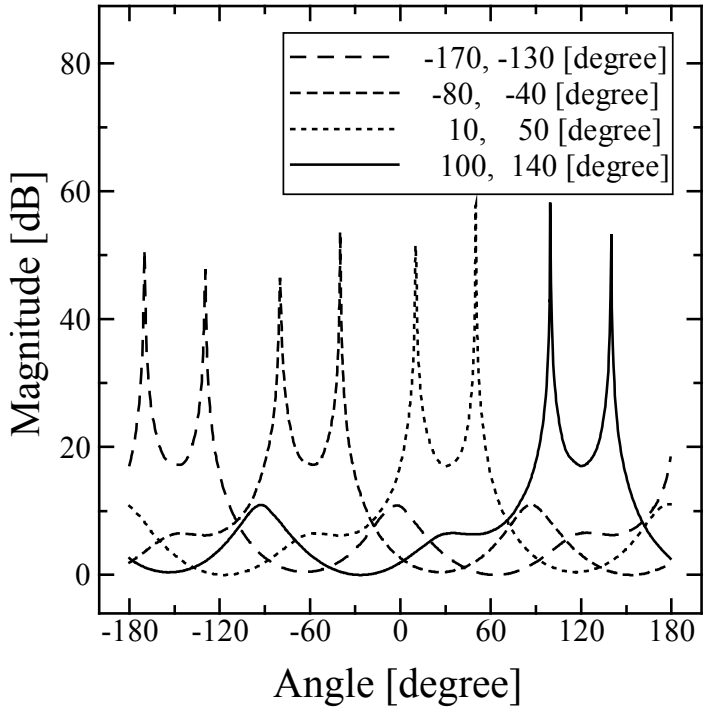

Fig. A-4 Simulation results of the MUSIC spectrum (Incoherent waves)

A.3.3 Characteristics in the case of coherent waves

The characteristics of the proposed method were evaluated by performing simulation in the case of two coherent waves. The array form was a 3 × 3 planar array, antenna elements were monopole antennas, the interval between elements was 0.45 wavelengths, and the size of the infinite ground plane was 1.35 × 1.35 wavelengths. The subarray form was a 2 × 2 planar array. RMSE was calculated by estimating DOA with changing angle from 0° to 360° where the difference between two coherent waves with equal powers was fixed to 40°. The calibration table was computed using Eq. (22) with the F/B spatial smoothing procedure. Elevation angles were 0°. The other simulation specifications were the same as in Sec. A.3. The results of the MUSIC spectrum are shown in Fig. A-5. As shown in this figure, it was confirmed that the proposed method can distinguish two waves with accuracy. RMSE was 0.13°. These results indicated that the proposed method can estimate DOA in the case of two incoherent waves.

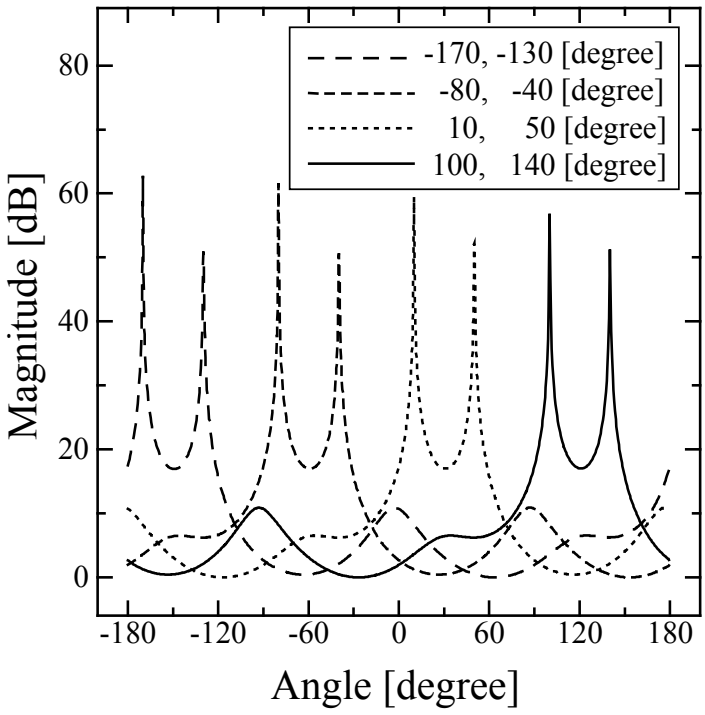

Fig. A-5 MUSIC spectrum (Coherent waves)

A.4 Evaluation of the prototype system

The performance of the proposed method during calibration was evaluated by several experiments. First, a comparison with the conventional method was performed. Then, the results with changing elevation were determined. Finally, experiments with two incoherent waves were performed.

A.4.1 Comparisons with the conventional method

The performance of the proposed method was evaluated by conducting experiments in the case of one wave in an anechoic chamber. Antennas were adjusted to the same height. The elevation angle was 0°. The radio frequency was a sinusoidal wave of 900 MHz that was not modulated. In this experiment, IF of a receiver was about 20 MHz. The data were sampled at 80 MHz, and baseband signals were calculated by a digital down convert; these data were used for DOA estimation. The SNR computed by applying output signals from ADC to Fourier transform

was about 30 dB. The array form was a 2 × 2 planar array, of which the interval was 0.45 wavelengths. Data were measured twice—the first were used for calibration, and the second for evaluating DOA estimation. The performance of the proposed method was evaluated based on these results. RMSE was calculated using Eq. (22).

Fig. A-6 shows the estimation errors when the incident angle was changed. In these experiments, RMSE without calibration, with the conventional method, and with the proposed method were 3.7°, 2.4°, and 0.5°, respectively. Although estimation errors were large in the case without the calibration, the accuracy of DOA estimations was better using the method with known sources. Moreover, improvements in accuracy of about 2° were obtained using the proposed method. This experiment was performed to examine the case in which the elevation of arrival waves is 0°. However, the results with the conventional and proposed methods were the same in the simulation. Although the conventional method cannot consider fabrication errors or differences in each antenna element in real systems, the proposed method can calibrate these errors because they are included in the mode vectors used by the proposed method. Thus, the proposed method can estimate DOA without increasing the errors. The results of these experiments confirmed the effectiveness of the proposed method.

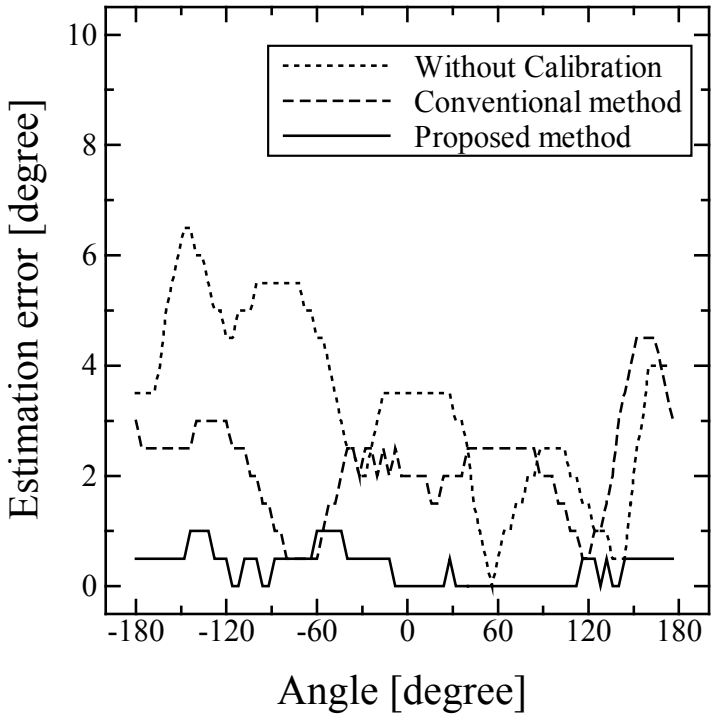

Fig. A-6 Experiment results

A.4.2 Elevation characteristics of the proposed method

The performance of the proposed method was evaluated by conducting experiments at several elevation angles. The number of arrival waves was one, and this experiment is conduced in an anechoic chamber. The heights of the antennas were adjusted such that the elevation of the arrival waves was –20, 0, 20, or 40°.

Data were measured twice at each elevation angle—the first were used for calibration, and the second for evaluating DOA estimation. The performance of the proposed method was evaluated based on these results. RMSE was calculated by Eq. (22). The other specifications were the same as in Sec. A.4.1. Fig. A-7 shows examples of radiation patterns of antenna elements at –20°, 0°, and 20°. As shown in this figure, the radiation patterns are illegal because of the influence of mutual couplings, infinite ground plane, and fabrication errors. Moreover, antenna patterns changed when the elevation angles were varied. Thus, DOA may not be estimated accurately at several elevations when only one calibration table is prepared.

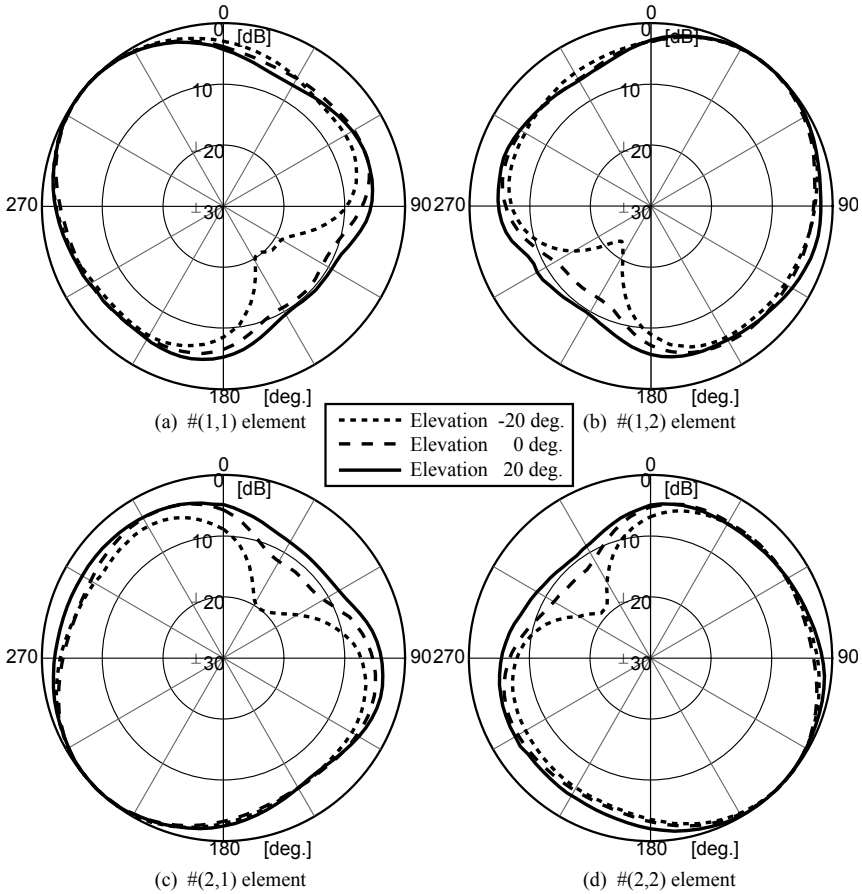

Fig. A-7 Antenna patterns (Experiments)

Table A-2 Elevation specifications

	Elevation for calibration [degree]	Elevation for evaluating estimation errors [degree]	Calibration method
Case 1	0	20	Reference signals
Case 2	20	20	Reference signals
Case 3	20	20	Proposed method
Case 4	0	40	Reference signals
Case 5	40	40	Reference signals
Case 6	40	40	Proposed method
Case 7	0	–20	Reference signals
Case 8	–20	–20	Reference signals
Case 9	–20	–20	Proposed method

Fig. A-8 shows the results from Case 1 to Case 3. In these experiments, RMSE of Case 1, Case 2, and Case 3 were 2.7°, 2.4°, and 0.27°, respectively. Although the accuracy of DOA estimation was not improved by changing the elevation for the calibration with the conventional method, the accuracy at each elevation was the same as that with an elevation angle of 0° using the proposed method.

Fig. A-9 shows the results from Case 4 to Case 6. In these experiments, RMSE of Case 4, Case 5, and Case 6 were 4.0°, 3.8°, and 0.9°, respectively. The errors were greater than with an elevation of 20°. This was due to the increased influence of scattering waves from the edge of the infinite ground plane and because antenna mode cannot be assumed as single mode; thus, errors increased in the case of the conventional method. On the other hand, the proposed method could estimate accurately because these influence were included in the calibration table. The experimental results confirmed that the proposed method is useful in the case of high elevations.

Finally, Fig. A-10 shows the results from Case 7 to Case 9. In these experiments, RMSE of Case 7, Case 8, and Case 9 were 3.3°, 2.3°, and 0.6°, respectively. These results showed that the proposed method can calibrate the errors accurately when arrival waves have depression angles. These results confirmed that arrival waves with high elevation and depression angles can be estimated with the proposed method by preparing and using calibration tables of several elevation angles.

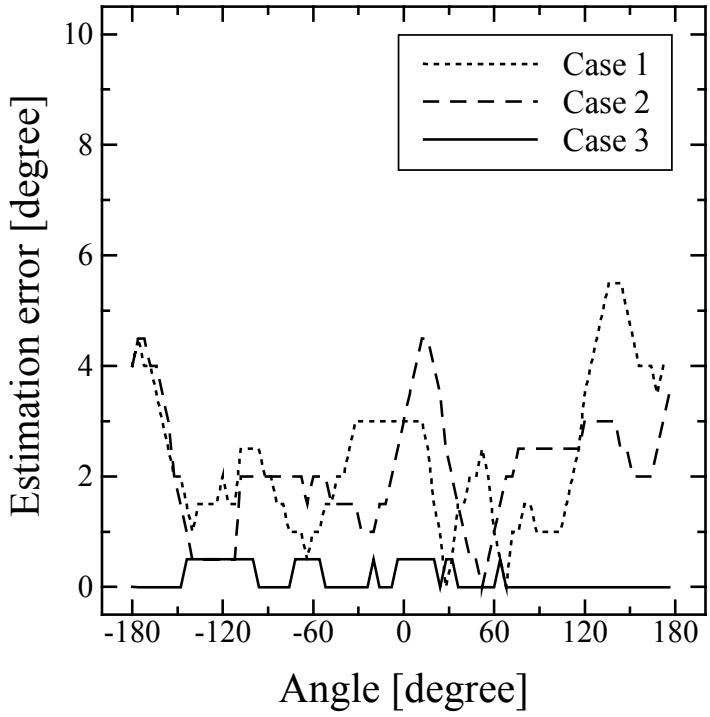

Fig. A-8 Estimation errors (elevation 20°)

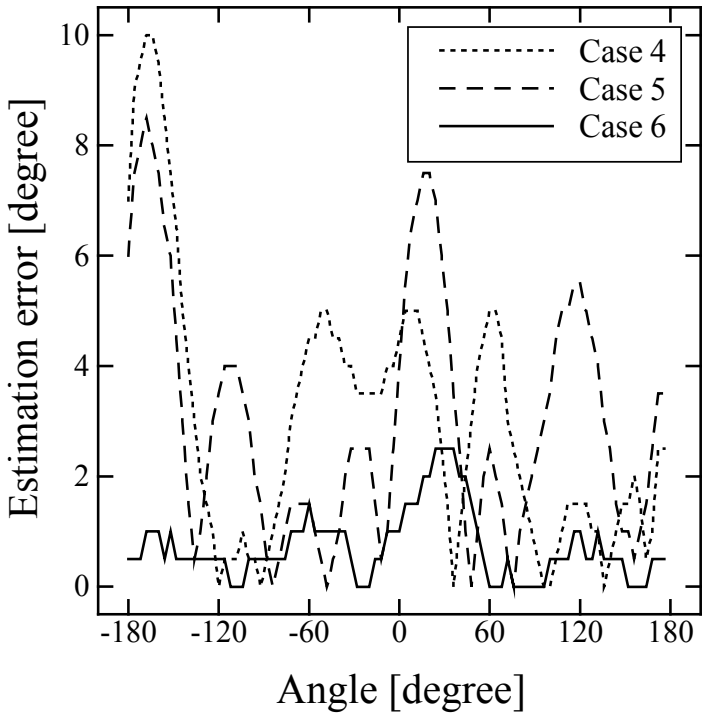

Fig. A-9 Estimation errors (elevation 40°)

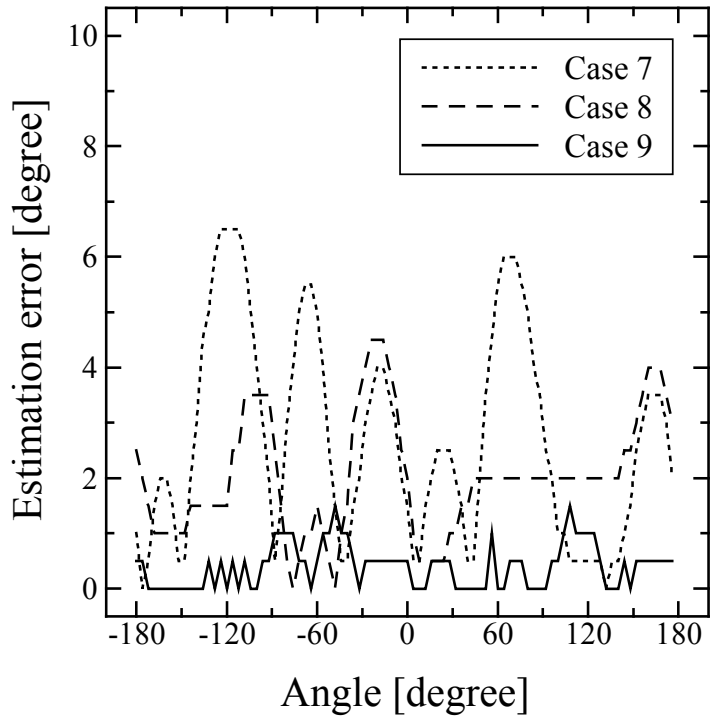

Fig. A-10 Estimation errors (elevation –20°)

A.4.3 Characteristics in the case of incoherent waves

The performance of the proposed method was evaluated by conducting experiments in the case of two incoherent waves. This experiment was conduced in an anechoic chamber. The antennas were adjusted to the same height. Incident waves were sinusoidal waves of 900 MHz that were not modulated. The frequencies of two waves were different by 7 MHz, and thus the arrival waves were incoherent waves. Transmission powers were equal. The angle difference was fixed to 40°, and arrival waves were measured with rotation of the array antenna by 360°. In this experiment, the SNR computed by applying output signals from ADC to Fourier transform was about 30 dB. The other specifications were the same as in Sec. A.4.1. RMSE was calculated by Eq. (22).

Fig. A-11 shows examples of MUSC spectra at several angles. The results shown in this figure confirmed that the system with the proposed method can distinguish two waves, and estimate DOA. These results confirmed the useful of the proposed method.

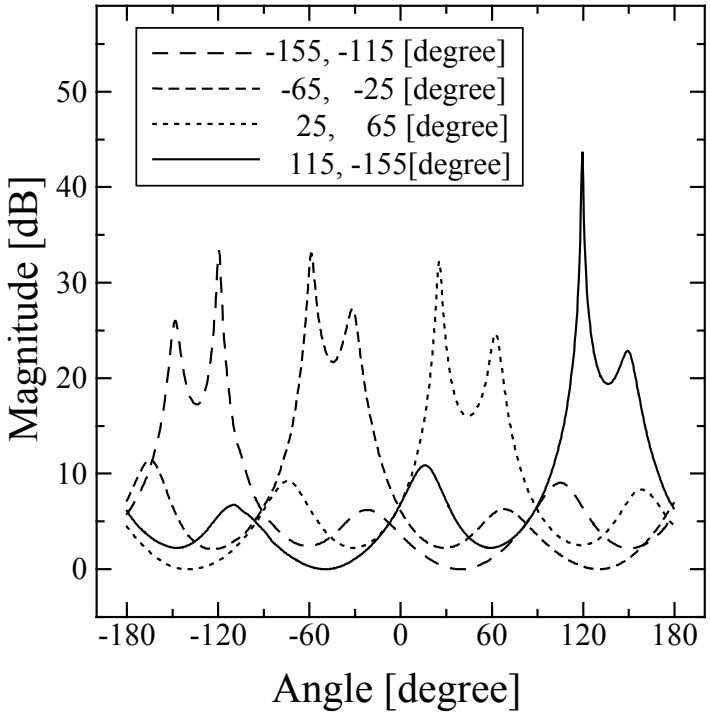

Fig. A-11 Experiment results (two arrival waves)

A.5 Conclusions

This appendix described the modified calibration method for the MUSIC method with a planar array. The proposed method can calibrate including the errors due to position errors and differences between antenna elements. Thus, this method is effective for DOA estimation. In addition, the proposed method can be applied to the F/B spatial smoothing method, and thus can be used for estimation of coherent waves. The effectiveness in the case of high elevation was confirmed by simulations. Moreover, experiments were conduced with the trial system, and the results confirmed that arrival waves with high elevation or depression angles can be estimated more accurately using the proposed method in comparison with the conventional method. These results confirmed that the proposed method provides effective calibration.

Appendix B DOA estimation system using virtual planar array with sequential measurements

B.1 Introduction

The quality of mobile communication must be improved, particularly in urban areas. Thus, it is important to estimate DOA from base stations and repeaters, and a planar array is effective for obtaining such measurements. However, systems with planar arrays require many elements for F/B SSP. This results in a high expenditure on receivers with a corresponding increase in the weight and size of the estimation system. This dissertation presented a DOA estimation system with a T-shaped array antenna to reduce the cost, and described the results of experiments confirming the effectiveness of the proposed method. The T-shaped array remains at rest in the proposed method when data of arrival waves are measured. On the other hand, if measurements of arrival waves are conducted while moving the T-shaped array, the usefulness of measurement of arrival waves was improved. Therefore, this appendix discusses evaluation of the DOA estimation method while moving the T-shaped array antenna. It is possible that there may be errors when measurements are obtained while moving the T-shaped array. Errors in measurement positions as shown in Fig. B-1 may increase when arrival waves are measured continuously. These errors are referred to as position errors in this appendix. Moreover, if the T-shaped array antenna is moving when data of arrival waves are obtained, this removes the cause of estimation errors. These errors are referred to as shifting errors in this appendix.

The influences of position and shifting errors were evaluated during DOA estimation by simulations and experiments. Although the method of shifting the T-shaped array continuously can be applied to the three methods proposed in this dissertation, the method using eigenvectors was used for synthesizing data of the virtual planar array.

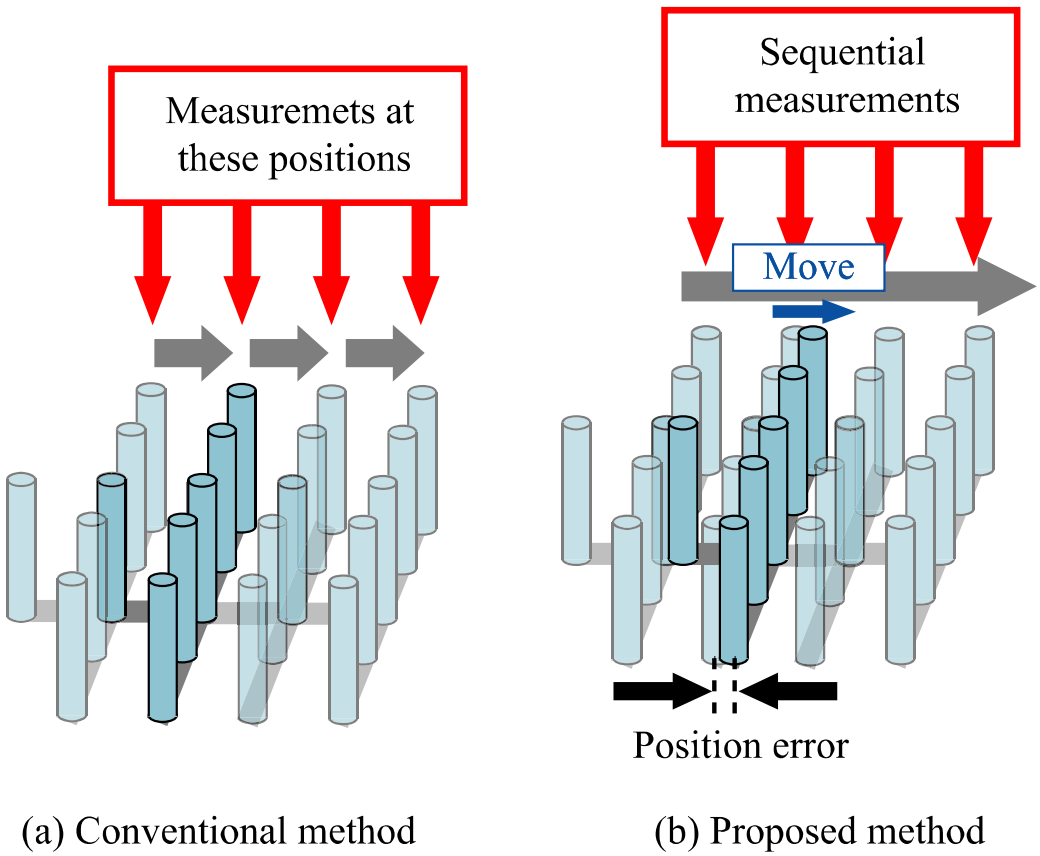

Fig. B-1 Measurement methods

B.2 Simulations

This section presents the results of simulation of the proposed method with sequential measurements during DOA estimation. Table B-1 shows the simulation specifications. Arrival waves were measured continuously with a T-shaped array as shown in Fig. B-1, and then DOA was estimated from the data of the virtual planar array synthesized using eigenvectors. The estimation algorithm used was MUSIC, the number of arrival waves was 6, and the averages of estimation errors were computed. In this case, there were errors due to measurement while shifting and position errors as shown in Fig. B-1. The array form was a 7 + 1 T-shaped array antenna, and a 7 × 4 virtual planar array was synthesized by shifting 3 times.

Fig. B-2 shows the simulation results. It was confirmed that the influence of these errors on DOA estimation was small. For example, position errors were about 0.004 wavelengths and shifting errors were about 3×10^{-5} wavelengths in the trial system described in Sec. B.3. Thus, there were no errors during DOA estimation due to sequential measurements. These results confirmed the possibility of sequential measurements using this method.

Table B-1 Simulation specifications

Array form	T-shaped array antenna (7 + 1 elements)
Number of virtual planar array elements	7 × 4 (28 elements)
Number of subarray elements	3 × 3 (9 elements)
Interval between elements	0.4 λ
Number of arrival waves	6 (–140°, –40°, –10°, 70°, 100°, 160°,)
SN ratio	20 dB
Number of snapshots	2000

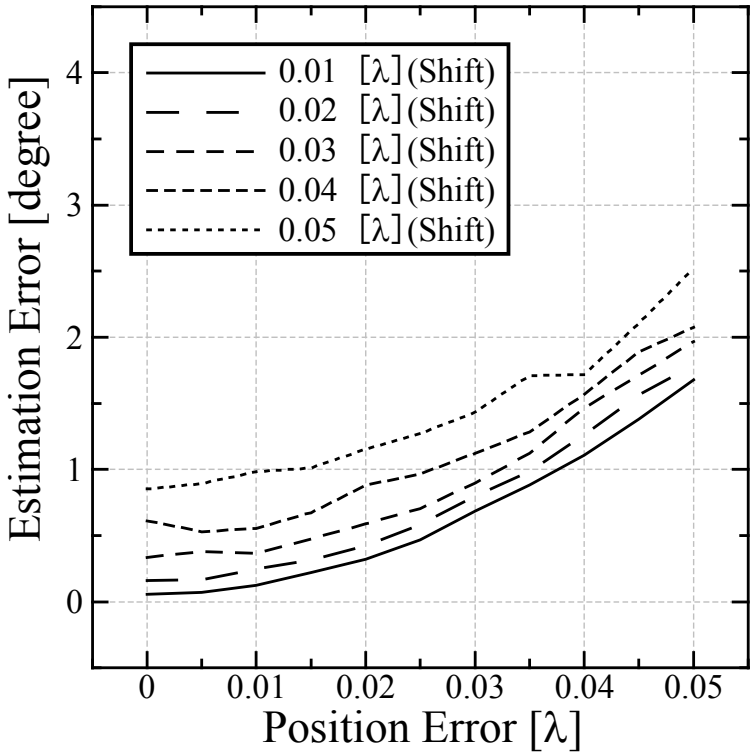

Fig. B-2 Simulation results

B.3 Experiments in an anechoic chamber

The performance of the proposed method during DOA estimation was evaluated by several experiments. The experiments were conducted in an anechoic chamber using the trial system. Table B-2 shows the experimental specifications. The interval between elements was 0.45

wavelengths, and a 5 × 4 virtual planar array was synthesized by shifting 5 + 1 T-shaped array antenna 3 times. RF was 2 GHz, DOA was changed every 30° from 0 to 180°, and estimated. Fig. B-3 shows a schematic view of the experiment. In the trial system, terminals were set up at measurement points, the other terminals were set up at the shifted array antenna, and terminals were connected to SG and AD as shown in Fig. B-3. When the array antenna reached the measurement points, signals from SG were transmitted to ADC because of the contacts between terminals at measurement points and the array antenna. The ADC samples data received by the T-shaped array antenna when the input is received at the ADC. The velocity of shifting the T-shaped array was about 10 [cm/s], and the measurement time was about 2 seconds. Under these conditions, position errors were 0.004 wavelengths, and shifting errors were 3×10^{-5} wavelengths. The simulation results indicated that there were no position or shifting errors. Fig. B-4 shows the experiment results. The average error of this experiment was 1.5. The results of this experiment confirmed the effectiveness of sequential measurement.

Table B-2 Experimental specifications (one arrival wave)

Array form	T-shaped array antenna (5 + 1 elements)
Number of virtual planar array elements	5 × 4 (28 elements)
Number of subarray elements	3 × 3 (9 elements)
Interval between elements	0.45 λ
Number of arrival waves	1
Sampling frequency of ADC	20 dB
Radio frequency	2 GHz
Intermediate Frequency	40 MHz
Number of snapshots	2000

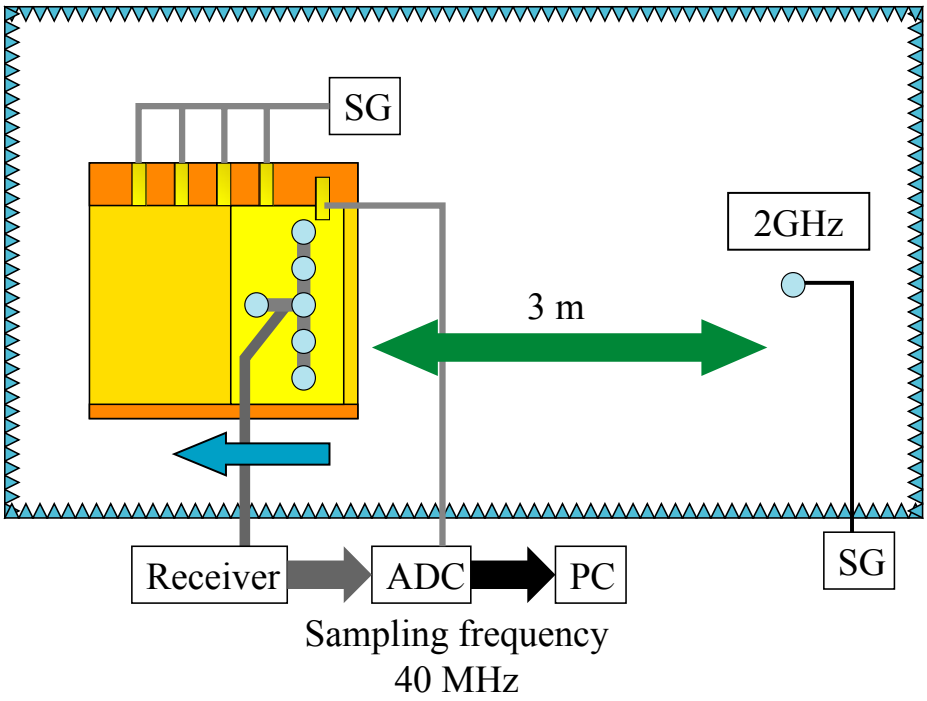

Fig. B-3 Schematic view of experiment (one arrival wave)

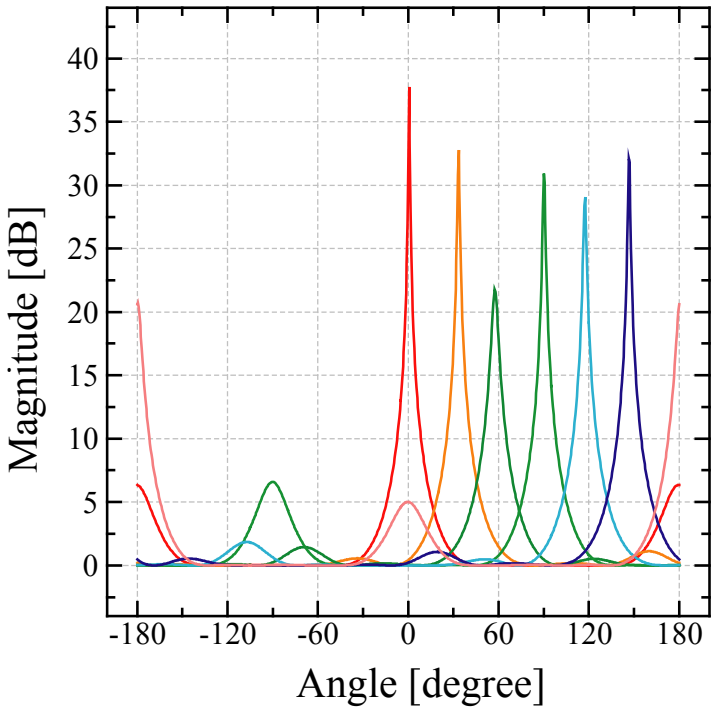

Fig. B-4 Results of DOA estimations (one arrival wave)

Then, experiments were conducted to examine the case of two arrival waves. The angle difference between the two arrival waves was 30°. The other specifications were the same as in the above experiments. Fig. B-5 shows the experiment results. It was confirmed that two arrival waves could be distinguished and estimated. These results confirmed the effectiveness of sequential measurement.

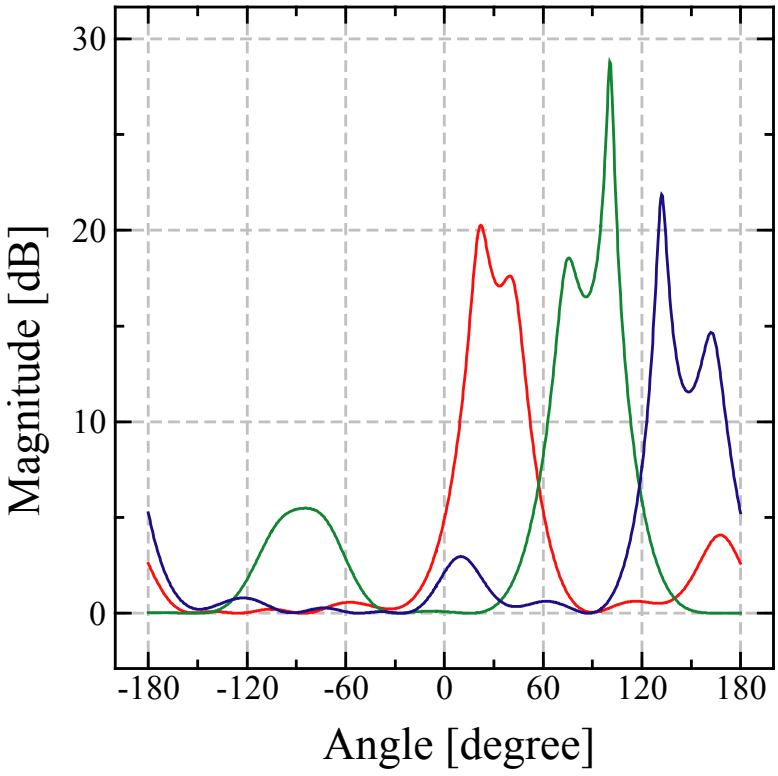

Fig. B-5 Results of DOA estimation (two arrival waves)

B.4 Conclusions

This appendix described evaluation of the influences of position and shifting errors during DOA estimation determined by simulations and experiments. These results confirmed that DOA can be estimated using a virtual planar array with sequential measurements.

Bibliography

[1] ARIB, RCR STD-28, Dec., 1993.

[2] DECT, “Digital European cordless system – common interface specications,” Code RES-3(89), DECT, 1989.

[3] T. Matsuura, “PHS obtains over 80 milion users from the world,” IEICE Journal, vol.88, no. 9, pp.745-750, Sep., 2005.

[4] T. Ohya, H. Yoshino, N. Umeda and T. Miki, “Technnologies and Standardization toword Beyond 3G Mobile Comunication System,” Microwave Workshop Digest, MWE2005, WS2-1, pp.47-52, Nov. 2005.

[5] http://www.soumu.go.jp/s-news/2005/050811_1.html

[6] T. Suzuki, “Trend and Vision of Wireless Techonologies for Beyond 3G,” Microwave Workshop Digest, MWE2005, WS2-2, pp53-58, Nov.2005.

[7] Y. Karasawa, “Radiowave Progapation Fundamentals for Digital Mobile Communications,” CORONA PUBLISHING CO., LTD., 2003.

[8] G. Arredondo, W. Chriss, and E. Walker, “A multipath fading simulator for mobile ratio,” IEEE Trans. Veh. Techno., vol. VT-22, pp.241-244, Nov. 1973.

[9] R. A. Comroe, “All-digital fading simulator,” in *Proc.* Nut. *Electron. Conf.,* vol. 32, pp. 136-139. 1978.

[10] J. R. Ball, “A real-time fading simulator for mobile radio,” *Radio Electron. Eng.,* vol. 52, pp. 475-478, Oct. 1982.

[11] R. A. Goubran, H. M. Hafez, and A. U. H. Sheikh, “Real-time programmable land mobile channel simulator,” in *P m* . 36th *IEEE Veh. Technol.* Soc. *Cony* ., Dallas, TX, pp. 215-218, May 1986.

[12] Y. Kamio, S. Sampei, H. Sasaoka and M. Yokoyama, ”A new type fading simulator with DSP,” Trans. IEICE, vol. E70, no.4, pp. 379-382, April 1987.

[13] S. Arata, K. Kaiga, S. Manabe, T. Yamaguchi, K. Miwa, K. Sakaguchi, S. Suyama and K. Araki, “4x4 MIMO Fading Simulator -- Development of Reconfigurable Platform --,” Proc. of 2005 IEICE Society Conf., B-17-2, Sep. 2005.

[14] Y. Okumura, E. Ohmori, T. Kawano, and K. Fukuda, “Field strength and its variability in VHF and UHF land-mobile radio service,” *Rev. Elec. Commun. Lab.*, vol. 16, pp. 825–873, 1968.

[15] M. Hata, “Empirical formula for propagation loss in land mobile radio services,” IEEE Trans. Veh. Technol., vol. VT-29, pp. 317–325, Aug. 1980.

[16] R. Steele and V. K. Prabhu, “High-user-density digital cellular mobile radio systems,”

Prve. Inst. Elec., Eng., pt. F, no. 5, pp. 396-404, Aug. 1985.

[17] G. Y. Delisle, J. P. Lefevre, M. Lecours and J. Y. Chouinard, “Propagation loss prediction; a comparative study with application to the mobile radio channel,” IEEE Trans. Veh. Technol., vol. VT-34, no. 2, pp. 86-96, May 1985

[18] J. H. Whitteker, “Measurements of path loss at 910 MHz for proposed microcell urban mobile systems,” IEEE Trans. Veh. Technol., vol. 37 pp. 125-129, Aug. 1988.

[19] R. J. C. Bultitude and G. K. Bedal, “Propagation characteristics on microcellular urban mobile radio channels at 910 MHz,” IEEE J. Select. Areas Commun., vol. 7, pp. 31-39, Jan. 1989.

[20] Y. Nagata,, Y. Furuya, E. Moriyama, T. Saruwatari, I. Kamiya, S. Hattori, “2GHz band radio propagation characteristics in microcellular mobile systems under tall building environments,” Technical report of IEICE, A· P90-84, pp.1-7, Dec. 1990.

[21] A. J. Rustako, N. Amitay, G.J. Owens, R. S. Roman, “Radio propagation at microwave frequencies for line-of-sight microcellular mobile and personal communications,” IEEE Trans. Veh. Technol., vol. 40, pp. 203-210, Feb. 1991.

[22] Y. Oda, T. Tanaka, “Microwave band path loss characteristics in microcellular mobile communications,” Technical report of IEICE, A· P94-105, pp.9-14, Jan. 1995.

[23] T. Furuno, T. Taga, “Delay spread in microcellular environment for personal communication systems,” IEICE Trans., vol. E79-B, no. 9, pp. 1199-1204, Sep. 1996

[24] T. Taga, T. Furuno, “Multipath delay mechanism in low antenna height line-of-sight microcells,” IEICE Trans. B-Ⅱ, vol. J80-B-Ⅱ, no. 10, pp.848-861, Oct., 1997.

[25] J. S. Colburn, Y. Rahmat-Samii, M. A. Jensen, G. J. Pottie, “Evaluation of personal communications dual-antenna handset diversity performance,” IEEE Trans., vol. 47, pp.737-746, Aug., 1998.

[26] T. Taga, S. Ichitsubo, Y. Ogawa, K. Itoh, “1.9-GHz-band radio propagation characteristics in an open urban environment and tree loss prediction using a loss layer model,” IEICE Trans. B, vol. J82-B, no. 8, pp.1538-1548, Aug., 1999.

[27] E. F. T. Martijn, M. H. A. J. Herben, “Characterization of radio wave propagation into buildings at 1800 MHz,” IEEE Lett. Antennas and Wireless Propagation, vol. 2, pp. 122-125, 2003.

[28] A. S. Bajwa and J. D. Parsons, “Small-area characterization of UHF urban and suburban mobile radio propagations,” IEE Proceedings, vol.129, pt.F, no.2, pp.95–101, Apr. 1982.

[29] S. Sakagami, “Experimental Results on Multipath Propagation in 900 MHz Mobile Communication Path –Amplitude-Frequency Characteristics and Angle of Arrival,” IEICE Trans., vol.J-70-B, no.12, pp.1522–1528, Dec. 1987.

[30] T. Ohgane, S. Sampei, Y. Kamio, H. Sasaoka, and M. Mizuno, “UHF Urban and Suburban Multipath Propagation Characteristics in Wideband Mobile Radio Communications,” IEICE Trans., vol.J72-B-II, pp.62–71, Feb. 1989.

[31] H. J. Thomas, T. Ohgane, and M. Mizuno, “A novel antenna measurement of the angular distribution of received waves in the mobile radio environment as a function of position and delay time,” Proc. IEEE Vehicular Technology Conf., pp.546–549, May 1992.

[32] T. Furuno and T. Taga, “Study on Identification of Propagation Path from Low Antenna Height Base Station in Urban Area,” Technical report of IEICE RCS, RCS95-126, Jan. 1996.

[33] K. Murota, and K. Hirade, “GMSK modulation for digital mobile radio telephony,” IEEE Trans. Commun., vol. COM-29, no. 7, pp.1044-50, July 1980.

[34] K. Kinoshita, M. Hata, and H. Nagabuchi, “Evaluation of 16kbit/s digital voice transmission,” IEEE Trans. Commun., vol. VT-33, no. 4, pp. 321-26, Nov. 1984.

[35] K. Honma, E. Murata, and Y. Riko, “On a method of constant envelope modulation for digital mobile communications,” IEEE ICC’80, pp. 24.1.1-24.1.5, Jun. 1980.

[36] Y. Akaiwa, I. Takase, S. Kojima, M. Ikoma, and N. Saegsa, “Performance of baseband bandlimited multi-level FM with discriminator detection for digital mobile telephony,” IEICE Trans., vol. E64, pp. 463-69, Jul. 1981.

[37] F.D. Jager, C. B. Dekker, “Tamed frequency modulation, a novel method to achieve spectrum economy in digital transmission,” IEEE Trans. Commun., vol. COM-26, no.5, pp. 534-42, May 1978.

[38] Y. Akaiwa, Y. Nagata, “Highly efficient digital mobile communications with a linear modulation method,” IEEE J. of Sel. Areas Commun., vol. 5, no. 5, pp. 890-895, Jun. 1987.

[39] K. Feher, Wireless digital communications, Modulation & spread spectrum applications, Prentice-Hall, Upper Saddle River, New Jersey, 1995.

[40] A. Bateman, “Feedforward transparent tone-in-band: Its implementation and applications,” IEEE Trans. Veh. Technol., vol. 39, no. 3, pp. 235-243, Aug. 1990.

[41] S. Sampei, and T. Sunaga, “Rayleigh fading compensation for QAM in land mobile radio communications,” IEEE Trans. Veh. Technol., vol. 42, no. 2, pp. 137-147, May 1993.

[42] L. Hanzo, R. Steele, and P.-M. Fortune, “A subband coding, BCH coding and 16QAM system for mobile radio speech applications,” IEEE Trans. Veh. Techonl., vol. 39, no. 4, pp. 327-339, Nov. 1990.

[43] S. Saito and H. Suzuki, “Fast carrier-tracking coherent detection with dual-mode carrier

recovery circuit for land mobile radio transmission," IEEE J. of Select. Area in Commun. vol. 7, no. 1, pp.130-139, Jan. 1989.

[44] S. Saito, T. Takami and H. Yamamoto, "Adaptive Carrier Tracking (ACT) demodulation for QPSK mobile radio transmission," IEICE Trans., vol. J75-B-Ⅱ, no.8, pp.499-507, Aug. 1992.

[45] S. Sampei, IEICE Trans. Vol.J72-B-Ⅱ, no. 4, pp. 125-132, Apr. 1989.

[46] M. Yokoyama, "BPSK with sounder to combat Raleigh fading in mobile radio communications," IEEE Trans. Vech. Tech., vol. VT-34,1, pp.35-40, Feb. 1985.

[47] X. Y. Hou, K.R. Wu, N. Morinaga and T. Namekawa, "Bit error rate performance of fading BPSK system with sounder in the presence of cochannel interference," IEICE Trans, vol. E70, no. 1, pp. 42-48, Jan 1987.

[48] F. Davarian, "Mobile digital communication via tone calibration," IEEE Trans. Veh. Tech., vol. VT-36, no. 2, pp.55-62, May 1987.

[49] P. S. K. Leung, K. Feher, "Transparent tone in band (TTIB) aided GMSK/MSK modem system," IEEE Veh. Tech. Conf., San Francisc, pp.249-255, May 1989.

[50] J. K. Cavers, F. R. Marchetto, F.S. and Carlson, S. D., " A new spectral notch generator for pilot tone systems," 40th IEEE Veh. Tech. Conf., Orlando, pp.547-551, May 1990.

[51] M. K. Simon, "Dual-pilot tone calibration technique," IEEE Trans. Veh. Tech., vol.VT-35, no. 2, pp.63-70, May 1986.

[52] A. Bateman, G. Lightfoot, A. Lymer and P. J. McGeehan, "Speech and data communications over 942 MHz TAB and TTIB signal sideband mobile radio systems incorpolating feed-forward signal regeneration," IEEE Trans. Veh. Tech., vol. VT-34, no. 1, pp. 13-21, Feb. 1985.

[53] M. P. Martin, A. Bateman, P. J. McGeehan and D. J. Marvill, "The implementation of a 16QAM mobile data system using TTIB based fading correction techniques," 38th IEEE Veh. Tech. Conf., Philadelphia, Pennsylvania, pp. 71-76, June 1988.

[54] A. Bateman, "Feedforward transparent tone-in-band: Its implementations and applications," IEEE Trans. Veh. Technol., vol. 39, no. 3, pp. 235-243, Aug. 1990.

[55] L. M. Moher and H. J. Lodge, "TCMP – A modulation and coding strategy for Rician fading channels," IEEE J. Select. Areas Commun., vol. 7, no. 9, pp.1347-1355, Dec. 1989.

[56] A. Aghamohammadi, H. Mayer and G. Ascheid, "A new method for phase synchronization and automatic gain control of linearly modulated signals in frequency-flat fading channels," Trans. IEEE Commun., vol COM-39, no. 1, pp. 25-29, Jan. 1991.

[57] J. K. Cavers, "An analysis of pilot symbol assistes modulation for rayleigh fading

channels," Trans. IEEE Veh. Tech., vol. VT-40, no. 4, pp. 686-693, Nov. 1991.

[58] S. Sanpei and T. Sumaga, "Rayleigh fading compensation for QAM in land mobile radio communications," Trans. IEEE Veh. Technol., vol. 42, no. 2, pp. 137-147, May 1993.

[59] A. Salmasi and S. K. Gilhousem, "On the system design aspects of code division multiple access (CDMA) applied to digital cellular and personal communication networks," 41st IEEE Veh. Tech. Conf., St. Louis, Missouri, pp. 57-62, May 1991.

[60] V. K. Garg, K. Smolik and J. E. Wilkes, "Applications of CDMA in wireless/personal communications," Prentice-Hall, Inc., 1997.

[61] M. Schwartz, W. R. Bennett and S. Stein, "Communication systems and techniques," McGraw-Hill, 1966.

[62] P. Monson, "Fading channel communications," IEEE Commun. Mag., vol. 18, no. 1, pp.16-25, Jan. 1980.

[63] S. Sampei, "Applications of digital wireless technologies to gtlobal wireless communications," Pearson Education, Inc., 1997.

[64] S. Sampei, "Development of Japanese adaptive equalizing technology toward high bit rate data transmission in land mobile communications," IEICE Trans., vol. E74, no. 6, pp. 1512-1521, Jun. 1991.

[65] D. G. Jr. Forney, "Maximum-likelihood sequence estimation of digital sequences in the presence of intersymbol interference," IEEE Trans. Inf. Theory, vol. IT-18, no. 3, pp. 363-378, May 1972.

[66] G. ungerboeck, "Adaptive maximum-likelihood receiver for carrier-modulated data-transmission systems," IEEE Trans. Commun., vol. COM-22, no. 5, pp. 624-634, May 1974.

[67] D. Godard, "Channel equalization using a Kalman filter for fast data transmission," IBM J. Res. Develop., vol. 18, pp.267-273, May 1974.

[68] S. Muller, "Least squares algorithms for adaptive equalizer," Bell Syst. Tech. J., vol. 60, no. 8, pp. 1905-1925, Oct. 1981.

[69] D.D. Falconer and L. Ljung, "Application of fast Kalman estimation to adaptive equalization," IEEE Trans. Commun., vol. COM-26, no. 10, pp. 1439-1446, Oct. 1978.

[70] S. Hara and R. Prasad, "Overview of multicarrier CDMA," IEEE Commun., Mag., pp. 126-133, Dec. 1997.

[71] M. Umehira and T. Sugiyama, "OFDM/CDMA technologies for future broadband mobile communication systems," IEICE Trans., vol. E85-A, no. 12, pp. 2804-2812, Dec. 2002.

[72] R. Gallager, "Low-Density Parity-Check Codes," IEEE Trans. IT, vol. 8, pp. 21-28, Jan.

1962.

[73] D. J. C. Mackay, “Good Error-Correcting Codes based on very sqarse matrices,” IEEE Trans. IT, vol. 45, pp. 399-431, Mar. 1999.

[74] T. Fujii, H. Masui and A. Nagate, “Prospects and issues of 4th generation mobile communication systems,” MWE 2005 Microwave workshop Dig., WS2-3, pp. 59-64, Nov. 2005.

[75] Y. Fujitsuka, K. Iimuro, H. Tanigawa, M. Iida, M. Shimada, K. Kataoka and T. Hamai, “A field test for the PHS base station with adaptive array antenna,” Proc. 1998 Commun. Society Conference of IEICE, B-5-74, Sept. 1998.

[76] H. Suzuki, “Interference canceling techniques in mobile communications,” IEICE Journal, vol. 79, no. 6, pp. 570-582.

[77] M. Nakano, M. Hirono, Y. Sato, T. Miyamoto, M. Karikome, A. Hirota, K. Ichige, H. Arai,”Direction of arrival detection : overview,” B-1-248, Sept. 2005.

[78] T. Inaba, T. Hirai, “Moving target indicator for FMICW radar,” IEICE Trans., vol. J88-B, No. 4, pp. 795-803, Apr. 2005.

[79] M. I. Skolnik, Introduction to radar system, McGraw-Hill, New York, 1962.

[80] F. E. Nathanson, Radar Design Principle, McGraw-Hill, NewYork, 1969.

[81] M. Ohtsuka, I. Chiba, T. Katagi, T. Suzuki, “Consideration for beam direction of difference pattern in a monopulse phased array antenna,” IEICE Trans., vol. J82-B, no. 3, pp.427-434, Mar. 1999.

[82] F. Pasqualucci, “Drop size distribution measurements in convective storms with a verthically pointing 35 GHz Doppler radar,” Radio Science, vol. 19, no. 1, pp. 177-183, Jan.-Feb. 1984.

[83] R. S. Kropfili, W. R. Moringer and F. Pasqualucci, “Circular depolarization ratio and Doppler velocity measurements with a 35 GHz radar during the cooperative precipitation experiment, ” Radio Science, vol. 19, no. 1, pp. 141-147, Jan.-Feb. 1984.

[84] J. B. Mead, A. K. Pazmany, S. M. Sekelsky and R.E. McIntosh, “Millimeter-wave radars for remotely sensing clouds and precipitation,” Proc. IEEE, vol. 82, no. 12, pp. 1891-1906, Dec. 1994.

[85] M. Uneda and H. Hokazono, “Compensation of amplitude and phase variations of the channels for applying the high resolution angular measurement processing by the large aperture equivalent uniformly circular array antenna of the measurement instrumention radar,” IEICE Trans., vol. J85-B, no. 7, pp. 1120-1129, Jul. 2002.

[86] N. Odachi, M. Uneda, J. Suzuki, H. Shoki, T. Watanabe, H. Hokazono, “2-D direction of arrivals estimation of coherent signal waves using adding virtual waves method and stepped interpolation SSP MUSIC by a large aperture equivalent circular array

antenna," IEICE Trans., vol. J85-B, no. 12, pp. 2362-2370, Dec. 2002.

[87] S. Sakagami, "Experimental results on multipath propagation 900 MHz mobile communication path," IEICE Trans., vol. J70-B, no.12, pp.1522-1528, Dec. 1987.

[88] T. Furuno and T. Taga, "Study on identification of propagation path from low antenna height base station in urban area," Technical report of IEICE, RCS95-126, Jan. 1996.

[89] T. Furuno and T. Taga, "Identification of propagation path from low antenna height base station in urban area," IEICE Trans., vol. J83-B, no. 1, pp. 71-80, Jan. 2000.

[90] A.S.Bajwa and J.D.Parsons, "Small-area characteristion of UHF urban and suburban mobile radio propagation, " IEE Proceedings, vol.129, pt.F, no.2, pp.95-101, April 1982.

[91] T. Ohgane, S. Sampei, Y. Kamio, H. Sasaoka, M. Mizuno, "UHF urban and suburban multipath propagation characteristics in wideband mobile radio communications," IEICE Trans., vol. J72-B-II, pp.62-71, Feb. 1989.

[92] H.J.Thomas, T.Ohgane and M.Mizuno, "A novel antenna measurement of the angular distribution of received waves in the mobile radio environment as a function of position and delay time," Proc. IEEE Vehicular Technology Conf, pp.546-549, May 1992.

[93] Y. Ogawa and N. Kikuma, "High-resolution techniques in signal processing antennas," IEICE Trans. Commun., nol. E78-B, no. 11, Nov. 1995.

[94] S. Haykin,ed., "Array signal processing," Prentice-Hall, Englewood Cliffs, 1985.

[95] J. Capon, "High-resolution frequency-wavenumber spectrum analysis," Proc. IEEE, vol. 57, no. 8, pp. 1408-1418, Aug. 1969.

[96] S. M. Kay, "Modern spectral estimation: Theory and application," Prentice-Hall, Englewood Cliffs, 1988.

[97] H. Krim and M. Viderg, "Two decades of array signal processing research – The parametric approach-," IEEE Signal Processing Mag., vol. 13, no. 4, pp. 67-94, Jul. 1996.

[98] V. F. Pisarenko, "The retrieval of harmonics from covariance functions," IEEE Trans., vol. Ap-34, no. 3, pp. 276-280, Mar. 1986.

[99] W. F. Gabriel, "Spectral analysis and adaptive array supperresolution techniques," Proc. IEEE, vol. 68, no. 6, pp. 654-666.

[100] S. U. Pliiai, Array Signal Processing, Springer-Verlag New York Inc., 1989.

[101] K. Takao, M. Fujita and T. Nishi, "An adaptive antenna array under directional constraint," IEEE Trans. Antennas & Propag. Vo. AP-24, no. 5, pp. 662-669, Sept. 1976.

[102] R. T. Compton, Jr., Adaptive Antennas – Concepts and Performance, Prentice-Hall, Englewood Cliffs, 1988.

[103] R. T. Compton, Jr., "The power inversion adaptive array : Concept and performance," IEEE Trans. Aerosp. & Electron. Syst., vol. AES-15, no. 6, pp. 803-814, Nov. 1979

[104] R. O. Schmidt, “Multiple Emitter Location and Signal Parameter Estimation,” IEEE Trans. Antenna & Propagat., vol.34, no.3, pp.276-280, Mar. 1986.

[105] R.L. Johnson and G. E. Miner, “Comparison of super-resolution algorithms for radio direction finding,” IEEE Trans., Aerosp. Electron. Syst., vol. AES-22, no. 4, pp. 432-442, Jul. 1986.

[106] M. Kaveh and A. J. Barabell, “The statistical performance of the MUSIC and the minimum-norm algorithms in resolving plane waves in noise,” IEEE Trans. Acoust., Speech, Signal Processing, vol. ASSP-34, no. 2, pp. 331-341, Apr. 1986.

[107] P. Stoica and A. Nehorai, “MUSIC, maximum likelihood, and Cramar-Rao bound,” IEEE Trans. Acoust., Speech and Signal Processing, vol. 37, no. 5, pp. 720-741, May 1989.

[108] B. D. Rao and K. V. S. Hari, “Performance analysis of Root-MUSIC,” IEEE Trans., Acoust., Speech, Signal Processing, vol.ASSP-37, no. 12, pp. 1939-1949, Dec. 1989.

[109] M. Kim, K. Ichige, H. Arai, “Implementation of FPGA based fast DOA estimator using unitary MUSIC algorithm,” Proc. VTC 2003-Fall, vol. 1, pp. 213-217, Oct. 2003.

[110] M. Kim, K. Ichige, H. Arai, “Implementation of FPGA Based Fast Unitary MUSIC DOA Estimator,” IEICE Trans., vol. E87-C, no. 9, Sept. 2004.

[111] R. Roy and T. Kailath, “ESPRIT—Estimation of Signal Parameter via Rotational Invariance Techniques,” IEEE Trans. Accoust., Speech & Signal Proc., vol.37, pp.984-995, July 1989.

[112] B. Ottersten, M. Viberg and T. Kailath, “Performance analysis of the total least squares ESPRIT algorithm,” IEEE Trans. on Signal Processing, vol. SP-39, no. 5, pp. 1122-1135, May 1991.

[113] M Haardt and J. A. Nossek, “Unitary ESPRIT : How to obtain increased estimation accuracy with a reduced computational burden,” IEEE Trans. Signal Processing, vol. 43, no. 5, pp. 1232-1242, May 1995.

[114] M. D. Zoltowski, M. Haardt and C. P. Mathews, “Closed-Form 2-D angle estimation with rectangular arrays in element space or beamspace via unitary ESPRIT,” IEEE Trans. Signal Processing, vol. 44, no. 2, pp. 316-328, Feb. 1996.

[115] Y. Ogawa, N. Hamaguchi, K. Ohshima and K. Itoh, “High-Resolution analysis of indoor multipath propagation structure,” IEICE Trans., Commun., vol. E78-B, no. 11, pp.1450-1457, Nov. 1995.

[116] T. Kuroda, N. Kikuma, N. Inagaki, “DOA estimation and pairing method in 2D-ESPRIT using triangular antenna array,” IEICE Trans., vol. J84-B, no. 8, pp. 1505-1513, Aug. 2001.

[117] Y. Tanabe, Y. Ogawa and T. Ohgane, ”High-resolution estimation of multipath

propagation based on the 2D-MUSIC algorithm using time-domain signals." IEICE Trans., vol. J83-B, no. 4, pp. 407-415, Apr. 2000.

[118] P. Strobach, "Two-Dimensional equirotational stack subspace fitting with an application to uniform rectangular arrays and ESPRIT," IEEE Trans. on Signal Processing, vol. 48, no. 7, Jul. 2000.

[119] N. Kikuma, "Iterative DOA estimation using subspace tracking methods and adaptive beamforming," IEICE Trans. Commun., vol. E88-B, no. 5, May 2005.

[120] P. Strobach, "Bi-iteration SVD subspace tracking algorithms and applications," IEEE Trans. Signal Process., vol. 45, no. 5, pp. 1222-1240, May 1997.

[121] P. Strobach, "Fast recursive subspace adaptive ESPRIT algorithms," IEEE Trans. Signal Process., vol. 46, no. 9, pp. 2413-2430, Sept. 1998.

[122] P. Strobach, "Bi-Iteration multiple invariance subspace tracking and adaptive ESPRIT," IEEE Trans. Signal Process., vol. 48, no. 2, pp. 442-456, Feb. 2000.

[123] B. Yang, "Projection approximation subspace tracking," IEEE Trans., Signal Process., vol. 43, no, 1, pp. 95-107, Jan. 1995.

[124] R. T. Williams, S. Prasad, A. K. Mahalanabis, L. H. Sibul, "An Improved Spatial Smoothing Technique for Bearing Estimation in a Multipath Environment," IEEE Trans., vol.ASSP-36, pp.425-432, April 1988.

[125] A. R. Thompson, "The Response of a Radio-Astronomy Synthesis Array to Interfering Signals," IEEE Trans. Antenna & Propagat., vol.30, no.3, pp.450–456, May 1982.

[126] R. O. Schmidt, "Multiple Emitter Location and Signal Parameter Estimation," IEEE Trans. Antenna & Propagat., vol.34, no.3, pp.276–280, Mar. 1986.

[127] R. Roy and T. Kailath, "ESPRIT—Estimation of Signal Parameter via Rotational Invariance Techniques," IEEE Trans. Accoust., Speech & Signal Proc., vol.37, pp.984–995, Jul. 1989.

[128] Y. M. Chen, "On spatial smoothing for two-demensional direction-of-arrival estimation of coherent signals," IEEE Trans., Signal Processing, vol.45, pp.1689–1696, Jul. 1997.

[129] S. Sekizawa, K. Taira, Y. Kanio, and M. Mizuno, "Configuration and Performance of a Measuring System for Spatiotemporal Characteristics of Multipath Fading Channels Using a Virtual Planar Array," IEICE Trans., vol.J83-B, no.9, pp.1303–1313, Sep. 2000.

[130] S. Sekizawa, "Estimation of Arrival Directions Using MUSIC Algorithm with a Planar Array," ICUPC '98, pp.555–559, Oct. 1998.

[131] U. Kickel, "Angular superresolution with phased array radar: A review of algorithms and operational constraints," IEE Proc. F, Commun, Radar & Signal Process., vol. 34, no. 1, pp. 53-59, Feb. 1987.

[132] H. Aoyama, H. Arai, "Mutual coupling matrix estimation and null forming methods for

MBF Antennas," IEICE Trans. Commun., vol. E88-B, No. 6, pp. 2305-2312, Jun. 2005.

[133] M. D. Zoltowski, M. Kauts and S. D. Silverstein, "Beamspace Root-MUSIC," IEEE Trans. Signal Process., vol. 41, no. 1, pp. 344-364, Jan. 1993.

[134] G. Xu, S. D. Silverstein, R. H. Roy and T. Kailath, "Beamspace ESPRIT," IEEE Trans. Signal Process., vol. 42, no. 2, pp. 349-356, Feb. 1994.

[135] K. M. Buckley, X. L. Xu, "Spatial-Spectrum estimation in a location sector," IEEE Trans. Acoust., Speech, Signal Processing, vol. 38, no. 11, pp. 1842-1852, Nov. 1990.

[136] T. Ohira, K. Gyouda and S. Denno, "Microwave signal processing adaptive beamforming and electronically steerable passive array radiator antenna," IEICE Technical Report, AP99-61, Jul. 1999.

[137] E. Taillefer, C. Plapous, C. Jun, K. Ligusa, T. Ohira, "Reactance-domain MUSIC for ESPAR antennas (experiment)," Proc. of WCNC 2003, vol. 1, pp. 98-102, Mar. 2003.

[138] E. Taillefer, A. Hirata, T. Ohira, "Reactance-Domain ESPRIT algorithm for hexagonally shaped seven-element ESPAR antenna," IEEE Trans. Antenna & Propagation, vol. 53, pp. 3486-3495, Nov. 2005.

[139] E. Taillefer, A. Hirata, T. Ohira, "Direction-of-arrival estimation using radiation power pattern with an ESPAR antenna," IEEE Trans. Antennas & Propagation, vol. 53, pp. 678-684, Feb. 2005.

[140] R. O. Schmit, "Multilinear array manifold interpolation,"IEEE Trans., Signal Processing, vol. 40, pp. 857-866, Apr. 1992.

[141] T. Arai, R. Hara, H. Yamada and Y. Yamaguchi, "Calibration technique for superresolution array," Technical report of IEICE, AP2002-28, May. 2002.

[142] K. Chiba, H. Yamada and Y. Yamaguchi, "Experimental verification of antenna array calibration using known sources," Technical report of IEICE, AP2002-41, Jun. 2002.

[143] I. J. Gupta and A. A. Ksienski, "Effect of Mutual Coupling on the Performance of Adaptive Arrays," IEEE Trans., Antenna & Propagat., vol.AP-31, no.5, pp.785-791, Sept. 1983.

[144] H. T. Hui, "Reducing the Mutual Coupling Effect in Adaptive Nulling Using a Re-defined Mutual Impedance," IEEE Trans. Microwave and Wireless Components Lett., vol.12, no.5, pp.178-180, May 2002.

[145] H. Yamada, R. Hara, Y. Ogawa and Y. Yamaguchi, "On performance comparison of calibration techniques for mutual coupling effect in array antennas," Technical report of IEICE, AP2002-218, Mar. 2003.

[146] R. S. Adve and T. K. Sarkar, "Compensation for the Effects of Mutual Coupling on Direct Data Domain Adaptive Algorithm," IEEE Trans. Antenna & Propagat., vol.48, no.1, pp.84-94, Jan. 2000.

[147] K. R. Dandekar, H. Ling, and G. Xu, “Experimental study of mutual coupling compensation in smart antenna applications,” IEEE Trans, Wireless Commun., vol.1, no.3, pp.480-487, Jul. 2002.

[148] B. Friedlander, and A. J. Weiss, “Direction Finding in the Presence of Mutual Coupling,” IEEE Trans. Antennas Propag., vol.39, no.3, pp.273-284, Mar. 1991.

[149] Q. yuan, Q. Chen, K. Sawaya, “Accurate DOA Estimation Using Array Antenna with Arbitrary Geometry,” IEEE Trans., vol.53, no.4, pp.1352-1357, Apr. 2005.

Publication list

Related works

Journal Papers

1. Akimichi Hirota, Koichi Ichige, Hiroyuki Arai, Kyeong-sik Min, Dong-chul Kim, Jng-hun Kim and Masayuki Nakano, “A DOA estimation system in 900MHz by ‘T’-type array antennas,” IEICE Trans. Commun., vol.J86-B no.10, pp.2153-2165, Oct. 2003 (in Japanese).
2. Akimichi Hirota, Hiroyuki Arai and Masayuki Nakano, “Direction-of-arrival estimation System for multipath propagation with Synthesized virtual planar array using pilot signals,” IEEE Trans. Vehicular Technology (submitted in 2005).
3. Akimichi Hirota, Takehiro Miyamoto, Masayuki Nakano and Hiroyuki Arai, “Modified calibration method for MUSIC method with a rectangular array,” IEICE Trans. Commun. (submitted in 2005).

Proceedings of International Conferences

4. Akimichi Hirota, Koichi Ichige and Hiroyuki Arai, "DOA Estimation by 'T'-Type Array Antenna and Its Evaluation," Proc.URSI General Assembly,No.C2.P.4, Maastricht, The Netherlands, August 2002.
5. Akimichi Hirota, Hiroyuki Arai, and Tatsuo Itoh, "The Antenna of The CRLH TL Using Multilayers Substrate," URSI EMTS 2004, pp.888-890, Pisa, Italy, May, 2004.
6. Akimichi Hirota, Hiroyuki Arai, and Masayuki Nakano, "DOA Estimation System by A Synthesized Virtual Planar Array Using Pilot Signals," Proc. ISAP'04, pp.21-24, Sendai, Japan, Aug. 2004.
7. Akimichi Hirota, Hiroyuki Arai, and Masayuki Nakano, ” On Performance Comparison of the Methods for a Realizing uniform Planar Array”, Proc. 2004 KJJC, pp.117-120 Seoul, Korea, Nov. 2004
8. Akimichi Hirota, Hiroyuki Arai, and Masayuki Nakano, ” System with synthesized virtual planar array using eigenvectors, ” Proc. 2005 ANTEM, No.W2D1, Saint-Malo, France, June. 2005.
9. Akimichi Hirota, Hiroyuki Arai, and Masayuki Nakano, ” Experimental Study of DOA System with Synthesized Virtual Planar Array Using Eigenvectors, ” Proc.URSI General Assembly, No.C02.3, New Delhi, India, Oct. 2005.

Domestic Meetings

10. Akimichi Hirota, Koichi Ichige, Hiroyuki Arai, Kyeong-sik Min, Dong-chul Kim, Jng-hun Kim and Masayuki Nakano, "DOA Estimation system in 900MHz Band and Its Evaluation," IEICE Technical Report, AP-2002-3, Apr. 2002.
11. Akimichi Hirota, Hiroyuki Arai, and Masayuki Nakano, "DOA estimation system using virtual rectangular array with eigenvectors," IEICE Technical Report, AP-2005-56, Jun. 2005.
12. Akimichi Hirota, Koichi Ichige and Hiroyuki Arai, "DOA and electric power estimation by an adaptive array antenna installed on a car," IEICE Society Conference, B-1-32, Sept. 2001.
13. Akimichi Hirota, Yuki Inoue, Koichi Ichige and Hiroyuki Arai, "DOA and electric power estimation experiment by adaptive array antenna," IEICE General Conference, B-1-20, Mar. 2002.
14. Akimichi Hirota, Koichi Ichige and Hiroyuki Arai, "DOA estimation system in 900MHz band and its evaluation," IEICE Society Conference, B-1-7, Sept. 2002.
15. Akimichi Hirota, Koichi Ichige, Hiroyuki Arai, Kyeong-sik Min, Dong-chul Kim, Jng-hun Kim and Masayuki Nakano, "A note on array shape of DOA estimation system in 900MHz band," IEICE General Conference, B-1-21, Mar. 2003.
16. Akimichi Hirota, Atsushi Sanada, Christophe Caloz, Hiroyuki Arai, and Tatsuo Itoh, "Near-field measurements of a zeroth-order resonator using a composite right/left-handed transmission line," IEICE General Conference, C-2-96, Mar. 2004.
17. Akimichi Hirota, Hiroyuki Arai and Masayuki Nakano, "Experiments of DOA estimation system using pilot signals in outdoor," IEICE Society Conference, B-1-168, Sept. 2004.
18. Akimichi Hirota, Hiroyuki Arai and Masayuki Nakano, "DOA estimation system using eigenvectors," IEICE General Conference, B-1-203, Mar. 2005.
19. Akimichi Hirota, Hiroyuki Arai and Masayuki Nakano, "DOA estimation system using virtual planar array by sequential measurements," IEICE Society Conference, B-1-263, Sept. 2005.

Joint Work

Journal Papers

20. Jun Yaezawa, Akimichi Hirota and Hiroyuki Arai, “Study of array antenna calibration in outdoor environments,” IEICE Trans. on Commun., (submitted in 2006)

Proceedings of International Conferences

21. Jun Yaezawa, Akimichi Hirota and Hiroyuki Arai, “Outdoor-calibration method of the 3 × 3 planar array antenna,” Proceedings of ISAP 2005, WE3-4, pp. 309-312, Aug. 2005.

Proceedings of IEICE General / Society Conferences (Domestic)

22. Jun Yaezawa, Akimichi Hirota and Hiroyuki Arai, “Calibration method for array antenna by using spread code,” IEICE Society Conference, B-1-203, Sept. 2004.
23. Jun Yaezawa, Akimichi Hirota and Hiroyuki Arai, “Examination of self-calibration for 3 × 3 rectangular array antenna,” IEICE General Conference, B-1-235, Mar. 2005.
24. Jun Yaezawa, Akimichi Hirota and Hiroyuki Arai, “An experimental study of self-calibration with 3 × 3 planar array antenna,” IEICE Society Conference, B-1-198, Sept. 2005.
25. Msayuki Nakano, Hirofumi Hirono, Yukio Sato, Takehiro Miyamoto, Masahiro Karikomi, Akimichi Hirota, Koichi Ichige and Hiroyuki Arai, “Direction of arrival detection system: Overview,” IEICE Society Conference, B-1-248, Sept. 2005.
26. Takehiro Miyamoto, Msayuki Nakano, Akimichi Hirota and Hiroyuki Arai, “Direction of arrival detection system: Improvement of MUSIC estimation precision using a modified calibration method,” IEICE Society Conference, B-1-250, Sept. 2005.
27. Hirofumi Hirono, Msayuki Nakano, Takehiro Miyamoto, Yukio Sato, Yurie Shiwa, Bryan Robinson, Akimichi Hirota and Hiroyuki Arai, “Direction of arrival detection system: laboratory measurements,” IEICE Society Conference, B-1-252, Sept. 2005.